

SOUND DISSIPATION IN
POROUS MEDIA

by

K. ATTENBOROUGH

Thesis submitted for the degree
of Doctor of Philosophy
March 1969

Department of Civil Engineering
The University of Leeds

Table of Contents

Chapter 1	Introduction and Preface	
Chapter 2	Review of literature	
Chapter 3	Scattering theory for fluids	
Chapter 4	Single scatterer theory	
Chapter 5	Multiple scattering theory	
Chapter 6	Experimental results	
Chapter 7	Discussion and conclusions	
Appendix A	waves in fluids	
Appendix B	waves in solids	
Appendix C	scattering coefficients	
Appendix D	Energy dissipation calculations	101
Appendix E	Synthesis, basis of	
Appendix F	List of samples	107
Appendix G	Viscoelastic absorber-scattering coefficients	110
Appendix H	Spherical scatterer-cells	110
Appendix I	cross sections	
	Photographs	
	Table of sample data	
	Graphs	
	References	

...sound penetrates porous bodies more freely than would have been expected... On the other hand a hay-stack seems to form a very perfect obstacle.

- Lord Rayleigh

10

Acknowledgements	CONTENTS	Page
List of Symbols		2
Chapter 0	Introduction and Abstract	6
Chapter 1	Review of Literature	8
Chapter 2	Scattering Theory for fibrous media	23
Chapter 3	Single scatterer theory	31
Chapter 4	Multiple scattering theory	41
Chapter 5	Experimental results	56
Chapter 6	Discussion and conclusions	61
Appendix A	Waves in fluids	74
Appendix B	Waves in solids	80
Appendix C	Scattering coefficients	83
Appendix D	Expressions for computer program	95
Appendix E	Energy dissipation calculations	101
Appendix F	Constants, basic expansions, List of samples	107
Appendix H	Viscoelastic absorber-scattering coefficients	110
Appendix G	Spherical scatterer-solid stress components	116
	Photographs	
	Resumé of sample data	
	Graphs	
	References	

Acknowledgements

I should like to record my deep gratitude to Professor R.H. Evans until recently, Head of the Faculty of Applied Science, for realising that there was room for such work as has formed the basis of this thesis, and for making available the necessary financial support for three years.

I am also indebted to my Uncle, Mr. William Houghton-Evans, Senior Lecturer in Architecture, for his consistently wise counsel and constant encouragement; and both to Mr. Alan Yettram, at present Reader in Structures in the Mechanical Engineering Department at Brunel University, and Mr. Paul Yaneske, my former "acoustical research" colleague, for many helpful discussions.

The work involved in performing the relevant computations was made relatively simple by the assistance of my colleagues Dr. Debendra Nath Hazarika, in the writing, and Mr. Dipeskanti Bhattacharrya, in the execution of the computer programs.

I sincerely thank Mr. Roy Duxbury of the technical staff, for taking the photographs necessary and Miss Pam Bennion of the Earth Sciences Department for performing the arduous and complicated task of typing.

Lastly, but by no means least, I offer my sincere thanks to Dr. "John" L.A. Walker, Lecturer in Building Science and my supervisor throughout this work, for his careful encouragement of my often wild endeavours and for his painstaking checking of the substance of this work, despite the many and frequent other demands upon his time.

List of Symbols

Superscripts:

f refers to fluid property

s refers to solid property

l defined in context below

* complex conjugate

Subscripts:

D signifies dilatational wave property

TH " thermal " "

T " viscous shear " "

b " bulk value

o " equilibrium value

 a_o

normal incidence absorption coefficient

 \tilde{A}

viscous wave vector potential

 A_n^B, C_n^D coefficients in expansion of series for wave potentials.
Defined in 3.123 \tilde{a}_1 unit vector in ξ_1 direction a, b, c products of fibre radius and propagation constants,
at normal incidence a^1, b^1, c^1

ditto, at oblique incidence

B

radius of volume of integration (Appendix E)

 $B = \rho^t (\partial P / \partial \rho^t)_T$

Bulk modulus

 C_b

bulk wave velocity

 Co^f, Co^s

dilatational isothermal wave velocities

 C_p, C_v

specific heats

 d^1

product of fibre radius and axial phase constant

d

slab thickness

 d_{ij}

rate of strain tensor

 δ_{ij}

Kronecka delta

 ∇

gradient operator

$\nabla \cdot ()$	divergence operator
$\nabla \times ()$	curl operator
e_{ij}	strain tensor
E	wave energy per unit normal area per unit time
E_0	incident wave energy per unit normal area per unit time
F	surface
g	far-field scattering amplitude (as defined by Twersky)
h_1, h_2, h_3	curvilinear coordinate parameters
i	$\sqrt{-1}$
J_n, H_n	Cylindrical Bessel functions of order n
K	axial phase constant
\underline{K}	propagation vector
K_b	bulk propagation constant
K^f, K^s	thermal conductivities
K_D^f, K_{TH}^f, K_T^f K_D^s, K_{TH}^s, K_T^s	} propagation constants of dilatational, thermal and viscous (shear) waves, respectively
ℓ	projected distance of any point from origin of coordinate system (fig. 3.11 page 31)
L	length of cylindrical fibre
N	concentration of fibres
N	outward drawn normal from surface F (App. E only)
N^f, N^s	coefficients (Ch. 3), defined in Appendicies A and B
P	pressure
\downarrow P_{ij}	viscous part of fluid stress tensor
P_{ij}	total fluid stress tensor
P_{AT}	atmospheric pressure
r	radial coordinate (fig. 3.11 page 31)
\hat{r}	unit vector in r -direction

R	radius of fibre
$\text{Re} ()$	real part of ()
$\text{Im} ()$	imaginary part of ()
t	time
T	temperature
U	specific internal energy
\vec{u}	displacement vector
\vec{v}	velocity vector
$u_{j^{\text{th}} j}^v$	j^{th} component of displacement, velocity
V	volume
W	time averaged total energy loss in volume V with surface F
W_{μ}, W_{σ}	viscous and thermal energy loss (time averaged) respectively in region of W .
x, y, z	cartesian coordinates (fig. 3.11 page 31)
\hat{z}	unit vector in z -direction
Z_n	surface normal impedance
$\beta = -\frac{1}{\rho_0} \left(\frac{\partial \rho}{\partial T} \right)_P$	coefficient of volume expansion
γ	ratio of specific heats
e_n	cipher $\begin{cases} (1) n = 0 \\ (2) n > 0 \end{cases}$
ξ_1, ξ_2, ξ_3	curvilinear coordinates
θ	polar angle measured in xy plane
θ^f, θ^s	angles between propagation vectors of scattered viscous (shear) waves and x -axis
$\hat{\theta}$	unit, vector in the θ -direction
λ, μ^s	Lamé's constants of the solid

μ^+	coefficient of viscosity
ν	kinematic viscosity
γ	coefficient of compressional viscosity
$\rho, \rho^+, \rho^s, \rho_b$	densities
σ_{ij}	total solid stress
σ	dissipation cross-section
σ^+, σ^s	thermal diffusivities
φ	angle of incidence with respect to normal to cylinder axis
$\varphi_D^+, \varphi_{TH}^+$	angles between propagation vectors of scattered fluid) dilatational, thermal waves and x-axis solid)
$\varphi_D^s, \varphi_{TH}^s$	
$\phi, \bar{\phi}$	scalar potentials
ϕ_i	incident potential
$\phi_D^+, \phi_{TH}^+, \phi_D^s, \phi_{TH}^s$	scalar dilatational and thermal wave potentials
ψ, χ	scalar potentials associated with viscous (shear) wave
ψ_M, ψ_σ	viscous and thermal dissipation functions, respectively
ψ_+, ψ_-	forward and backward travelling plane wave potentials
ψ_R, ψ_T	reflected and transmitted plane wave potential amplitudes
ω	angular frequency
\int_F, \int_V	surface and volume integral respectively
$\langle \rangle_{AV}$	time average
x^*	complex conjugate of x
\sim	of the order of
\simeq	approximately equal to

SOUND DISSIPATION IN POROUS MEDIAINTRODUCTION AND ABSTRACT

0.1 The particular field that has been the concern of this work is that of Building Science. The porous media of interest are consequently those commonly used as absorbents in Architectural Acoustics.⁽¹⁾

The object of the work has been to formulate quantitatively a theory of the dissipation of sound in such materials, so that a basis can be laid for optimising and predicting their coefficients of absorption. The theory has aimed at avoiding the inclusion of empirical constants.

0.2 A review of literature is made involving a somewhat wider range of porous media, including those of interest in the fields of Geophysics and Engineering Geology. Porous fluids, a term employed by A.B. Wood (in "A textbook on Sound" Ch.3), as they occur, for instance, in Underwater Acoustics are also considered. Further, the literature concerned with sound propagation in more general inhomogeneous and composite fluids and solids, is examined, where the theoretical techniques are relevant to our study.

0.3 It is found that the literature specifically related to sound absorbing materials and also to unconsolidated or consolidated granular media:-

(a) develops theories which are essentially macroscopic and do not allow adequately for the microstructure of non-isotropic flexible framed media i.e. fibrous media.

(b) provides little realistic description of the dissipation in closed pore viscoelastic absorbers e.g. cellular rubber.

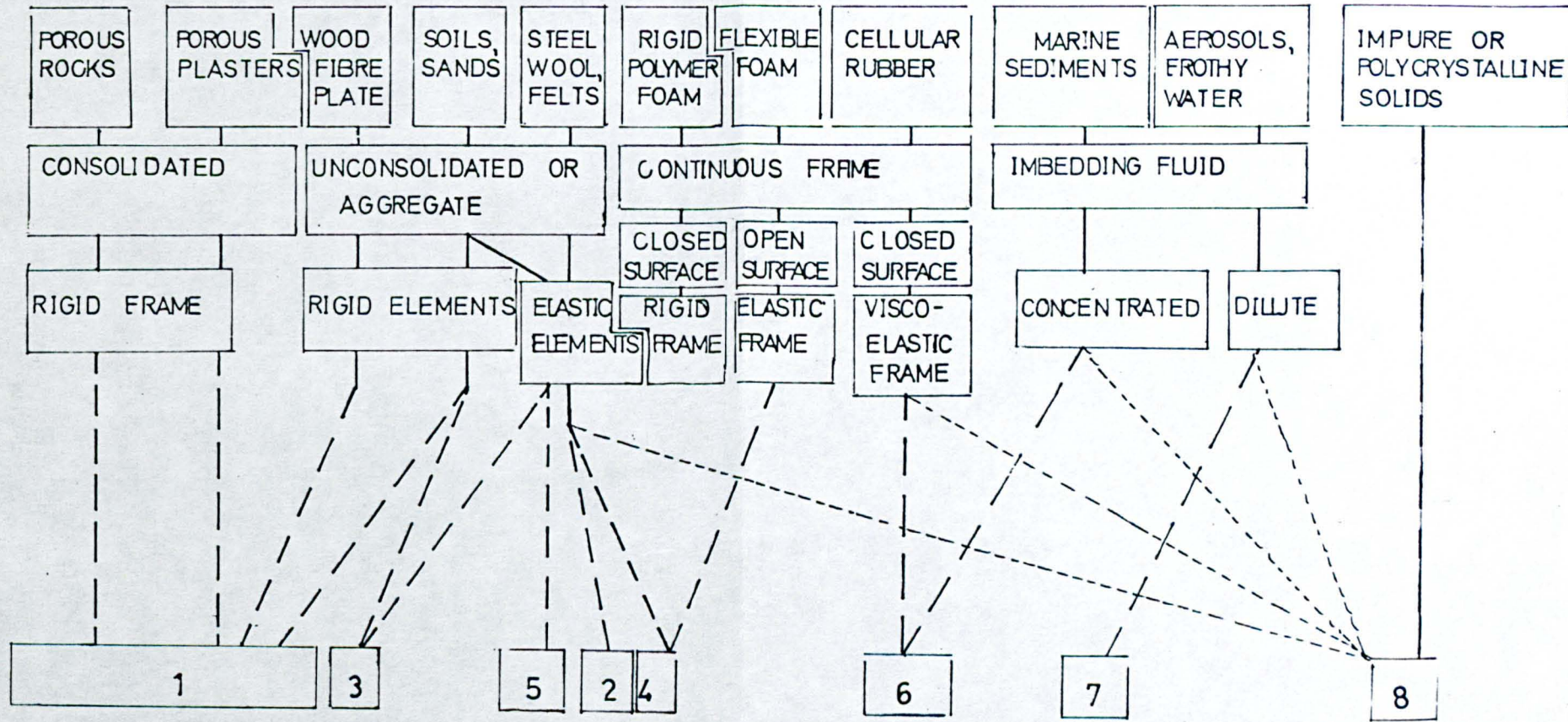
0.4 A theoretical technique, previously reserved for problems in underwater acoustics and sound propagation in suspensions is applied, as an alternative, to cases of fibrous and viscoelastic foam media.

POROUS MEDIA

COMPOSITE MEDIA

TYPES OF MEDIA

MODELS USED



————— LINKS REVIEWED

- - - - - LINKS SUGGESTED

The predictions of absorption thus obtained for fibrous media are found to correlate reasonably with experimental data on glass fibre block samples.

Further, an explanation of the physics of sound absorption in cellular viscoelastic media is suggested and conclusions and observations of previous literature are corroborated.

The literature is examined in the wider context previously mentioned. As might be expected, the field of interest has determined the particular type of porous medium considered; the model assumed; and often the theoretical technique.

The fold-out diagram shows these links, together with those discussed in the thesis and provides a classification for the review. Models numbered in the chart are now discussed.

Chapter 1

Review of Literature

1.1 Model 1. This is the basic conceptual model which underlies most of the work on sound absorbing materials.

Essentially, the porous medium is assumed to have a rigid solid, continuous frame containing a number of parallel cylindrical pores open at the surface of the material and normal to this surface.

1.11 After initial work by Rayleigh⁽³⁾ and Crandall⁽⁴⁾ dissipation can be postulated to take place according to such a model by:

(a) viscous losses in the boundary layer of the walls of each capillary tube owing to relative motion between the contained viscous, conducting and compressible fluid and the solid walls; and

(b) heat conduction, i.e. exchanges of heat energy between contained fluid and pore walls during cycles of fluid compression and rarefaction.

This stems from the Helmholtz-Kirchoff theory for sound propagation in a rigid walled tube containing a compressive, viscous conducting fluid.

1.12 Zwikker and Kosten⁽⁵⁾ extend this theory to a complete medium corresponding to Model 1. In order to allow for irregularity in the pore cross sections; viz. deviations from circular cross-section and changes in effective radius causing a variation in the fluid particle velocity across each capillary pore (superimposed on the variation due to viscous drag at the pore walls); the fluid particle velocity is replaced by an average particle velocity over the cross-section of any pore. This can then be related to the volume flow through the porous material by Dupuit's Relation⁽⁶⁾:-

$$\text{volume flow} = \left[\text{porosity} \times \text{average particle velocity} \right]$$

1.13 The viscous drag effects in the separate capillary pores are combined⁽⁸⁾ by the introduction of the specific resistance or flow resistance coefficient (σ) for the porous material which relates volume flow with the pressure variation through the material. Its steady state value corresponds to the case where the equation of motion in the individual pores reduces to that for Poiseuille flow. Then the equation of motion for volume flow in the total medium is Darcey's empirical law⁽⁶⁾ (for non-turbulent flow) and the flow resistance is equivalent to an inverse permeability coefficient.

The high frequency extreme where the Helmholtz annular effect⁽⁷⁾ can be considered to exist in the capillary pores is given an approximate value by Crandall. An expression for the flow resistance coefficient which applies at intermediate frequencies is computed by Zwikker and Kosten.⁽⁹⁾

The characteristic impedance and propagation constant for a medium corresponding to Model 1. are derived considering viscous and thermal effects in

1.2 Model 2 - a generalisation of model 1.

The porous medium is regarded as having a continuous solid flexible frame containing pores, the structures of which are not specified, apart from the requirement that the medium be homogeneous and isotropic.

1.21. Zwikker and Kosten⁽¹⁶⁾ extend their previous work for the rigid framed model 1 to the more general flexible frame model 2, by introducing the concept of a coupling factor. This factor includes the inertial and viscous coupling between the solid frame and the pore fluid resulting from their relative motion. The parameters of porosity, structure factor and flow resistance coefficient are retained in modified equations of motion and continuity for both pore fluid and solid frame. This procedure does not require the more rigorous calculations for complex density and stiffness for the rigidly framed model 1. The solution of these equations provides for the existence of two types of coupled waves, which become decoupled into separate compressional waves for frame and pore fluid at certain frequencies depending on the compressibility of the frame.

1.22 Other authors,^(17,18,19) using a similar general flexible frame model based on a rigid frame approach, define parameters less easily identifiable with the structural properties of actual materials. In particular an effective dynamic mass factor (m) is introduced; defined as the ratio of the effective mass of air in the pores to the mass of an equal volume of "free" air. This is meant to contain the effect of the presence and motion of the solid skeleton on the motion of the fluid. This parameter reduces to unity i.e. to the same value as Zwikker and Kosten's structure factor, for a medium corresponding to Model 1 with a rigid frame and all the pores parallel to the wave vector of the incident (plane) sound wave. Rettinger⁽²⁰⁾ defines a slightly different parameter representing the amount of vibrating

air mass per unit volume of the medium. This differs by a factor of bulk density from the above definition due to Morse and Bolt.⁽¹⁸⁾

1.23 Beranek⁽²¹⁾ applies the coupling factor approach to model 2 type media. However, greater concern with fibrous materials is shown, in that friction between fibres is introduced as a further consideration, in the equation of motion of the solid frame. Kosten and Janssen⁽²²⁾ express doubt as to the correctness of Beranek's⁽²¹⁾ derivation of the coupling factor and point out his misinterpretation of the structure factor as a "dynamic mass" coefficient similar to m . Further⁽²²⁾ the coupling factor derivation of Zwikker and Kosten⁽¹⁶⁾ is adapted to include the more complete expressions for complex density and complex stiffness of air in a rigid-walled pore.⁽⁵⁾

It is remarked that to be fully rigorous these expressions should in fact be developed for a gas contained in a flexibly walled cylindrical pore.

1.24 Zwikker and Kosten⁽²³⁾ compare their theoretical predictions for model 2 with experimental observation for wood-fibre plate and hair-felt. Kosten and Janssen⁽²²⁾ further compare the modified theory with experimental results for more flexibly framed fibrous media. The correlation in this latter case is found good, if, as is required for the earlier theory,⁽⁵⁾ some suitable estimation of the structure factor is made.

Paterson⁽²⁴⁾ applies the Zwikker and Kosten⁽⁵⁾⁽¹⁶⁾ theory further to fluid-saturated granular materials and obtains reasonable correlation with experimental results.

1.3 Model 3 - applied particularly in the context of fluid-saturated granular media, where concern is more with sound propagation than sound absorption.

The porous medium is regarded as a fluid-saturated aggregate of closely-packed spheres. The spheres are assumed elastic and in contact such that applied isotropic pressure causes changes in the area of contact between adjacent spheres. The saturating fluid is assumed incompressible and inviscid.

Brandt⁽²⁵⁾ considers a randomly packed array of four different sphere sizes such that each smaller size completely fills the voids of the next larger size to a constant fraction. A non-linear stress-strain relationship for such a model is obtained by calculating the dilatational deformation of sphere radius as a function of the force between the particles.

A similar model is used by Duffy and Mindlin⁽²⁶⁾, however tangential as well as normal contact pressure is included, and the frictional loss per cycle due to slip is considered. In both cases the velocity of compressional waves through such a frame is calculated.

1.4 Model 4 - of fibrous materials.

The fibre block is considered as an air-fibre composite medium in which parallel fibres of uniform diameter and length are either freely suspended in air, or bound elastically to fixed positions in space.

1.41 Kawasima⁽²⁷⁾ chooses this model as an alternative to models 1 or 2 for the case of a flexible and fibrous acoustic material. The incident sound is restricted theoretically to plane waves propagating in the direction perpendicular to the fibre axes. In the elastically bound case, a string model and a bonded rigid bar model are differentiated. In the former case the fibres are assumed to move as clamped strings i.e. as though the major fraction ($8/\pi^2$) of their length were a rigid bar, and the remainder fixed permanently at the equilibrium position. The latter case is a simplification of this, where the whole of the fibre is assumed to oscillate as a rigid bar, constrained according to Hooke's Law.

1.42 The clamped string model is developed as a general case and the other two cases are considered to be special cases of this. Equations of continuity, introducing porosity, motion of fibres, and volume flow of air are deduced, together with equations of motion of fibres and air, derived from Hamilton's Principle, and incorporating a resistance coefficient for each fibre. This resistance coefficient is given by Stoke's law for a "long ellipsoid of gyration" and gives a frequency dependent expression for specific flow resistance when the equations of motion for fluid and fibres are combined in terms of relative velocity.

The general form, because of the model assumed, predicts total absorption at resonant frequencies of the elastically bound fibres.

1.43 A similar model of an array of identical parallel rods uniformly spaced in air has been adopted by Lang (104) in discussing the absorption properties of cellular plasters e.g. polyurethane foam. The theory used is essentially based on Zwikker and Kosten. However, by choosing this particular model he avoids the use of their structure factor. Thermal dissipation is not considered.

1.5. Model 5 - of particular importance in discussion of sound propagation through unconsolidated, granular, fluid-saturated media where dissipation is also considered.

The medium is considered to consist of an elastic solid matrix, saturated with a compressible, viscous fluid. No specific assumptions are made about micro-structure. However, certain restrictions apply at some stages.

1.51 The literature based on this type of model is more concerned with the formal derivation of the equation of motion of the solid frame via a stress-strain constitutive relation than the previously discussed theories. (5,7,8-23)

A linear stress-strain relationship involving porosity is derived by Biot.⁽²⁸⁾ Analytic expressions for the resulting six elastic coefficients are obtained from three equations of equilibrium and three equations representing a generalised form of Darcy's law.⁽⁶⁾ Biot⁽²⁹⁾ uses this formulation together with a Lagrangian form of the equations of motion to derive wave equations.

1.52 The coupling factor of Zwikker and Kosten⁽¹⁶⁾ and Beranek⁽²¹⁾ is split up into its inertial and viscous components for this model. The inertial coupling is introduced into the equations of motion via three "mass" coefficients derived empirically. The viscous coupling is introduced allowing for the variation of the viscous dissipation with the micro-velocity field across the pores ~~i.e. variation of the viscous dissipation with the micro-velocity field across the pores~~ i.e. variation with frequency and with change of cross-sectional pore shape. These effects are combined into a viscosity function which depends on frequency, a characteristic dimension of the pore (extremes of shape being parallel walled slits and circular capillaries), tortuosity⁽⁶⁾ and the kinematic viscosity of the pore fluid. The effect of tortuosity of the pores, in particular is contained by a structural factor.⁽³⁰⁾ The frequency dependent viscosity function is a more comprehensive, microstructurally sensitive representation of the dynamic flow resistance coefficient than that used by other authors.⁽¹⁶⁻²¹⁾

1.53 In a later paper, Biot⁽³¹⁾ rederives the elastic stress-strain relation for a porous medium, considering both "closed" (fluid not free to circulate in and out of the medium) and "open" pore situations, (as do Gassman⁽³²⁾ and Paterson⁽²⁴⁾ for model 3). Anisotropy of the medium is also considered in this paper, together with the effects of heat conduction between grains and porefluid and internal friction between the grains of the unconsolidated solid.

The latter two considerations are introduced under the general heading of "thermoelastic effects" and previous theories⁽³³⁾ of irreversible thermodynamics are evoked, resulting in the replacement of the elastic coefficients by operators. The equations of motion are derived in a different form, reducing the three mass coefficients used previously⁽²⁹⁾ to a single coefficient dependent on the pore geometry, i.e. more simply analogous to the inertial part of the coupling factor.^(16,21)

Another paper⁽³⁴⁾ sees the introduction of a viscodynamic operator in an equation of relative motion of fluid in the pores. This represents a generalisation of a method previously used to obtain the complex viscosity function. The equation of relative motion, together with an equation of motion representing the time derivative of the total momentum of the fluid-solid mixture, are used rather than separate equations of motion for fluid and solid respectively.^(28,29,31) A wave equation is then derived which can be analysed as previously,^(28,29,31) into two compressional and one shear wave.

1.54 Hardin and Richart⁽³⁵⁾ point out that the elastic constants introduced by Biot^(28,29) are difficult to measure in practice. In their theory therefor the Young's modulus of the elastic frame is derived from Duffy and Mindlin's analysis⁽²⁶⁾ according to model 3, and this is substituted into the Biot theory.⁽²⁴⁾ Brutsaert⁽³⁶⁾ extends analysis based on Model 5 to the case of a three phase medium; a porous granular medium saturated with air, some grains being covered with a wetting fluid. A Lagrangian approach, for the equations of motion, similar to that of Biot's isotropic medium theory⁽²⁹⁾, is used. The difficulty with Biot's elastic coefficients^(28,33,34) is partially avoided by employing Brandt's approach⁽²⁵⁾ for elasticity of Model 3, pointing out that the remainder of Brandt's theory for the compressional wave velocity assumes that the fluid and solid move together and exhibit the same displace-

ments. Viscous effects in the air are included according to Zwikker and Kosten for Model 1,⁽⁵⁾ and those in the liquid according to Biot's viscosity function.⁽²⁹⁾ The effects of change of pore shape, tortuosity of pores, and heat conduction are not considered and it is assumed that the two fluids do not occupy the same pore at the same time.

1.6 Model 6 - represents a "finite element" approach to the problem.

The medium is considered to consist of a number of identical elements of volume or "cells" containing proportions of fluid and solid.

1.61 A rigid, porous, sound absorbing material is compared by Beranek⁽³⁷⁾ to a model containing a series of rectangular cells divided into proportions of rigid solid and fluid according to the volume porosity. Flow resistance is also introduced into a theory in which the equations of continuity and fluid motion are deduced from first principles, making no specific assumptions about pore characteristics but making a number of restricting approximations. This model and approach were rejected by Beranek⁽²¹⁾ in favour of Model 2.

However, McGrath⁽³⁸⁾ points out that an analytic solution for model 6 is possible without the number of approximations used and that reasonable results can be obtained with two acoustic materials with fairly rigid frames.

1.62 Tyutekin⁽³⁹⁾ develops a theory for a hypothetical rubber-like material containing an array of parallel cylindrical ducts with their axes normal to the incident plane wave front. The medium is treated as if it consisted of an array of identical close-packed hexagonal "prisms", each of which contains an infinitely long cylindrical channel. Each "prism" or cell is approximated to a cylinder with a radially fastened external surface for the purpose of applying simple boundary conditions for continuity of radial displacement and transverse stress of the boundary. The boundary conditions together with the requirement of continuity of direct and transverse stress

at the channel boundaries furnish a wave equation for each cell corresponding to that for the propagation of axially symmetric elastic waves in a solid rod with a free surface.

1.63 A cell model approach is also used by Nesterov^(40a) to describe sound propagation in a concentrated suspension of heavy, rigid solid particles in a viscous fluid. Each cell is postulated to consist of a double plug i.e. a cylindrical solid plug surrounded by a coaxial cylindrical liquid plug. For a regular array of particles, the assumed cylindrical shape of the liquid plug is an approximation to the rectangular box shape obviously required for a representation of the actual medium.

Neglecting thermal effects, equations of motion for the liquid and the solid are obtained and used to define a complex density for the suspension which includes the viscous effects in much the same way as the complex density derived by Zwikker and Kosten⁽⁵⁾ for the rigid walled tube.

Bysova and Nesterov^(40b) extend this cell model to include thermal effects. In this case the spherical shape is chosen for the liquid-solid plug. A complex compressibility is thus defined expressing the thermal attenuation within the concentrated suspension (c.f. Zwikker and Kosten⁽⁵⁾'s complex stiffness for a medium with rigid walled pores). The theory^(40a, b) is suggested as being more applicable to concentrated suspensions than other theories⁽⁴¹⁾ which do not include interactions between the particles.

1.7 Model 7 - applicable to various types of suspensions in fluids; and of inhomogeneous or composite solids.

1.71 The suspension or inhomogeneous solid is considered to contain a distribution of discontinuities according to the following forms:-

(a) spherical fluid discontinuities in a denser fluid medium

- (b) spherical fluid discontinuities in a less dense fluid medium
- (c) spherical rigid or elastic solid discontinuities in a fluid medium.
- (d) spherical or arbitrarily shaped solid, fluid or cavity discontinuities in a solid medium.

When dissipation is calculated for (a), (b) or (c) it is based on the solution of the scattering problem for a single scatterer and extended by simple addition to the total medium. i.e. the scatterers are assumed to have only a slight effect on the properties of the imbedding medium.

1.72 Rayleigh⁽⁴²⁾ develops the spherical harmonic approach to the single scatterer problem where the incident wavelength is large compared with the radius of the scattering obstacle. Lamb⁽⁴³⁾ extends this analysis to include viscous effects and derives scattering coefficients for a rigid sphere free to move, from rate of change of momentum considerations. The first application to a number of obstacles is made by Sewell⁽⁴⁴⁾ for a suspension of fixed, rigid, solid obstacles in a viscous fluid. A correction is applied in this treatment to account for movement of the obstacles. A more rigorous approach, for suspensions of types (a), (b) and (c) is given by Epstein⁽⁴⁵⁾ This is revised and extended by Epstein and Carhart⁽⁴⁶⁾ for types (a) and (b), to include the effects of heat exchange between particles and imbedding medium. It is shown that the irreversible effects due to viscosity and heat conduction are simply additive to within a close approximation, at audio-frequencies. The attenuation coefficient for the medium is correspondingly calculated from dissipation functions representing viscous loss and thermal loss separately. Chow⁽⁴⁷⁾ considers suspensions of type (a) and (b) and includes surface tension effects. The theory⁽⁴⁶⁾ is shown to be applicable even in the case of large displacements of the scatterers⁽⁴⁷⁾

i.e. the boundary conditions used for each scatterer retain the same form when either the origin of coordinates is fixed in space or allowed to move with the scatterer. Wood⁽²⁾ considers attenuation in bubbly water by a scattering procedure. The same problem is considered by Devlin⁽⁴⁸⁾ by a somewhat different technique considering the passage of the sound wave as a small perturbation on the volume of the bubble (c.f. model 3). The equations of motion are derived using generalised coordinates and a Lagrangian approach. Zink and Delsasso^(49a) apply the Epstein and Carhart⁽⁴⁶⁾ theory to suspensions type (c); pointing out Epstein's conclusion⁽⁴⁵⁾ that when only viscous attenuation is considered, dissipation becomes almost independent of density, (when the density of the solid obstacles is much greater than that of the imbedding fluid). It is further remarked that, in such media, losses due to (i) thermal effects within the scatterers (ii) relaxation phenomena and (iii) spherical scattered wave formation (removing energy from the incident plane wave front - unimportant in reverberation measurements⁽⁴⁵⁾) are negligible compared with the effects of viscous and thermal attenuation.

1.73 Attenuation in inhomogeneous solids of type (d) is considered by Ying and Truell.⁽⁵⁰⁾ The particular obstacles considered are (i) isotropic elastic sphere, (ii) rigid sphere and (iii) spherical cavity embedded in an elastic solid. The average energy removed as a fraction of the incident energy per unit area per particle by spherical compressional and shear wave formation in scattering, is calculated.

The case of scattering of high frequency sound by arbitrarily shaped and orientated grains in polycrystalline materials is developed by Bhatia⁽⁵¹⁾ as a problem of "slight" scattering i.e. where the properties of the scattering medium differ only slightly from those of the imbedding medium. The effect

of multiple scattering, i.e. the effect of the material surrounding a single grain, being granular and not bulk material, is disregarded because of the grains' random orientation with respect to each other.

1.74 Urick and Ament⁽⁴¹⁾ consider the propagation of sound in a finite slab region, (thickness d), containing a concentrated suspension of elastic, solid particles, the imbedding fluid being viscous and non conducting. Model 7 conditions are assumed within the slab i.e. the wave incident normally on the slab is assumed to be a close approximation to that incident on each of the particles. The inhomogeneous nature of the slab medium is brought into account by assuming plane reflected and transmitted waves either side of the slab which are respectively the sum of the backward scattered and forward scattered waves from the particles. The single scatterer coefficients for an elastic sphere free to move in a non-conducting viscous fluid as calculated by Lamb⁽⁴³⁾ are used for each particle. The propagation constant and complex velocity of the model are calculated on the supposition that the scattering from the inhomogeneous slab region is identical with transmitted/reflected components from the homogeneous slab. The viscous attenuation expression is shown to be the same as predicted by the relevant single scatterer theory.^(43,45) Correlation is also shown with the derivation of Urick⁽⁶⁸⁾ based on a theory of the viscous drag process between fluid and particles according to Stoke's Law. Duykers⁽⁹²⁾ shows that this in turn can be related to Biot's theory^(28,31) for viscous attenuation in a relevant model.

1.8 Model 8 - a more concentrated version of model 7.

This model applies where the wave incident on each scatterer within the suspension is not necessarily approximately the same as the source plane wave i.e. the obstacles do not scatter independently to any reasonable approximation.

1.81 Morse and Feshbach,⁽⁵²⁾ Waterman and Truell⁽⁵³⁾ and Twersky⁽⁵⁴⁻⁵⁶⁾

include the interaction between the particles of model 8 caused by multiple scattering. The first⁽⁵²⁾ is concerned with propagation in bubbly waters and bases the technique of solution on the construction of a Green's function for the complete case. The other references⁽⁵³⁻⁵⁶⁾ deal with a more general class of problems by constructing integral equations for the exciting field on any scatterer in the medium. Twersky⁽⁵⁶⁾ derives bulk parameters for a multiple scattering slab medium containing a random array of similarly aligned, identical scatterers of general shape. In a first formalism⁽⁵⁴⁾ these are computed in terms of the properties of the imbedding medium and the single scattering coefficients for an isolated scatterer in the imbedding medium. A second formalism⁽⁵⁵⁾ derives the bulk parameters in terms of a generalised isolated scattering amplitude corresponding to each scatterer being excited by the coherent multiple scattering field but radiating into the imbedding medium. This is considered to be more accurate than the first formalism.

Embleton⁽⁵⁷⁾ applies the first formalism⁽⁵⁴⁾ to the attenuation of sound by compressional wave scattering in forests by considering the case of sound incident on a slab region of parallel rigid cylinders, their axes normal to the incident plane wave vector.

Fibrous materials are now very commonly used as sound absorbing materials and a large variety of proprietary brands are available.⁽¹⁾ They also provide the best sound absorption characteristics⁽⁵⁹⁾, in the audio-frequency range. Thus, it is important that there should be adequate theoretical work available to explain their performance and lay the basis for their design.

2.1 Criticism of existing models, theories and resulting parameters

Although several authors specifically concerned with Architectural Acoustics have suggested that their theories^(5, 17-21) are applicable to fibrous media, certain inadequacies of their work can be pointed out. These stem basically from the differences between the microstructure of the conceptual models (1.2) behind their theoretical work and that of the materials under consideration. It is proposed that the material parameters on which the dissipative capacity depends tend to represent macroscopic properties⁽¹⁴⁾ and are often frequency dependent.^(17,18) The most comprehensive treatments are those due to Zwikker and Kosten⁽⁵⁾ and Biot,⁽²⁸⁻³¹⁾ thus their parameters are the primary ones reviewed.

2.11 Structure Factors

As remarked in 1.14, the structure factor⁽¹⁰⁾ is introduced to allow for effects of orientation of pores and of side-holes. Also, at least for that theory based on the rigid framed Model 1, the factor is required to include the effect of the motion of the frame⁽¹⁰⁾ i.e. a slight frequency dependence is introduced as in the effective air mass parameter.^(17,18,21) The result for all absorbing materials is a factor which cannot be exactly measured⁽¹²⁾ and is calculated simply as a factor required to bring theoretical prediction into line with experimental observation. It can

only be predicted in fact for special cases of "artificial media" e.g. stacked glass straws⁽⁵⁹⁾ which are unlikely to correspond in structure to materials used for sound absorption, of the high flexibility, low flow resistance category,^(5,21) such as glass fibre wool. The structure factor may be more viable for high density, high flow resistance materials, such as wood-fibre plate; where it would serve as a "persistence factor"⁽⁶⁰⁾ measuring the persistence of a pore in direction and cross-sectional area in a section parallel to the "common" direction of the fibres. For such materials it may be expected that the fibres are close-packed i.e. in contact for the major portion of their length with other fibres and thus such concepts as capillary pores, side-holes, orientation⁽¹⁰⁾ and tortuosity^(6,30) have meaning. For loosely compacted fibre wools, where the fibres cannot be expected to be in contact for any appreciable portion of their length such concepts as these have little place. Only that of tortuosity of streamline flow⁽⁶⁾ retains any meaning.

2.12 Flow Resistance

This parameter is introduced by authors^(5,14-21) to express the viscous boundary layer action, at the solid-fluid interfaces within porous materials, in the equations of motion. It is given an accurate representation (1.13) as a frequency dependent function only for Model 1 (carried over to Model 2) i.e. for the case of periodic motion of a viscous, compressible fluid in a fixed, rigid walled, circular, cylindrical pore. For model 5 (1.52), a viscosity function⁽²⁹⁾ is introduced to express the more general periodic micro-velocity field situation across a pore of arbitrary shape, with a limited motion of the rigid pore wall, i.e. unidirectional motion parallel to the induced pressure gradient. An analysis of incompressible, viscous fluid flow inside a cylindrical tube with elastic

walls, which are massive and capable of three dimensional motion, is made by Womersley⁽⁶¹⁾, the analytic solution being in terms of uncharted functions. Fibrous material in which capillary pores can be defined, such as the wood-fibre plates already mentioned, would require an analysis of viscous, compressible, conducting fluid motion within pores of arbitrary shape, possessing massive, conducting elastic walls, capable of three dimensional motion. Clearly for this case, and for loosely compacted woollen materials where capillary pores cannot be defined, an analytic expression for the dynamic flow resistance coefficient necessary in the relevant theories^(5, 14-21) even in terms of the measurable static coefficient,⁽⁶²⁾ presents a somewhat intractable problem. Thus the practicability of dynamic flow resistance as a parameter for flexible, fibrous absorbing media must be questionable.

2.13 Concept of a continuously framed and isotropic medium

The theories of propagation, based on models 2, 3 and 5, predict plane "frame waves", coupled or decoupled with the motion of the saturating fluid. This requires the existence of a continuous solid frame through the medium or at least a discontinuous frame which will transmit the effect of periodic loading on the "front" surface of the medium. A continuous rigid solid frame, of course, is an integral specification of model 1.

The requirement of continuity of frame is met in actual materials of the acoustic plaster, wood fibre plate (from the observations of 2.11), and granular, types. Where the wood fibre and granular materials may be expected to show a non-linear elasticity due to their essential discontinuity - is pointed out by some authors concerned with models 3 and 5 (1.3 and 1.54) and by Jones.⁽⁶³⁾

However, the correlation achieved by Kawasima⁽²⁷⁾ between theory based on the unbonded version of Model 4⁽⁶⁴⁾ and experimental observation on glass fibre material, would seem to indicate that in such materials, for the small displacements and velocities involved in an acoustic disturbance the fibres react quite independently of each other, at least at high frequencies. This is not true in the presence of resin bonding.

Further, the condition of isotropy, required in many of the continuum mechanical theories^(5,19,21,35,36) based on models 2, 3 and 5, is not necessarily satisfied by fibrous materials if the fibres have a "preferred" direction. Thus materials must come under the category of materials not adequately described in their sound absorbing properties by theories based on homogeneous, isotropic media.⁽⁶⁵⁾

2.2 Application of the unbonded version of Model 4

2.21 Kawasima's Theory - advantages and disadvantages

By choosing a model for the fibrous material as described in 1.4 Kawasima avoids many of the difficulties mentioned in the previous section. However, new problems are introduced in attempting to apply a continuum mechanical approach to this model. An approximation is introduced with the resistance coefficient⁽⁶⁶⁾ i.e. an application of Stoke's Law for motion of a body through a viscous fluid. Further, the heat conduction effect can only be introduced assuming a square array of fibres.⁽⁶⁷⁾ Also, the compressibility, and three dimensional strain of the elastic fibres are not taken into account by the assumed rigid fibre model.

2.22 A scattering theory

Model 4, at least with unbound or lightly bound conditions, may also be regarded as a version of model 7 or 8. Thus the fibrous medium may be considered to be a suspension of fibres in air and the techniques of

analysis reviewed in 1.7 and 1.8 may be applied. Each fibre may be compared to an elastic, cylindrical, conducting solid scatterer immersed in a viscous conducting, compressible fluid medium. The tractability of this approach is ensured for most materials in use as sound absorbing materials by the very small dimensions of the component material fibres (diameters between 3 and 10 microns in most instances). This means that the harmonic functions used in the scattering theory are rapidly convergent and need only be expanded for the first few orders of their arguments; i.e. Rayleigh scattering conditions exist, the wavelength of the incident sound being much greater than the radius of the scattering obstacles for the frequency range (100-6000 c/s) of interest.

2.23 Dissipation in Fibrous Media on a scattering model

Epstein and Carhart⁽⁴⁶⁾ analyse sound propagation in a viscous, conducting, compressible fluid medium into three types of waves; two compressional waves and one rotational or shear wave. Within a small approximation one of the compressional waves is shown to be ascribable purely to thermal effects, the other corresponding to dilatational propagation in an inviscid, non-conducting fluid. It is noticed that the shear (viscous) wave and the "thermal" wave are rapidly attenuated in air and water. The attenuation of sound in its passage through fluid suspensions, as described in 1.7, can then be attributed to the "mode conversion" of incident plane dilatational waves into thermal and viscous waves by scattering at the various obstacles (suspended particles).

This mode conversion into viscous waves ^{is} accepted by Urick⁽⁶⁸⁾, Chow⁽⁴⁷⁾ and OCartensen and Schwan⁽⁶⁹⁾ as equivalent to the more conventional representation of viscous drag. Urick⁽⁶⁸⁾ shows that the attenuation coefficient derived by Lamb⁽⁴³⁾ can be divided into two parts related to the scattering loss and viscous loss respectively, and proceeds to verify that the viscous part can be derived independently by means of Stoke's equation. Chow⁽⁴⁷⁾ similarly shows, that the first order (low frequency) approximation of the viscous drag (as a function of relative velocity) on water droplets in air, subject to an incident sound wave according to the Epstein and Carhart⁽⁴⁶⁾ formulation, is equivalent to Stoke's law for spheres moving with the same velocity. Further, Chow⁽⁴⁷⁾ derives the first order (low frequency) approximation of the heat transfer rate for this formulation, including heat conduction effects for each droplet, as equivalent to the standard expression for heat transfer to a sphere when Reynolds number tends to zero and heat exchange is by conduction only.

It may therefore be expected that the expressions for dissipation given by mode conversion within Model 4 (as a type of Model 7) are accurate representations of the mechanisms of dissipation in an ideal fibrous medium previously inaccurately represented by theories using flow resistance etc. The main parameters in this approach are; radius of fibres, their elasticity, number (average) per unit volume and properties of the imbedding medium (air). Such quantities are readily measurable compared with the less convenient parameters previously required, and indeed a scattering theory is more directly related to the microstructure of a fibrous material.

2.3. Restrictions and assumptions required in applying a scattering theory

2.31 The unbonded version of Model 4 is the only one which corresponds to Model 7. Each fibre is assumed freely suspended in air so that boundary conditions of continuity of pressure, velocity, temperature and heat flow can be applied to any point on its surface. Thus the contact between fibres, necessarily occurring in actual materials, is neglected, introducing a systematic error in so far as they induce "frame" waves.

Friction between fibres is also neglected, as is the effect of resin bonding which alters the apparent elasticity of the fibres, their orientation and degree of contact with each other. The influence of resin or cross bonding of the fibres is to decrease the sound absorption at low frequencies and increase it at high frequencies⁽⁷⁰⁾. It may be considered that a bonded material is more amenable to analysis based on continuous frame models (2.13) than a loose pile.

2.32 When a single scattering approach specific to Model 7 is used, the time average of the power dissipated per scatterer, as a fraction of the incident energy, is calculated to give the attenuation coefficient of the medium. The power dissipated per scatterer is found by integrating the dissipation functions over a large volume surrounding each scatterer. This volume must be at least large enough for the viscous and thermal waves to have died out before reaching its surface. Thus a minimum radius of the volume of integration must be the wave decrement distance for the viscous and thermal waves (roughly equal⁽⁴⁶⁾). It follows that this method of calculation requires the scatterers to be separated by at least twice this distance so that the viscous and thermal waves do not interfere. The required separation in air has been calculated to be

$0.02 \text{ cm}^{(46)*}$. In a fibrous block, this requirement is unlikely to be met over the whole length of every fibre, and must provide another source of systematic error.

2.33 In view of the concentration of fibres to be expected in actual media and the variation in their separation, the single scattering theory can only provide a crude approximation. The multiple scattering theory appropriate to model 8 should improve on this by introducing the possibility of scattered dilatational wave interference. In the multiple scattering theories available, however, for general situations, viscous and thermal wave multiple scattering are not considered.

The work of Waterman and Truell⁽⁵³⁾ would seem to indicate that symmetry arguments discount any effect of viscous (shear) wave multiple scattering among spherical scatterers. More general situations, however, require modification of the theoretical arguments used to allow for shear wave interaction.

Further, the first formalism of Twersky⁽⁵⁴⁾, although allowing for random spacing of the fibres, requires them to be parallel along their whole length. The extra refinement of scattered wave interaction therefore limits the flexibility of the single scattering technique as regards the orientation of each fibre with respect to the incident wave front.

* for frequencies $> 550 \text{ Hz}$

The scattering approach to the problem of sound dissipation in a fibre block, as indicated in the previous chapter, requires the solution of the scattering problem for a single fibre.

Each fibre may be approximated by an elastic, conducting solid cylinder, which is suspended in a viscous, conducting fluid viz. air, for the cases of interest.

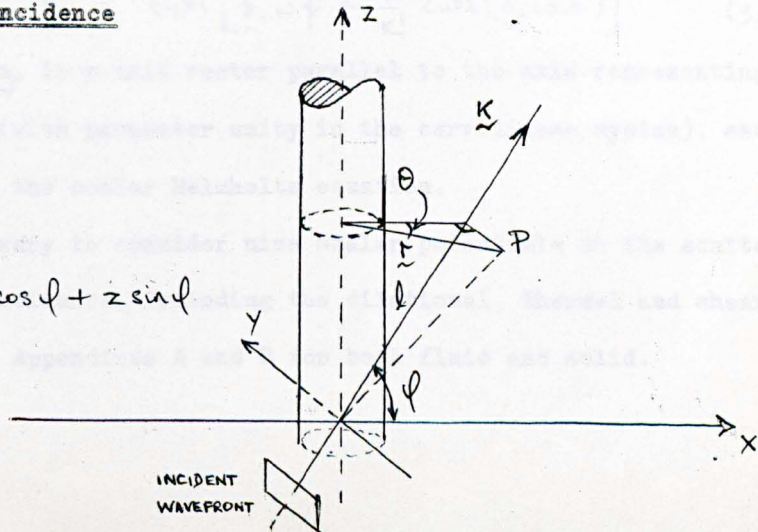
Scattering by solid cylindrical objects is considered by Lamb⁽⁸⁰⁾, Morse⁽⁸¹⁾, Morse and Feshbach⁽⁸²⁾ and Lyamshev⁽¹¹⁰⁾. Further the cylindrical scattering problem for plane acoustic waves is investigated by White⁽⁷⁷⁾ and Tyutekin^(78,79), both for normal and oblique incidence on fluid filled or evacuated cavities. The treatment of White⁽⁷⁷⁾ allows both shear and compressional wave incidence.

None of the literature, however, considers dissipation, due to the scattering of viscous and thermal waves, around a cylindrical object; this, therefore, must be investigated.

3.1. Scattering by an elastic, conducting, solid cylinder imbedded in a viscous, conducting fluid

3.11. Oblique incidence

$$l = x \cos \phi + z \sin \phi$$



Following White⁽⁷⁷⁾, consider a plane compressional wave incident on the cylinder, choosing a system of coordinates as shown above, with their origin inside the cylinder, and the z-axis coincident with the axis of the cylinder.

For simplicity^(77,79) the incident wave vector is chosen to lie in the xz-plane. The incident wave potential may therefore be written

$$\phi_i = \exp(-i\omega t) \exp \left[ik_0^f (x \cos \psi + z \sin \psi) \right]$$

using the convention that this represents a progressive wave, travelling in the positive x direction, and stipulating that ϕ_i must satisfy the scalar Helmholtz equation.

3.12. Other potentials

In general as both the fluid and the solid are allowed to support shear, it is necessary to consider more general solutions of the vector Helmholtz equation.

For certain coordinate systems $[\xi_1, \xi_2, \xi_3]$, by (83), it is possible to represent the vector potentials of the velocity fields in terms of two scalar potentials:-

$$\underline{A} = \text{curl} \left[\underline{a}_0 \omega \psi + \frac{1}{k_0^f} \text{curl}(\underline{a}_0 \omega \chi) \right] \quad (3.121)$$

where $\omega = \omega(\xi_1)$ and \underline{a}_0 is a unit vector parallel to the axis representing the coordinate ξ_1 (with parameter unity in the curvilinear system), and ψ, χ both satisfy the scalar Helmholtz equation.

Thus it is necessary to consider nine scalar potentials in the scattering problem for oblique incidence, including the dilational, thermal and shear potentials derived in Appendices A and B for both fluid and solid.

According to the conventional treatments (80,81) it is possible to expand the incident plane wave together with scattered and induced wave potentials, as solutions of the scalar Helmholtz equation, in cylindrical harmonics viz. writing $x = r \cos \theta$, $\kappa = \kappa_D^f \sin \varphi$, $\kappa_D^f = \kappa^f \cos \varphi$ and $\epsilon_n = \begin{cases} 1, & n=0 \\ 2, & n>0 \end{cases}$

$$\phi_i = \exp(ikz) \sum_{n=0}^{\infty} \epsilon_n i^n J_n(\kappa_D^f r) \cos(n\theta) \quad (3.122)$$

where the J_n are cylindrical Bessel functions of the first kind and order n , and the time dependence $\exp(-i\omega t)$ is understood.

The outgoing fluid scattered waves may similarly be written, further suppressing time dependence:

$$\left. \begin{aligned} \phi_D^f &= \exp(ikz) \sum_{n=0}^{\infty} A_n^f i^n H_n(\kappa_D^f r) \cos(n\theta) \\ \phi_{TH}^f &= \exp(ikz) \sum_{n=0}^{\infty} B_n^f i^n H_n(\kappa_{TH}^f r) \cos(n\theta) \\ \psi^f &= \exp(ikz) \sum_{n=0}^{\infty} C_n^f i^n H_n(\kappa_T^f r) \cos(n\theta) \\ \chi^f &= \exp(ikz) \sum_{n=0}^{\infty} D_n^f i^n H_n(\kappa_T^f r) \sin(n\theta) \end{aligned} \right\} (3.123)$$

where the H_n are Hankel functions of the first kind and order n (representing outgoing waves).

The induced solid wave potentials may also be written in expansions of cylindrical harmonics, again suppressing time dependence.

$$\left. \begin{aligned} \phi_D^s &= \exp(ikz) \sum_{n=0}^{\infty} A_n^s i^n J_n(\kappa_D^s r) \cos(n\theta) \\ \phi_{TH}^s &= \exp(ikz) \sum_{n=0}^{\infty} B_n^s i^n J_n(\kappa_{TH}^s r) \cos(n\theta) \\ \psi^s &= \exp(ikz) \sum_{n=0}^{\infty} C_n^s i^n J_n(\kappa_T^s r) \cos(n\theta) \\ \chi^s &= \exp(ikz) \sum_{n=0}^{\infty} D_n^s i^n J_n(\kappa_T^s r) \sin(n\theta) \end{aligned} \right\} (3.124)$$

where

$$\kappa_{TH}^f = \kappa_{TH}^f \cos \varphi_{TH}^f; \quad \kappa_T^f = \kappa_T^f \cos \theta^f;$$

$$\kappa_D^{1S} = \kappa_D^S \cos \phi_D^S ; \quad \kappa_{TH}^{1S} = \kappa_{TH}^S \cos \phi_{TH}^S ; \quad \kappa_T^{1S} = \kappa_T^S \cos \theta^S ;$$

and the z dependence of all the waves relates the scattered and refracted angles to the angle of incidence, assuming a "generalised Snell's law"⁽⁸⁵⁾ to hold viz. $\psi = \phi_D^f$;

$$\kappa = \kappa_D^f \sin \psi = \kappa_{TH}^f \sin \phi_{TH}^f = \kappa_T^f \sin \theta^f = \kappa_D^S \sin \phi_D^S = \kappa_{TH}^S \sin \phi_{TH}^S = \kappa_T^S \sin \theta^S \quad (3.125)$$

The expressions (3.123) and (3.124) introduce eight sets of unknown coefficients. However, there are 8 boundary conditions which may be applied at the surface ($r = R$) of the cylindrical fibre viz. continuity of pressure (three components), continuity of velocity (three components); continuity of temperature and continuity of heat flow.

3.13. Boundary conditions

3.131 Velocity (or displacement)

It is necessary to deduce the components of velocity \underline{v} of the fluid or displacement \underline{u} of the solid from the form

$$\left. \begin{matrix} \underline{v} \\ \underline{u} \end{matrix} \right\} = -\nabla \phi + \text{curl} \underline{A} \quad (\text{see Appendix A})$$

in cylindrical polars.

Now from (3.121) the particular case of cylindrical polars gives⁽⁸³⁾ $\omega(\xi_1) = 1$ and $\underline{a}_1 = \hat{z}$ (unit vector in the Z direction)

Thus the expression required for \underline{v} and \underline{u} is

$$\text{curl} \underline{A} = \text{curl} \text{curl} \left(\frac{\hat{z}}{r} \psi \right) + \frac{1}{\kappa_T} \text{curl} \text{curl} \text{curl} \left(\frac{\hat{z}}{r} \chi \right)$$

Calling upon the vector identities⁽⁸⁴⁾:-

$$\begin{aligned} \text{curl} \text{curl} () &= \text{grad} \text{div} () - \nabla^2 () \\ \text{div} (\phi \underline{a}) &= \phi \text{div} (\underline{a}) + (\text{grad} \phi) \cdot (\underline{a}) \\ \text{curl} (\phi \underline{a}) &= \phi \text{curl} (\underline{a}) + (\text{grad} \phi) \times (\underline{a}) \end{aligned}$$

and the scalar Helmholtz equations satisfied by ψ and χ viz:-

$$(\nabla^2 + \kappa_T^2) \begin{pmatrix} \psi \\ \chi \end{pmatrix} = 0$$

The expression for $\text{curl} \underline{A}$ can be transformed to

$$\text{curl} \underline{A} = \hat{r} \left[\frac{\partial^2 \psi}{\partial r \partial z} + \frac{\kappa_T}{r} \left(\frac{\partial \chi}{\partial \theta} \right) \right] + \hat{\theta} \left[\frac{1}{r} \frac{\partial^2 \psi}{\partial \theta \partial z} - \kappa_T \frac{\partial \chi}{\partial r} \right] + \hat{z} \left[\frac{\partial^2 \psi}{\partial z^2} + \kappa_T^2 \psi \right] \quad (3.1311)$$

Thus from (3.1311) and the expression for $\nabla(\)$ in cylindrical polars (84)

$$\nabla(\) = \hat{r} \frac{\partial}{\partial r}(\) + \frac{\hat{\theta}}{r} \frac{\partial}{\partial \theta}(\) + \hat{z} \frac{\partial}{\partial z}(\)$$

the components of fluid velocity or solid displacement may be written

$$\begin{aligned} r \text{ component} &= -\frac{\partial \phi}{\partial r} + \frac{\partial^2 \psi}{\partial z \partial r} + \frac{\kappa_r}{r} \frac{\partial \chi}{\partial \theta} \\ \theta \text{ component} &= -\frac{1}{r} \frac{\partial \phi}{\partial \theta} + \frac{1}{r} \frac{\partial^2 \psi}{\partial \theta \partial z} + \left(-\kappa_r \frac{\partial \chi}{\partial r} \right) \\ z \text{ component} &= -\frac{\partial \psi}{\partial z} + \frac{\partial^2 \psi}{\partial z^2} + \kappa_r^2 \psi \end{aligned} \quad (3.1312)$$

Substitution of the relevant potential expansions (3.123) and (3.124), where the solid fibre velocity components are given by the partial derivative w.r.t. time of the displacement components, and remembering that the total fluid field must include both scattered and incident potentials, then yields, for example, for continuity of r component of velocity $\left[v_r = \dot{u}_r \right]_{r=R} :-$

$$\begin{aligned} & -\exp(ikz) \left\{ \sum_{n=0}^{\infty} A_n^f i^n \kappa_D^f H_n'(k_D^f r) \cos(n\theta) + \sum_{n=0}^{\infty} B_n^f i^n \kappa_{TH}^f H_n'(k_{TH}^f r) \cos(n\theta) \right. \\ & \quad \left. + \sum_{n=0}^{\infty} C_n^f i^n \kappa_D^f J_n'(k_D^f r) \cos(n\theta) \right\}_{r=R} \\ & + ik \exp(ikz) \left\{ \sum_{n=0}^{\infty} C_n^f i^n \kappa_T^f H_n'(k_T^f r) \cos(n\theta) \right\}_{r=R} \\ & \quad + \frac{\kappa_{KT}}{r} \exp(ikz) \left\{ \sum_{n=0}^{\infty} D_n^f i^n H_n(k_T^f r) \cos(n\theta) \right\}_{r=R} \\ & = -i\omega \left[-\exp(ikz) \left\{ \sum_{n=0}^{\infty} A_n^s i^n \kappa_D^s J_n'(k_D^s r) \cos(n\theta) + \sum_{n=0}^{\infty} B_n^s i^n \kappa_{TH}^s J_n'(k_{TH}^s r) \cos(n\theta) \right\} \right]_{r=R} \\ & \quad - i\omega \left[ik \exp(ikz) \left\{ \sum_{n=0}^{\infty} C_n^s i^n \kappa_T^s J_n'(k_T^s r) \cos(n\theta) + \frac{\kappa_{KT}}{ikr} \sum_{n=0}^{\infty} D_n^s i^n J_n(k_T^s r) \cos(n\theta) \right\} \right]_{r=R} \end{aligned}$$

where the notation $R'_n(x) \equiv \frac{d}{dx} [R_n(x)]$ is understood for the cylindrical Bessel Functions.

This boundary condition may then be simplified by multiplication through with the factor:-

$$\frac{\epsilon_n R}{\pi} i^{(-n)} \exp(-ikz) \int_0^\pi \cos(m\theta)$$

such that the orthogonality of $\cos(m\theta)$ is invoked viz.

$$\int_0^\pi \cos(m\theta) \cos(n\theta) d\theta = \begin{cases} 0 & m \neq n \\ \pi/2 & m = n \neq 0 \\ \pi & m = n = 0 \end{cases}$$

This has the effect of picking out the $m = n$ terms. Similar factors may be used for simplification of the other boundary conditions: in particular the continuity of θ compt. of velocity and $r\theta$ compt. of stress require the corresponding orthogonal property of $\sin(m\theta)$.

$$\begin{aligned} \text{Introducing the notation } \kappa_D^f R &= a^f; \quad \kappa_{TH}^f R = b^f; \quad \kappa_T^f R = c^f; \\ \kappa_D^s R &= a^s; \quad \kappa_{TH}^s R = b^s; \quad \kappa_T^s R = c^s; \end{aligned}$$

The velocity boundary conditions finally yield the forms:-

$$\begin{aligned} -a^f [e_n J_n'(a^f) + A_n^f H_n'(a^f)] - b^f B_n^f H_n'(b^f) + ikc^f C_n^f H_n'(c^f) + n\kappa_T^f D_n^f H_n'(c^f) \\ = -iw \left\{ -a^s A_n^s J_n'(a^s) - b^s B_n^s J_n'(b^s) + ikc^s C_n^s J_n'(c^s) + n\kappa_T^s D_n^s J_n'(c^s) \right\} \end{aligned}$$

$$\begin{aligned} (3.1313) \quad n \left[e_n J_n(a^f) + A_n^f H_n(a^f) + B_n^f H_n(b^f) - ikC_n^f H_n(c^f) \right] - \kappa_T^f c^f D_n^f H_n'(c^f) \\ = -iw \left\{ n \left[A_n^s J_n(a^s) + B_n^s J_n(b^s) - ikC_n^s J_n(c^s) \right] - \kappa_T^s c^s D_n^s J_n'(c^s) \right\} \end{aligned}$$

$$\begin{aligned} -ik \left[e_n J_n(a^f) + A_n^f H_n(a^f) + B_n^f H_n(b^f) \right] + (\kappa_T^f - \kappa^2) C_n^f H_n(c^f) \\ = -i\omega \left[A_n^s J_n(a^s) + B_n^s J_n(b^s) \right] - i\omega (\kappa_T^s - \kappa^2) C_n^s J_n(c^s) \end{aligned}$$

3.132. Pressure and stress

from Appendix A, the total fluid stress may be written:-

$$P_{ij} = [2\mu^f \nabla^2 \phi + i\omega \rho_0^f \phi] \delta_{ij} + \mu^f \left(\frac{\partial v_i}{\partial x_j} + \frac{\partial v_j}{\partial x_i} \right)$$

and from Appendix B, the total solid stress is given by

$$\begin{aligned} \sigma_{ij} &= \lambda \operatorname{div} \underline{u} - \beta^s B^s (T - T_0) \delta_{ij} + \mu^s \left(\frac{\partial u_i}{\partial x_j} + \frac{\partial u_j}{\partial x_i} \right) \\ &= [2\mu^s \nabla^2 \phi + \rho^s \omega^2 \phi] \delta_{ij} + \mu^s \left(\frac{\partial u_i}{\partial x_j} + \frac{\partial u_j}{\partial x_i} \right) \end{aligned}$$

Further, from the expressions for the strain components in cylindrical polars, given in Appendix B, which apply equally well to the rate of strain components, where displacements are replaced by velocities for the fluid, it may be seen that:-

$$\begin{aligned} P_{rr} &= 2\mu^f \left\{ \frac{1}{r} \frac{\partial \phi}{\partial r} + \frac{1}{r^2} \frac{\partial^2 \phi}{\partial \theta^2} + \frac{\partial^2 \phi}{\partial z^2} + \frac{\partial^2 \phi}{\partial r \partial z} + \kappa_T^f \left(\frac{\partial^2 \chi^f}{\partial r \partial \theta} - \frac{1}{r} \frac{\partial \chi^f}{\partial \theta} \right) + \frac{\kappa_T^f}{2} \phi \right\} \\ (3.1321) \quad P_{r\theta} &= \mu^f \left\{ -2 \frac{\partial^2 \phi}{r \partial r \partial \theta} + 2 \frac{\partial^3 \phi}{r^2 \partial r \partial \theta^2} + 2 \frac{\partial \phi}{r^2 \partial \theta} - 2 \frac{\partial^2 \phi}{r^2 \partial \theta \partial z} + \kappa_T^f \left(\frac{1}{r} \frac{\partial \chi^f}{\partial r} - \frac{\partial^2 \chi^f}{\partial r^2} + \frac{1}{r^2} \frac{\partial^2 \chi^f}{\partial \theta^2} \right) \right\} \\ P_{rz} &= \mu^f \left\{ -2 \frac{\partial^2 \phi}{r \partial r \partial z} + 2 \frac{\partial^3 \phi}{r^2 \partial z^2} + \kappa_T^f \frac{\partial \chi^f}{\partial r} + \frac{\kappa_T^f}{r} \frac{\partial \chi^f}{\partial \theta \partial z} \right\} \end{aligned}$$

Also, identical forms for σ_{rr} , $\sigma_{r\theta}$, σ_{rz} exist, where the fluid potentials are replaced by corresponding solid potentials and the fluid constants are replaced by the relevant solid constants.

Use is made in each case of $\kappa_T^{f2} = \frac{i\omega \rho_0^f}{\mu^f}$; $\kappa_T^{s2} = \frac{\omega^2 \rho^s}{\mu^s}$ respectively.

Introducing the further notation $\kappa R = d^f$, the continuity of stress

at the fibre boundary gives, essentially by the procedure outlined in

3.131:-

$$\left[P_{rr} = \sigma_{rr} \right]_{r=R}$$

$$\mu^f \left\{ \begin{aligned} & \epsilon_n \left[a^f J_n'(a^f) + \left(\frac{c^f}{2} - d^f - n^2 \right) J_n(a^f) \right] + A_n^f \left[a^f H_n'(a^f) + \left(\frac{c^f}{2} - d^f - n^2 \right) H_n(a^f) \right] \\ & + B_n^f \left[b^f H_n'(b^f) + \left(\frac{c^f}{2} - d^f - n^2 \right) H_n(b^f) \right] + i k c^f C_n^f H_n''(c^f) + n \kappa_T^f D_n^f \left[c^f H_n'(c^f) - H_n(c^f) \right] \end{aligned} \right\}$$

$$= \mu^s \left\{ \begin{aligned} & A_n^s \left[a^s J_n'(a^s) + \left(\frac{c^s}{2} - d^s - n^2 \right) J_n(a^s) \right] + B_n^s \left[b^s J_n'(b^s) + \left(\frac{c^s}{2} - d^s - n^2 \right) J_n(b^s) \right] \\ & + i k c^s J_n''(c^s) C_n^s + n \kappa_T^s D_n^s \left[c^s J_n'(c^s) - J_n(c^s) \right] \end{aligned} \right\}$$

Further, from the expressions for the stress

$$\left[P_{r\theta} = \sigma_{r\theta} \right]_{r=R}$$

$$\mu^f \left\{ \begin{aligned} & n \left[\epsilon_n \left[a^f J_n'(a^f) - J_n(a^f) \right] + A_n^f \left[a^f H_n'(a^f) - H_n(a^f) \right] + B_n^f \left[b^f H_n'(b^f) - H_n(b^f) \right] \right. \\ & \quad \left. - i k C_n^f \left[c^f H_n'(c^f) - H_n(c^f) \right] \right. \\ & \quad \left. + \frac{D_n^f \kappa_T^f}{2} \left[c^f H_n'(c^f) - c^{f2} H_n''(c^f) - n^2 H_n(c^f) \right] \right\} \end{aligned} \right\}$$

3.1322

$$= \mu^s \left\{ \begin{aligned} & n \left[A_n^s \left[a^s J_n'(a^s) - J_n(a^s) \right] + B_n^s \left[b^s J_n'(b^s) - J_n(b^s) \right] - i k C_n^s \left[c^s J_n'(c^s) - J_n(c^s) \right] \right] \\ & \quad + \frac{D_n^s \kappa_T^s}{2} \left[c^s J_n'(c^s) - c^{s2} J_n''(c^s) - n^2 J_n(c^s) \right] \end{aligned} \right\}$$

$$\left[P_{rz} = \sigma_{rz} \right]_{r=R}$$

$$\mu^f \left\{ \begin{aligned} & -i k \left[\epsilon_n a^f J_n'(a^f) + A_n^f a^f H_n'(a^f) + B_n^f b^f H_n'(b^f) \right] + c^f C_n^f \left(\frac{\kappa_T^f}{2} - \kappa^2 \right) H_n'(c^f) \\ & \quad + i n \frac{\kappa_T^f}{2} D_n^f H_n(c^f) \end{aligned} \right\}$$

$$= \mu^s \left\{ \begin{aligned} & -i k A_n^s a^s J_n'(a^s) + B_n^s b^s J_n'(b^s) + c^s C_n^s \left(\frac{\kappa_T^s}{2} - \kappa^2 \right) J_n'(c^s) + i n \frac{\kappa_T^s}{2} D_n^s J_n(c^s) \end{aligned} \right\}$$

3.133. Temperature and Heat flow

From Appendix A, the following expression for the temperature variation within the fluid holds:-

$$T^f = f(\phi_i + \phi_D^f) + F\phi_{TH}^f$$

where $f = \gamma \left[\omega^2 - \kappa_D^f \left(\frac{c_0^f}{\gamma} - i\omega N^f \right) \right] (\beta c_0^f i\omega)^{-1}$

and $F = \gamma \left[\omega^2 - \kappa_{TH}^f \left(\frac{c_0^f}{\gamma} - i\omega N^f \right) \right] (\beta c_0^f i\omega)^{-1}$

which from eqn (A.20) $\sim -(\beta \sigma^f)^{-1}$ neglecting small quantities $\frac{i\omega \delta}{\beta c_0^f}, \frac{i\omega N^f}{\beta c_0^f}$ compared with $(\beta \sigma^f)^{-1}$

Further, from Appendix B, for the solid

$$T^s = -G\phi_{TH}^s$$

where $G \sim -\frac{i\omega \rho^s}{\beta^s \sigma^s} \left(i\omega \rho^s + \frac{N^s}{\sigma^s} \right)$ on the assumption that $\delta^s \sim 1$ and $N^s = c_0^s \delta^s$

Thus temperature continuity at the fibre surface gives

$$f \left[\epsilon_n J_n(a^f) + A_n^f H_n(a^f) \right] + F B_n^f H_n(b^f) = -G B_n^s J_n(b^s) \quad (3.1331)$$

and continuity of heat flow viz. $\left[\kappa^f \frac{\partial T^f}{\partial r} = \kappa^s \frac{\partial T^s}{\partial r} \right]_{r=R}$ gives

$$\kappa^f \left\{ f a^f \left[\epsilon_n J_n'(a^f) + A_n^f H_n'(a^f) \right] + F b^f B_n^f H_n'(b^f) \right\} = -\kappa^s G b^s B_n^s J_n'(b^s) \quad (3.1332)$$

From the eight boundary conditions (3.1313), (3.1322), (3.1331) and (3.1332) the coefficients A_n^f required (see Appendix E) for attenuation calculations, for normal or oblique incidence, may be calculated (see Appendix C), showing their dependence on fluid and fibre properties (Appendix D).

3.2. Attenuation due to a single cylindrical scatterer

From Appendix E, the energy loss per scatterer per unit time is given by

$$W = -2\omega \rho_0^f L \operatorname{Re} (A_0^f + A_1^f)$$

for a normally incident plane wave, for which the energy carried per unit time through unit area normal to its direction may be written $(46, 47) \frac{1}{2} \omega \rho_0^f \kappa_b^f = E_0$

Thus a "dissipation cross section" (σ), for each unit length of cylindrical scatterer parallel to the incident wave front may be defined by

$$\sigma = \frac{W}{E_0 L} = -\frac{4}{k_D^f} \operatorname{Re}(A_0^f + A_1^f) \quad (3.21)$$

Chapter 4 ABSORPTION OF A NORMALLY INCIDENT PLANE SOUND WAVE BY A FIBROUS BLOCK, BACKED BY A RIGID PLANE.

In the discussion of chapters 1 and 2 it is suggested that a model for the fibrous block similar to that used by Kawasima⁽²⁷⁾ may be chosen. In particular, if the block is regarded as a region of space (imbedding fluid) containing an array of parallel fibres, which are completely separate and free to move in the incident field, a scattering approach is suitable. This approach may be based on either the single scattering technique associated with model 7 or the multiple scattering techniques used with model 8.

The special circumstance of a rigid plane backing is also considered in order to correspond with the physical situation of impedance tube measurement.

4.1. Single Scattering Theory

4.1.1 Attenuation constant

Each fibre is considered to be a right circular cylinder, so that the analysis of chapter 3 applies.

If the wave incident on each fibre is assumed to be identical with that incident on the block surface and all the fibres are assumed parallel, then the total energy removed from the incident wave front by scattering, per unit volume of the fibre block is (NW) , i.e. the product of the average number of fibres crossing unit area normal to their axes and the time average of the overall energy loss throughout a volume that is large compared with the decrement distance of the thermal and viscous waves (Appendix E). Thus, if E represents the time averaged energy flux, then the energy loss during traversal of thickness element dx of the block is given by

$$dE = -Nw dx = -N\sigma E_0 dx \quad (\text{from Appendix E and 3.2})$$

where x is the direction of propagation of the incident wave front.

The solution of this is

$$E = E_0 \exp(-N\sigma x)$$

and hence $N\sigma$ may be regarded as the attenuation coefficient of the medium.

Writing $\psi = A \exp(i k_b x - \omega t)$ to represent the internal field potential for

the model, with bulk propagation constant, $k_b = a + ib$

the form of b may be deduced i.e.

$$b = \frac{N\sigma}{2} \quad (4.1.1)$$

since

$$E \propto |\psi|^2$$

It may be noted^(4.9b) that this definition of b , includes only the effects of conversion of the incident plane wave into viscous and thermal waves at the fibre boundaries.

To be complete other effects, mentioned in 1.72, should be included. Of these, the dissipation due to normal wave motion within the imbedding fluid has already been neglected in the derivation of W , by assuming κ_p^f to be real.

Further, the time averaged power loss identifiable with the conversion of the incident plane wave into cylindrical scattered dilatational waves at the fibre boundaries, under Rayleigh scattering conditions may also be neglected, as follows:-

The time averaged power per unit length of scatterer, carried out (through surface F , of a large volume V surrounding the scatterer) by the scattered dilatational wave can be shown to be given by

$$\frac{1}{T} \left\{ \frac{1}{2} \operatorname{Re} \int_F [\langle P_{Nj}^* v_j \rangle_{Av.}]_{\text{Scattered Wave}} dF \right\}$$

The process of integration used previously in Appendix E, then gives the following expression for this term:-

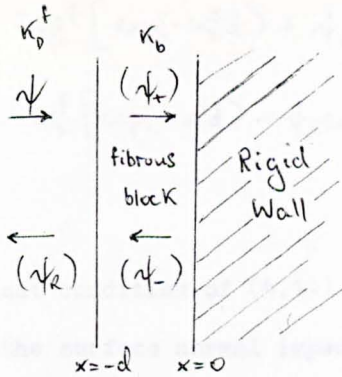
$$\frac{1}{2} \operatorname{Re} \left\{ 4\omega\rho_0^f \sum_{n=0}^{\infty} A_n^f A_n^{f*} \right\} \quad (4.1.2)$$

This expression is of the same order as the second term of W (E.10) and thus may be neglected by the argument of Appendix (E.3). As remarked by Epstein⁽⁴⁵⁾, this wave conversion will not anyway, represent energy "loss" in reverberation measurements, since the energy re-enters the enclosure.

It should be mentioned that the similarity of the expression for the scattered energy above, and that for the total energy loss in the region surrounding a scatterer, given by E.1. of Appendix E, is fortuitous. The latter has considered viscous and thermal dissipation throughout a volume, and develops (Epstein and Carhart) to the form E.1. only after some manipulation. The "Rayleigh Scattering" expression above is a first statement of the scattered energy carried across a surface. The subsequent evaluations of these expressions must differ since the dissipation integral includes both incident and scattered dilational potentials (ϕ_i and ϕ_D^f), whilst with the scattering integral ϕ_D^f alone is involved.

4.12 Surface normal impedance

For a single scatterer therefore σ (3.21) represents the main part of the dissipation of energy from the incident beam.



From the above argument the single scattering model, predicts dissipation as in (4.11). As a first approximation this may be considered as the only effect of the presence of the fibres on the properties of the imbedding medium.

Thus, in the following simple analytic treatment, the fibre block is replaced by a homogeneous attenuating medium having a propagation constant given by

$$k_b = k_b^f + \frac{iN\sigma}{2} \quad (4.1.3)$$

Assuming the forms $\psi = \exp(ik_b^f x) \exp(-i\omega t)$ for the incident wave
 $\psi_r \exp(-ik_b^f x) \exp(-i\omega t)$ for the reflected wave
 $\psi_+ \exp(ik_b x) \exp(-i\omega t)$ for the forward wave
 $\psi_- \exp(-ik_b x) \exp(-i\omega t)$ for the backward wave }
 inside the slab,

the latter pair assume the field inside the fibrous block to be plane and compressional.

Writing $\bar{\psi}$ for the total field potential at any point, the pressure and velocity along the +ve direction are given at any point by

$$P_{xx} = i\omega\rho_0^f \bar{\psi}$$

$$v_x = -\frac{\partial \bar{\psi}}{\partial x}$$

and the boundary conditions of continuity of normal pressure and velocity at $x = -d$ and zero velocity at $x = 0$, necessary for the "impedance tube" situation are given by

$$\begin{aligned}
 i\omega\rho_0^f \left[\exp(-i\kappa_b^f d) + \psi_R \exp(i\kappa_b^f d) \right] &= i\omega\rho_b \left[\psi_+ \exp(-i\kappa_b d) \right. \\
 &\quad \left. + \psi_- \exp(i\kappa_b d) \right] \\
 -i\kappa_b^f \left[\exp(-i\kappa_b^f d) - \psi_R \exp(i\kappa_b^f d) \right] &= -i\kappa_b \left[\psi_+ \exp(-i\kappa_b d) \right. \\
 &\quad \left. - \psi_- \exp(i\kappa_b d) \right]
 \end{aligned}
 \quad (4.1.4)$$

$$0 = -i\kappa_b [\psi_+ - \psi_-]$$

The last condition of (4.1.4) gives $\psi_+ = \psi_-$

Thus the surface normal impedance,

$$\begin{aligned}
 Z_n &= - \left. \frac{P_{xx}}{v_x} \right|_{x=-d} \\
 &= \frac{\omega\rho_0^f}{\kappa_b^f} \left\{ \frac{\exp(-i\kappa_b^f d) + \psi_R \exp(i\kappa_b^f d)}{\exp(-i\kappa_b^f d) - \psi_R \exp(i\kappa_b^f d)} \right\} \\
 &= \frac{\omega\rho_b}{\kappa_b} \left\{ \frac{\psi_+ \exp(-i\kappa_b d) + \psi_- \exp(i\kappa_b d)}{\psi_+ \exp(-i\kappa_b d) - \psi_- \exp(i\kappa_b d)} \right\}
 \end{aligned}$$

may be written

$$Z_n = \beta_0 c_b \left\{ \frac{1 + \exp(2i\kappa_b d)}{1 - \exp(2i\kappa_b d)} \right\} \quad (4.1.5)$$

where $c_b = \frac{\omega}{\kappa_b}$ is the complex velocity of sound waves in the bulk medium.

Writing $Z_n = \Gamma_n + i\alpha_n$

the normal incidence absorption coefficient is related to these expressions by (91)

$$a_0 = \frac{4 \Gamma_n \rho_0^f c_D^f}{(\Gamma_n + \rho_0^f c_D^f)^2 + \alpha_n^2}$$

where Γ_n and α_n derive from (4.1.5)

4.2 Multiple scattering theory

The single scattering approach previously detailed enables arrangement of the fibres obliquely to the surface of the block to be considered as the scattering coefficients used in σ may be made appropriate to either normal or oblique incidence conditions. Further, distributions of variously

inclined fibres may also be considered, requiring only that N_{ν} be replaced by an appropriate summation viz $\sum_{\alpha} N_{\alpha} \sigma_{\alpha}$, where N_{α} is the no. of (parallel) fibres inclined at angle α to the block surface (per unit volume of the block) and σ_{α} is the scattering cross section of these fibres employing the relevant oblique incidence scattering coefficients.

These straightforward relations together with (4.1.3) are only possible however if the interactions, between the various scattered compressional waves inside the block, are neglected. - 4.1.5)

Restricting, for the moment, the problem to one of normal incidence on a block containing fibres parallel to the block surface, the single scattering theory may be improved upon by using the first formalism of Twersky⁽⁵⁴⁾.

By this approach forward and backward plane waves representing the block's internal field are derived as integral summations of the forward and backward scattered waves within the relevant scattering region.

4.21 Single scattering amplitude

Initially, it is necessary to derive the single scattering amplitude of interest i.e. for a cylindrical fibre, in the form used by Twersky⁽⁵⁴⁾. Considering only normal incidence, the scattered dilational wave from any fibre is given by:-

$$\phi_D^f = \sum_{n=0}^{\infty} A_n^f i_n H_n(k_D^f r) \cos(n\theta)$$

At large r , the asymptotic form of the Hankel function (Appendix E) may be used viz.

$$H_n(k_D^f r) \sim \left(\frac{2}{\pi k_D^f r} \right)^{\frac{1}{2}} \exp \left[i k_D^f r - \frac{i\pi}{2} \left(n + \frac{1}{2} \right) \right]$$

$$= \left(\frac{2}{i\pi k_D^f r} \right)^{\frac{1}{2}} \exp(ik_D^f r) \frac{1}{i^n}$$

since $e^{-\frac{1}{2}i n \pi} = \left(e^{-\frac{i\pi}{2}} \right)^n = \frac{1}{i^n}$ and $e^{-\frac{i\pi}{4}} = i^{-\frac{1}{2}}$

Thus the far field form of ϕ_D^f is

$$\left(\frac{2}{i\pi k_D^f r} \right)^{\frac{1}{2}} \exp(ik_D^f r) \sum_{n=0}^{\infty} A_n^f \cos(n\theta) \quad (4.2.1)$$

In general, Twersky⁽⁵⁴⁾ (eqn. (2.7) p. 702) gives this far field form as

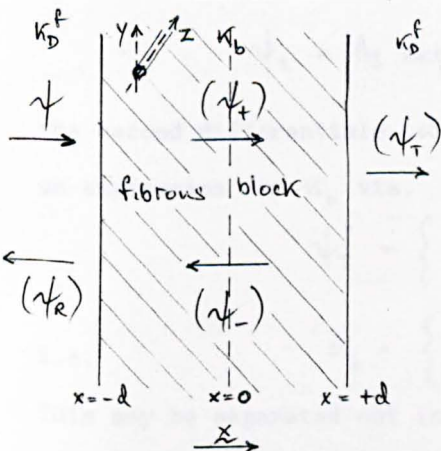
$$\mathcal{H}(k_D^f r) g(\varrho, \xi) \quad (4.2.2)$$

where $\mathcal{H}(k_D^f r) = \left(\frac{2}{i\pi k_D^f r} \right)^{\frac{1}{2}} \exp(ik_D^f r)$ and $g(\varrho, \xi) = g(\theta)$,

θ being the angle between the direction of incidence and observation

Comparing 4.2.1 and 4.2.2. $g(\theta) = \sum_{n=0}^{\infty} A_n^f \cos(n\theta) \quad (4.2.3)$

4.2.2. Internal field



Now, considering the general transmission case for the fibrous block, as shown, the forward and backward waves within the slab may be taken directly from equations (3.1) of Twersky⁽⁵⁴⁾ with suitable limit modifications viz.

$$(4.2.4) \quad \begin{cases} \psi_+(-d, x) = \exp(ik_b^f x) \left\{ 1 + \int_{-d}^x \exp(-ik_b^f \gamma) [C_g \psi_+(-d, \gamma) + C_g' \psi_-(\gamma, d)] d\gamma \right\} \\ \psi_-(x, d) = \exp(-ik_b^f x) \int_x^d \exp(ik_b^f \gamma) [C_g' \psi_+(-d, \gamma) + C_g \psi_-(\gamma, d)] d\gamma \end{cases}$$

(time dependence understood)

where, for normal incidence, and cylindrical scatterers, from (4.2.3)

$$\begin{aligned} g &= g(0) = \sum_n A_n^f \\ g' &= g(\pi) = \sum_n (-1)^n A_n^f \\ c &= \frac{2N}{k_b^f} \end{aligned}$$

(and the axes chosen here differ from Twersky's⁽⁵⁴⁾ i.e. $\frac{z}{\lambda}$ chosen to lie along the fibre axes, and x is as shown).

The total internal field $\psi_{\pm} = \psi_+ + \psi_-$, now represents a multiple scattering process in the imbedding fluid, the field at any fibre at point x inside the fibre block, being assumed to consist of contributions from the incident plane wave; the backward scattered waves from fibres beyond x ; and forward scattered waves from fibres in front of x .

4.2.3 Bulk propagation constant

If a bulk propagation constant k_b is now attributed to the scattering region, so that the internal waves may be written in the alternative form

$$\psi_{\pm} = A_{\pm} \exp(ik_b x) + B_{\pm} \exp(-ik_b x) \quad (4.2.5)$$

the second differentials (w.r.t. x) of (4.2.4) and (4.2.5) give together an expression for k_b viz.

$$\psi_{\pm}'' = \left\{ (ik_b^f + c_g)^2 - c^2 g^{12} \right\} \psi_{\pm} = -k_b^2 \psi_{\pm}$$

i.e.

$$k_b = \left\{ k_b^{f2} - 2ik_b^f c_g + c^2 (g^{12} - g^2) \right\}^{\frac{1}{2}} \quad (4.2.6)$$

This may be separated out into real and imaginary components a and b viz.

$$a = \left\{ \frac{1}{2} \left[A \pm (A^2 + B^2)^{\frac{1}{2}} \right] \right\}^{\frac{1}{2}}$$

$$b = \frac{B}{2a}$$

where $A \approx \kappa_0^{f2} + 4 \text{Im} N g - c^2 [\text{Re} A_1^f \text{Re} A_0^f - \text{Im} A_1^f \text{Im} A_0^f]$

and $B \approx -4 \text{Re} N g - c^2 [\text{Re} A_0^f \text{Im} A_1^f + \text{Im} A_0^f \text{Re} A_1^f]$

g and g^i here are taken to have approximate values,

$$g \sim A_0^f + A_1^f$$

$$g^i \sim A_0^f - A_1^f$$

which are consistent with the approximation of E.11.

4.2.4 Low concentrations

When C_g and C_g^1 are very small and can be neglected above first order,

$$\kappa_b^2 \approx \kappa_0^{f2} - 2i C_g \kappa_0^f$$

i.e. $\kappa_b \approx \kappa_0^f - \frac{2i N g}{\kappa_0^f}$ (4.2.7)

where use has been made of the Binomial expansion.

This situation corresponds to very sparse concentrations where the effect of multiple scattering is likely to be small. (4.2.7) indicates an attenuation constant given by $-\frac{2N}{\kappa_0^f} \text{Re} g$. This corresponds to (4.1.1), again if the A_n^f are small and may be neglected above first order.

However, it should be noted that the real part of κ_b in (4.2.7) i.e. the phase constant, is given by

$$a = \kappa_0^f + \frac{2N}{\kappa_0^f} \text{Im} g \quad (4.2.8)$$

This does not correspond to the assumption of the small perturbation theory in 4.1 i.e. the single scattering theory does not completely correspond to the low concentration situation as predicted by the multiple scattering theory.

Thus the multiple scattering theory predicts a change in phase as well as attenuation of the incident fluid wave.

4.2.5 Surface normal impedance

The coefficients introduced in equation (4.2.5) may be evaluated, for the fibrous block situation of interest, by using boundary conditions corresponding to the two dimensional forms of Twersky⁽⁵⁴⁾ modified for normal incidence and scatterers symmetrical to reflection in the surface(s) of the slab viz.

$$\left. \begin{aligned} A_- &= -QA_+ \\ B_+ &= -QB_- \\ A_+ e^{-ik_b d} + B_+ e^{ik_b d} &= e^{-ik_b^f d} \\ A_- e^{ik_b d} + B_- e^{-ik_b d} &= 0 \end{aligned} \right\} \quad (4.2.9)$$

where

$$Q = c_g^f / (ik_b^f + c_g + ik_b)$$

The first two equations of (4.2.9) are given by direct substitution of (4.2.5) into the first derivative of (4.2.4), namely,

$$\psi_{\pm}' = \pm (ik_b^f + c_g) \psi_{\pm} \pm c_g^f \psi_{\mp}$$

The third equation requires that the forward travelling wave at the surface ($x = -d$) of the slab must be the incident wave at the plane. Finally the fourth equation of (4.2.9) represents the requirement that the backward travelling wave must cease to exist at the surface $x = +d$.

(4.2.9) may be solved for A_{\pm} and the results substituted in the expression for the total internal field to give

$$\psi_I = \psi_+ + \psi_- = D(1-Q) \exp(i(k_b - k_b^f)d) [e^{ik_b x} + Q e^{ik_b(2d-x)}]$$

where

$$D = [1 - Q^2 e^{4ik_b d}]^{-1}$$

Similarly, the reflected wave amplitude is given by

$$(4.2.10) \quad [\psi_R \exp(-ik_b^f x)]_{x=-d} = \psi_-(-d, d)$$

$$(4.2.10) \quad \text{i.e.} \quad \psi_R = -Q \exp(-2i\kappa_b^t d) [1 - e^{4i\kappa_b^t d}] \mathcal{D}$$

and the transmitted wave amplitude by

$$\begin{aligned} [\psi_T \exp(i\kappa_b^t x)]_{x=d} &= \psi_+(-d, d) \\ \psi_T &= (1-Q^2) \exp[i(\kappa_b - \kappa_b^t)d] \mathcal{D} \end{aligned}$$

If now the impedance tube situation is considered, by replacing the part of the slab $0 \leq x \leq d$ by a rigid medium, providing a rigid plane at $x=0$, the method of images may be invoked to compute the new internal and reflected fields.

For a wave $\phi' = \exp(-i\kappa_b^t x)$, (the image of $\phi = \exp(i\kappa_b^t x)$), incident on the surface $x=-d$ of the slab, the new internal waves may be written

$$\underline{\psi}_\pm = A_\pm \exp(-i\kappa_b x) + B_\pm \exp(i\kappa_b x) \quad (4.2.11)$$

It is easily seen that the boundary conditions (4.2.9) are unchanged i.e. the A_\pm, B_\pm are identical for both ϕ and ϕ' incident. Thus the new internal wave potential $\underline{\psi}_I$ and the new reflected wave and transmitted wave amplitudes, $\underline{\psi}_R$ and $\underline{\psi}_T$ are given by replacing x by $-x$ in the expressions of (4.2.10).

The method of images requires that the total internal and reflected field potentials ($\underline{\phi}_I$ and $\underline{\phi}_R$) for the impedance tube situation previously referred to, should be given by

$$\underline{\phi}_I = \psi_I + \underline{\psi}_I$$

and

$$\underline{\phi}_R = (\psi_R + \underline{\psi}_T) \exp(-i\kappa_b^t x)$$

Thus $\underline{\phi}_I = \mathcal{D}(1-Q) [\exp i(\kappa_b - \kappa_b^t)d] [e^{i\kappa_b x} + Q e^{i(2d-x)\kappa_b} + e^{-i\kappa_b x} + Q e^{i\kappa_b(2d+x)}]$

i.e. substituting for D

$$\bar{\Phi}_I = \frac{(1-Q)e^{i(\kappa_b - \kappa_b^f)d} \{ e^{i\kappa_b x} + e^{-i\kappa_b x} \}}{(1 - Qe^{2i\kappa_b d})} \quad (4.2.12)$$

Similarly

$$\bar{\Phi}_R = - \frac{e^{-2i\kappa_b^f d} [Q - e^{2i\kappa_b d}] e^{-i\kappa_b^f x}}{(1 - Qe^{2i\kappa_b d})} \quad (4.2.13)$$

At this point, it is necessary to note that in the notation of Twersky⁽⁵⁴⁾, which has been used here, the wave potentials ψ, ϕ etc. correspond to acoustic pressure and not to acoustic velocity as required in Chapter 3 and 4.2.

The potentials can be transformed by

$$\bar{\Phi}_p = i\omega\rho\bar{\Phi}_v = \text{pressure}$$

and

$$-\frac{1}{i\omega\rho} \frac{\partial \bar{\Phi}_p}{\partial x} = -\frac{\partial \bar{\Phi}_v}{\partial x} = \text{velocity}$$

where $\bar{\Phi}_p$ refers to the potentials so far used in 4.2, and $\bar{\Phi}_v$ to the potentials required.

The surface normal impedance for the layer $-d \leq x \leq 0$ now follows from $z_n = \frac{-P_{xx}}{v_x}$ at $x = -d$ as in 4.1. The total potential required for calculation of P_{xx} and v_x may be taken to be either $\phi + \bar{\Phi}_R$ or $\bar{\Phi}_I$.

Thus

$$z_n = \frac{\frac{i\omega\rho_0^f}{\kappa_b^f} \left\{ \exp(-i\kappa_b^f d) - \frac{\exp(-i\kappa_b^f d)(Q - e^{2i\kappa_b d})}{(1 - Qe^{2i\kappa_b d})} \right\}}{\left\{ \exp(-i\kappa_b^f d) + \exp(-i\kappa_b^f d) \left[\frac{Q - e^{2i\kappa_b d}}{1 - Qe^{2i\kappa_b d}} \right] \right\}}$$

i.e.

$$z_n = \rho_0^f c_b^f \frac{(1-Q)}{(1+Q)} \left\{ \frac{1 + \exp(2i\kappa_b d)}{1 - \exp(2i\kappa_b d)} \right\} \quad (4.2.14)$$

This expression corresponds to (4.1.5) if $\left(\frac{1-Q}{1+Q}\right)$ may be taken to be the relative characteristic impedance of the material on a multiple scattering theory viz. if

$$\frac{\rho_b c_b}{\rho_0^f c_0^f} = \left(\frac{1-Q}{1+Q}\right) \quad (4.2.15)$$

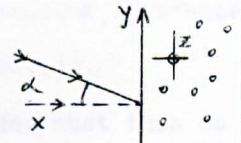
Thus using a multiple scattering theory on an idealised model, the fibrous block is shown to behave like a homogeneous medium, having a propagation constant κ_b given by (4.2.6) and a bulk density given by

$$\rho_b = \frac{\rho_0^f c_0^f}{c_b} \frac{(1-Q)}{(1+Q)}$$

i.e. substituting for Q and using the approximate form for g and g'

$$\rho_b = \frac{\rho_0^f \kappa_b (i\kappa_b^f + 2A_1^f c + i\kappa_b)}{\kappa_b^f (i\kappa_b^f + 2A_0^f c + i\kappa_b)} \quad (4.2.16)$$

The expression (4.2.15) is derived by Twersky⁽⁵⁴⁾ for the case of a slab region of scatterers $0 \leq x \leq d$ bounded by an infinite fluid. It can be seen that the conditions (4.2.9) replace, effectively in the multiple scattering case, the boundary conditions (4.1.4) for the single scattering case.



4.2.6. Oblique Incidence

The multiple scattering theory has, thus far, been restricted to normal incidence on the fibrous block. Twersky's⁽⁵⁴⁾ theory, however, allows more generally for arbitrary incidence.

(i) Oblique incidence in the xy plane

For this situation, the incident plane wave front is still normally incident on fibres with their axes running parallel to the z axis.

The forms of g and g' are therefore unaffected, and the only result of the oblique incidence is to introduce a phase dependence along the fibrous block surface normal to the x direction (parallel to the y direction). This alters the expressions both for the propagation constant

in the scattering region and for the effective relative characteristic impedance.

These are now given by

$$\kappa_b^2 = \kappa_b^{f2} - 4 \sin \alpha + \left(\frac{2N}{\kappa_b^f \cos \alpha} \right)^2 (g^{i2} - g^2) \quad (4.2.17)$$

and

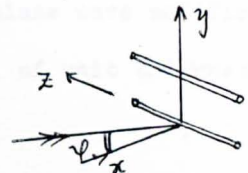
$$Z_{rel} = \frac{\beta_b c_b}{\rho_b^f c_b^f} = \frac{i \kappa_b^f \sin \alpha + C (g - g') + i \kappa_b}{i \kappa_b^f \sin \alpha + C (g + g') + i \kappa_b} \quad (4.2.18)$$

where

$$C = \frac{2N}{\kappa_b^f \cos \alpha} \quad (4.2.19)$$

for incidence at angle α in the xy plane.

(ii) Oblique incidence in the xz plane



For fibres with their axes parallel to the z axis oblique incidence in the xz plane will introduce a phase dependence along them according to the general theory of Chapter 3.

Thus g and g^1 must be calculated from the oblique incidence scattering coefficients A_o^f and A_i^f given in (C.1.1).

The alteration in these scattering amplitudes must then be superimposed on the expressions corresponding to (4.2.17) and (4.2.18) to give the relevant κ_b and Z_{rel} .

(iii) Departure from continuum behaviour

Both situations (i) and (ii) would indicate that the behaviour of the idealised model used for the multiple scattering theory, departs considerably from that of a continuum slab, when the angle of incidence of the incident plane wave is varied.

This follows from the fact that both the propagation constant and the relative characteristic impedance attributable to the model vary with the angle of incidence of incident sound.

A behaviour such as this is possibly to be expected in a model which allows the incident wave to penetrate, gradually altering in phase and amplitude, the internal incoherent field represented by $\overline{\Psi}_I$ being a limiting state.

This penetration can easily be seen from the simplified situation corresponding to small N (as in 4.2.7 and using 4.2.19) giving from Twersky⁽⁵⁴⁾ p. 708

$$\kappa_b \approx \kappa_b^t \cos \alpha - i c_g$$

i.e. the propagation constant is that of the incident plane wave modified in phase and amplitude by a single-scattering traversal of unit thickness of the material.

It is to be expected that the behaviour of actual fibrous blocks will differ from that of continuum materials to the extent that the blocks correspond to the idealised model used.

CHAPTER 5ABSORPTION MEASUREMENTS AND THEORETICAL RESULTS5.1. Experimental Procedure5.1.1. Absorption Coefficient

The absorption coefficient i.e. the fraction of incident sound energy absorbed, is the parameter of greatest practical significance in assessing the performance of absorbing materials in various situations.

In order to substantiate the theory developed in Chapter 4, the impedance tube method of measurement was used to obtain normal incidence absorption coefficients for several fibre glass materials.

5.1.2. Standing Wave Method

This method of measurement which requires relatively small samples of material, probes the sound field, generated at discrete frequencies within a closed tube. The sample, cut into the shape of a disc, is positioned at one end of the tube.

From the standard theory^(93, 95), the ratio of the magnitudes of the pressure maxima and minima, corresponding to the "pseudo"⁽⁹⁵⁾ standing wave pattern's nodes and antinodes, may be used to calculate the normal incidence absorption coefficient a_o :-

$$a_o = \frac{4}{n + \frac{1}{n} + 2} \quad \text{where } n = \frac{P_{MAX}}{P_{MIN}}$$

5.1.3. Materials

Samples of glass fibre quilt, (as specified in Appendix F); in layers of 2.54 cm and 5.08 cm thickness and 3 cm. and 10 cm. diameter, circular cross-section, were tested. The various bulk densities were computed by weighing a known volume of each of the sample types. The weight of the

enclosed volume of air was not taken into account, for the purpose of the theoretical calculation (Appendix D).

5.1.4. Apparatus

Use was made of the Bruel and Kjaer (B & K) Standing Wave Apparatus (Type 4002).

Basically this apparatus includes:

- (i) a large tube of internal diameter 10 cm which was found to be applicable in the frequency range 300 Hz - 1800 Hz
- (ii) a smaller tube of internal diameter 3 cm., applicable in the frequency range 1800 Hz - 6000 Hz.
- (iii) sample holders of appropriate and adjustable size.
- (iv) a speaker with a cone approximately 10 cm. diameter.
- (v) a condenser microphone with a wheeled carriage and probe tube attachments.

The speaker was driven by a B & K Beat Frequency Oscillator (Type 1022) and the microphone was connected to a B & K Frequency Analyser (Type 2107) used as an amplifier.

5.1.5. Errors

Values for the normal incidence absorption coefficients were read directly from the calibrated scales on the B & K Frequency Analyser. This procedure requires corrections for air-absorption and non-rigidity of the tube walls and terminations.

Further inaccuracies are introduced due to:

- (a) the small disturbance on the standing wave pattern in the tube caused by the geometrical shape of the ^{probe} tube (93, 94).
- (b) the non-infinitely high impedance of the probe tube opening.
- (c) the contradictory requirements for flexible, fibrous materials, of
- (i) an airtight sample fit
- and
- (ii) avoidance of a situation in which the impedance tube walls hamper the vibration of the materials constituent fibres by compression.
- (d) the non-plane and non-vertical front surfaces of the samples used
- (e) the leakages and resonances in the system e.g. the leakage around the probe tube channel passing through the speaker cone.
- (f) the possibility of the wavefronts, generated by the speaker, differing from plane wavefronts at the surface of the samples: this is a large problem when transverse modes are excited (93, 94).

5.1.6. Alternative Methods

Kosten and Janssen⁽²²⁾ review a method in which the whole tube is filled with circular discs of the material, each disc containing a triangular notch in its centre, to allow the passage of the probe tube. This allows the direct measurement of the characteristic impedance of the material, which is another quantity of interest. Furthermore, the problem of sample fit, in the standard method, is substantially reduced. Another method suggested by Taylor⁽⁹⁶⁾, dispenses with the probe tube, and hence the error of 5.1.5(a). The method uses a microphone diaphragm, as one end of the tube, and a piston which can be used to alter the effective length of the tube, as the other end.

However, the standard method used was considered adequate for observing the variation with fibre radius, slab density and slab thickness of the frequency dependant material absorptions. Further, the results of measurement are sufficiently accurate for comparison with the scattering theory predictions.

5.2. Comparison of calculated and measured absorption coefficients

The measured absorption-frequency characteristics are shown in graphs 1 and 2. Some of the calculated characteristics are plotted for comparison in graphs 3-7.

5.2.1. Low frequency discrepancy

The absorption-frequency characteristics calculated for the free fibre model have the same general shape as those measured for the relevant materials. However, it can be seen from graphs 3-5 that considerable differences in coefficient magnitudes exist at low frequencies. This discrepancy is greater (graphs 3 and 5c) for the 2.54 cm. layers than for the 5.08 cm. layers (graphs 4, 5a and 5b). Further for the latter thickness, better correlation is obtained the less dense the material considered.

5.2.2. Dependence on assumed fibre radius

The respective (average) fibre radii for the Rocksil materials and the Rocksil-K (resin bonded) materials are given to be 5μ (microns) and 3μ respectively. Therefore the computer programs were designed (Appendix D) to output a_0 values for both radii (for the same values of the other variables).

As may be seen from graphs 5a, 5b and 5c the multiple scattering calculation for the free fibre model is sensitive to the assumed fibre radius; however, greatest correlation is obtained by taking $R = 5$ microns for the Rocksil-K materials. The correlation is better, the thicker the layer considered.

5.2.3. Dependence on slab density and thickness

The calculated absorption characteristics show the expected improvement with increased thickness from 2.54 cm to 5.08 cm.

The improvement in absorption with slab density for 2.54 cm. layers (graph 1) is obtained with the calculated curves, if $R = 5$ microns is used for the Rocksil-K materials (graph 6). The measured curves for the 5.08 cm. layers show an inversion of the rank ordering according to density in the range 1250 Hz - 2500 Hz (graph 2). A similar inversion is observed in the calculated curves but (using $R = 3$ microns for the Rocksil-K materials) in a lower range viz. 600 - 1600 Hz (graph 7).

CHAPTER 6DISCUSSION OF RESULTS AND CONCLUSIONS6.1. Comparison of single scattering (SS) and multiple scattering (MS) theories6.1.1. Attenuation

The SS form of the attenuation constant - frequency characteristic for a particular density of fibres on the free fibre model (graph 9) is similar to that obtained by Epstein and Carhart⁽⁴⁶⁾ and Chow⁽⁴⁷⁾, for aerosols.

This indicates that with a scattering theory applied both to the fibre model and to a suspension of liquid droplets, neither the geometry nor the concentration of scatterers seriously alters the frequency dependence of the attenuation.

Epstein and Carhart^(46, fig.2) compare their calculated characteristic with measured values. It may be observed that the difference between these curves, corresponds roughly to the difference between the SS and MS attenuation characteristics on the free fibre model (graph 9). Thus neglect of multiple scattering effects by Epstein and Carhart, even at the sparse concentrations involved, must be a greater source of error than they estimate.

6.1.2. Absorption

MS also provides a considerable improvement on SS for the calculation of absorption - frequency characteristics (graph 3) by the methods of Ch. 4. The assumption of a real density for sound propagation, equal to the actual bulk density of the fibrous block, in the SS theory is, therefore, a

severely limiting one. It would seem that the MS prediction of a complex density for sound propagation in fibrous media is more accurate.

6.2. Limitations of MS theory for flexible, fibrous media

6.2.1. Motion of a single fibre

For a single fibre freely suspended and parallel to the incident wave front the mode of vibration resulting from the analysis of Chapter 3 may be taken to be that of simple oscillation without distortion, i.e. that derived by Epstein^(45, pp. 180-182) in the analogous situation for a spherical droplet. For oblique incidence where dependence along the fibre axis is introduced, end effects have been neglected by assuming the fibre length to be infinite. Clearly, end effects are also important where the fibres parallel to the incident wave front are bound, or must satisfy some boundary conditions of contact at their extremities. The situation inside fibrous materials embraces both variously orientated fibres and fibres bound or in contact at randomly distributed nodes. Therefore the theory for a single scatterer should be extended to include end effects and thus to allow flexural and torsional modes of vibration.

6.2.2. Macroscopic effects of bonding or contact

From a more macroscopic point of view the bonding or fibre contact will result in motion and distortion of "groups" of fibres rather than individual fibres. These groups of fibres will represent individual "frameworks of motion" within the total slab medium. The number of bonds defining a particular framework and the size of the framework will increase,

with increase in the wave length of the incident sound, until at low frequencies, where the wavelength is much larger than the thickness of the material, the slab will tend to move as a whole.

This picture is consistent with the theory of Kosten and Janssen (K. and J.)⁽²²⁾, which according to the discussion of 1.2 is the most refined of those concerning flexible sound absorbing materials and using a continuous framework model.

K & J predicts that:

(a) at high frequencies the flexible skeleton is so inert that it does not vibrate appreciably i.e. the air and skeleton are almost decoupled.

(b) at low frequencies, the coupling between air and frame is so tight that they tend to move together.

This means, in effect, that sound propagation in flexible fibrous media should be dominated by "frame action" in the low frequency range and by the air-wave at higher frequencies.

On the MS theory a comparison of absorption characteristics based on fibres (i) freely suspended and (ii) rigidly fixed in space, shows negligible differences above a clearly defined lower limit in the audible frequency range. Since the MS theory represents a purely "air-wave" for all frequencies in the "rigidly fixed" case, the correspondence of (i) and (ii) above a lower limiting frequency confirms prediction (a) of K & J.

Further the discrepancy between the absorption characteristics predicted by the free fibre MS theory and those measured (graphs 3-5c)

is largest at low frequencies and increases with decrease in frequency. This suggests that K & J's prediction (b) is correct and that the neglect of fibre contact and bonding (previously discussed in 2.3) is the principal error of the present theory. Thus the discussion of 6.2.1 indicates the required extension of the scattering theory.

6.2.3. Decoupling

The MS theory for free fibres makes some allowance for frame action. Thus the frequencies at which the MS absorption curves for fibres rigidly fixed in space begin to follow those for free fibres and give an indication of the decoupling frequencies discussed by Zwicker & Kosten⁽¹⁶⁾. From graphs 3 and 4 for "Acoustic Blanket", decoupling frequencies are seen to be approximately 1200 Hz for 2.54 cm., and 750 Hz for 5.08 cm. layers.

6.2.4. Impervious coverings

Zwicker and Kosten⁽¹⁶⁾ (Z & K) consider the effect of closing the surface of an elastic porous layer with a thin impervious covering, for the simplified case of unit porosity. Having deduced the propagation constant for an elastic porous layer, Z & K derive a_0 for a closed layer by altering the boundary conditions at the closed surface. These then express the fact that the enclosed fluid and the solid frame are constrained to move together at this surface.

This procedure cannot be used with the free fibre model, as no such frame exists. Moreover, the presence of a solid skin at $x = -d$, introduces the complication of "reflected" scattered waves into the analysis of the scattering theory (4.2.).

6.3. Effective Radius

The resin bonding in the Rocksil-K materials (Appendix H) can frequently be observed to bind fibres along the majority of their lengths. This "clumping" of fibres along their lengths represents a form of "framework of motion" not discussed in 6.2.2. As each fibre "clump" will move as an individual unit the effect of "clumping" must be to increase the apparent physical size of the fibres. Thus, assuming that small departures from a cylindrical cross section do not substantially affect the theory of Chapter 3, the effect of this type of bonding could be included in the MS theory, by taking the effective radius of the fibres to be greater than the actual mean radius. Evidence for this argument is given by the results discussed in 5.2.

Using MS theory, therefore, it must be possible to choose an "effective radius", giving greatest correlation between calculation and measurement for any given material, which radius will represent the extent of this type of fibre contact or bonding.

6.4. Prediction of oblique incidence behaviour

Zwikker and Kosten⁽⁹⁷⁾ argue that flexible porous layers should be locally reacting to incident pressure variation i.e. the velocity component perpendicular to the surface should depend only on the pressure and not on the angle of incidence of the incident wave. This argument depends on the high damping of the incident wave, predicted by their theory, and is affected only by the extent of interconnection of the pores in a "sideways" direction. Pyett⁽⁹⁸⁾

develops a "frame" theory for an anisotropic situation, which predicts considerable departure from locally reacting behaviour. A similar prediction is made by Ford, Landau and West⁽⁹⁹⁾ by a theory, in which both dilatational and shear waves are allowed to propagate in the solid part of a fluid-solid mixture as a result of obliquely incident waves.

Locally reacting behaviour requires that Z_n should be constant, and that the oblique incidence surface impedance (Z_α) from which the absorption coefficient $Q(\alpha)$ can be calculated, should be given by $Z_n \cos \alpha$ ⁽⁹⁷⁾. A plot of Z_α in the complex plane therefore, for a particular frequency, should yield a straight line of slope (χ_n/τ_n) for a range of α .

The MS theory, predicts angle dependent functions for both propagation constant and characteristic impedance (4.2.6 (iii)). It is therefore evident that the MS theory will predict considerable departure from locally reacting behaviour. In fact, graph 11 shows that this departure reduces considerably with increase in thickness of layer and reduces slightly with increase in frequency. The tendency towards locally reacting behaviour with increase in thickness is consistent with the extremely high damping of the internal wave calculated on the MS theory (graph 10), the effect being particularly marked at low frequencies. The absorption coefficient for the 1.27 cm. layer case increases rapidly with α i.e. the random incidence coefficient may be deduced to have a somewhat higher value than Q_0 , for thin layers. Thicker layers (5.08 cm) have calculated values of absorption coefficient which are roughly constant with α .

6.5. Angular Dependence of Dissipation for single fibre

The form of the expressions (C.2.4 - C.3.6) for A_0^f and A_1^f , indicate that (i) A_0^f represents the thermal part of the dissipation and (ii) A_1^f is associated primarily with viscous dissipation. These conclusions are deduced by Epstein and Carhart⁽⁴⁶⁾ for the case of a spherical droplet.

Thus the following interpretation may be placed on the results of the calculations (D.2) for the oblique incidence scattering coefficients, (by 'oblique' here is meant that φ in fig. 3.11 is other than zero) typical forms of which are shown in graph 12:-

- (i) the thermal dissipation increases steadily with obliquity of incidence
- (ii) the viscous dissipation decreases rapidly with obliquity of incidence

and apparently tends towards a limiting condition of zero dissipation at 90° i.e. grazing incidence.

(ii) might occur with the formation of surface waves along the cylinder at grazing incidence⁽¹⁰⁰⁾ whereby there would be no relative motion between the cylindrical fibre and the imbedding fluid.

6.6. Further application of MS theory

6.6.1. Granular media

R.W. Morse⁽¹⁴⁾ suggests the possibility of using a "microscopic" scattering theory for rigid grained granular media. Indeed the wave motion through a suspension of rigid, spherical scatterers may be analysed by a MS theory. However, such a model departs considerably from

granular media, where grain contact is inevitable, and problems of "interference" of the scattered fluid viscous and thermal waves at and around each inter-grain boundary of contact must be considered.

Any extension to elastic grain situations will introduce the problem (analogous to the fibrous one) of frame wave contribution. Further the problem of friction between the grains must be considered. This is probably greater than in fibrous media because of the rougher surfaces involved.

6.6.2. Consolidated media.

(i) Materials such as acoustic plaster do not lend themselves very readily to a wave analysis of the type employed in the MS theory. Consider first a general case, where the persistent direction of the pores is not normal to the surface of the model or the incident (plane) wave front. It is necessary to choose wave functions inside fluid and solid which must satisfy boundary conditions both at the pore walls and at the surface of the material. The surface would be a fluid/solid interface for the solid waves and a pore entrance for the fluid waves. The latter situation requires consideration of problems of diffraction effects at the edges of the pore entrances which will interact with reflected waves from the solid surfaces and radiation from the pore interior. Further for the case which should represent a simplified situation, where the pore axes are normal to the surface (model 1 with flexible frame), one finds an ambiguity in the wave analysis. This is due to the existence of surface waves along the pore boundaries⁽¹⁰⁰⁾.

Numerous authors^{(100) (101) (61)}, have considered relevant cases of fluid wave propagation in elastic walled tubes. Chester⁽¹⁰²⁾ has considered propagation in a rigid walled tube whose entrance is surrounded by an infinite baffle; a case, which might be applicable to Model 1 but tends to intricate analysis. Apart from this, a less refined approach could neglect near-surface diffraction effects by assuming that within a few wavelengths of the surface the wavelets would have recombined as an effective plane wave.

(ii) However, the scattering theory does give an explanation of the poor absorption characteristic observed with stiff framed, consolidated media when their front surfaces are sealed⁽¹⁰³⁾. In this situation, a reasonable model is one of a continuous "imbedding" solid frame containing a "suspension" of cylindrical, fluid-filled pores which do not cut the surface. The pores will scatter waves propagating from the solid surface and the single scatterer situation will correspond to the "inverse" of that analysed in Chapter 3. The energy calculation corresponding to Appendix E, therefore, predicts a dissipation cross-section (σ) dependent only on the internal friction of the solid. Even for very large concentrations of pores, the total dissipation is thus very small except when the solid is very elastic and has high internal losses.

6.6.3. Polymer foams

Many materials referred to as flexible "foams" have an open-celled structure which differs greatly from models 1, 2, 3 and 5 and are consequently unsuitable for the application of theories based on

these models. Taking polyurethane foam as an example of such media one can distinguish two cases:-

- (i) Rigid polyurethane foam (plate 3) has its porosity completely based on sealed off pores, thus corresponding to the previously discussed case of covered consolidated media (6.6.2).
- (ii) Flexible polyurethane foam consists essentially of a continuous three dimensional lattice of polygons (usually hexagons) of polymer fibre. Occasional "sides" of the lattice are filled in with skins of the polymer (plates 4 and 5).

With such a microstructure, one has the interconnected porous structure of a fibrous material interspersed with closed or "sealed-off" pores, where the polymer skins are concentrated.

In view of the facts that:

- (a) these materials have absorption characteristics very similar to those of glass fibre
 - and (b) Lang⁽¹⁰⁴⁾ obtains reasonable results with an analysis similar to that of Kawasima⁽²⁷⁾ (see 1.4);
- the MS theory should also be applicable.

However, the problem of a continuous network of "fibres" is there from the outset and some knowledge of the polymer elasticity is required. It is possible that an equivalent geometrical form (q.v. 6.3) could be devised which would make the scattering problem tractable. Further, scattering by geometrical forms other than sphere or circular cylinder must be solved.

6.7. Viscoelastic Absorbers

6.7.1. Cellular Rubber

This type of absorber is mentioned by Zwikker and Kosten⁽¹⁰⁵⁾ and Furrer⁽¹⁰⁶⁾. It is described as consisting of a rubber-like solid matrix containing a random distribution of closed pores. A particular porous medium model is not suggested. A qualitative assessment, only, of its performance is given⁽¹⁰⁵⁾ in terms of internal friction ascribing a complex stiffness (or bulk modulus) to the material.

6.7.2. MS description

A viscoelastic material may be regarded as having complex propagation constants for both dilatational and shear waves, signifying both compressional and shear viscosities. A rubber-like material in particular, exhibits very little effect due to compressional viscosity compared with that due to shear⁽¹⁰⁷⁾.

Thus a pore-discontinuity inside such a material will, from the scattering viewpoint, alter part of any incident compressional wave into shear wave by mode conversion at its boundary, thus causing dissipation (the shear wave being damped). This mechanism is similar to that previously cited for a fibre imbedded in a viscous fluid, but now with the solid as imbedding medium.

Vovk, Pasternak and Tyutekin⁽¹⁰⁸⁾ suggest the controlled manufacture of such absorbents with high absorption. Their main advantage over the traditional fibrous or "foam" absorbents would be, of course, that their surfaces are impervious i.e. they do not rely on the penetration of the incident fluid wave for their absorptive property. This means that their

surface acts as a vapour and/or dust barrier, these being important considerations, say, in swimming pools and hospitals. Vovk et sec⁽¹⁰⁸⁾ in fact consider the special case of a material containing cylindrical channels normal to the surface and radially fastened, following the cell model theory of Tyutekin⁽³⁹⁾ (see 1.6). The materials should still absorb, however, according to the MS description, whether or not the pores cut the surface. This statement is consistent with the observation by Kosten⁽⁹³⁾ that very flexible materials i.e. materials like sponge rubber (with a viscoelastic frame) do not have their absorption impaired by covering their surface with a light coating. Indeed, it is stated that coating improves the absorption at low frequencies, and is not particularly detrimental at high frequencies.

Thus choosing a "suspension" model for such a viscoelastic absorber enables a deduction of its absorptive behaviour in terms of:-(i) the number of discontinuities per unit volume (ii) their dimensions and (iii) the elastic properties of the imbedding viscoelastic matrix. In Appendix G, an outline is given of the theory for a single scatterer in this absorber following the work of Chapter 3. For simplicity, thermoelasticity is neglected, and the pore discontinuities are assumed evacuated. Moreover a phenomenological description is used for the viscoelastic behaviour. The theory therefore requires modification for a more exact theory of viscoelasticity and the presence of air in the pores. The propagation constant and characteristic impedance for a slab region of such discontinuities may then be derived, following 4.2. The impedance of a layer of viscoelastic absorber against a rigid backing, may subsequently be calculated by assuming the layer to be

homogeneous, containing forward and backward (plane) waves, with the propagation constant and characteristic impedance as previously derived.

This procedure, however, introduces some inconsistency into the macroscopic picture as the surface of the layer will act as a reflector of scattered waves, hence a problem similar to that mentioned in 6.2.3.

APPENDIX A. SMALL AMPLITUDE WAVE PROPAGATION IN A VISCOUS, CONDUCTING,
COMPRESSIBLE FLUID

For a compressible fluid, the equation of continuity⁽⁷¹⁾, may be written:-

$$\frac{d\rho^f}{dt} + \text{div}(\rho^f \underline{v}) = 0$$

thus where $\text{div}(\rho^f \underline{v}) = \rho^f \text{div} \underline{v} + (\text{grad} \rho^f) \cdot \underline{v}$

and $\frac{d\rho^f}{dt} = \frac{\partial \rho^f}{\partial t} + (\text{grad} \rho^f) \cdot \underline{v}$

then $\frac{d\rho^f}{dt} + \rho^f \text{div} \underline{v} = 0$ (A.1)

If the usual assumption for a normal acoustic disturbance is made i.e. that all the velocities, displacements, etc. are small, such that the products of the perturbations introduced may be neglected e.g. the density alters with $\rho^f = \rho_0^f + d\rho^f$, (ρ_0^f being the equilibrium value), and the product $(d\rho^f)(\text{div} \underline{v})$ may be neglected; then the equation of continuity becomes,

$$\frac{d\rho^f}{dt} + \rho_0^f \text{div} \underline{v} = 0$$
 (A.2)

Neglecting body force, the equation of motion⁽⁷²⁾ is,

$$\rho^f \frac{dv_i}{dt} = - \frac{\partial p}{\partial x_i} + \frac{\partial P'_{ji}}{\partial x_j}$$

where $\frac{\partial P'_{ji}}{\partial x_j} = \left(\gamma + \frac{1}{3}\mu^f\right) \underline{\nabla} \text{div} \underline{v} + \mu^f \nabla^2 \underline{v}$

Here, the summation convention is implied, and the viscosity coefficients γ, μ^f have been assumed isotropic.

Using the vector identity $\nabla \times (\nabla \times \underline{v}) = \nabla \text{div} \underline{v} - \nabla^2 \underline{v}$, and the small disturbance assumption, the above equation of motion may be transformed to:-

$$\rho_0^f \frac{dv_i}{dt} = -\nabla p + \left(\gamma + \frac{4}{3}\mu^f\right) \nabla \text{div} \underline{v} - \mu^f \nabla \times (\nabla \times \underline{v}) \quad (\text{A.3})$$

The energy equation⁽⁷³⁾ may be written

$$\rho^f \frac{dU}{dt} = -p \delta_{ij} d_{ij} + P_{ij}^I d_{ij} - \text{div} q$$

where $\underline{q} = -\kappa^f \nabla T$ and $d_{ij} = \frac{1}{2} \left(\frac{\partial v_i}{\partial x_j} + \frac{\partial v_j}{\partial x_i} \right)$

The second term in ^{the r.h.s. of} the energy equation, may be ignored, by the small disturbance assumption, leaving,

$$\rho^f \frac{dU}{dt} + (p \text{div} \underline{v}) - \kappa^f \nabla^2 T = 0 \quad (\text{A.4})$$

Further, for $U = U(\rho^f, T)$, then $\frac{dU}{dt} = \left(\frac{\partial U}{\partial \rho^f}\right)_T \frac{d\rho^f}{dt} + \left(\frac{\partial U}{\partial T}\right)_{\rho^f} \frac{dT}{dt}$ (A.5)

Thus with⁽⁷⁴⁾

$$\left. \begin{aligned} \left(\frac{\partial U}{\partial T}\right)_{\rho^f} &= c_v \\ \left(\frac{\partial U}{\partial \rho^f}\right)_T &= T\beta B - p \\ c_p - c_v &= T_0 \beta^2 B / \rho_0^f \\ \left(\frac{\partial p}{\partial T}\right)_{\rho^f} &= \beta B \end{aligned} \right\} \quad (\text{A.6})$$

(A.5) becomes

$$\frac{dU}{dt} = (-\rho_0^f \operatorname{div} \underline{v}) \left(-\frac{1}{\rho_0^f} \right) \left\{ \frac{\rho^f (\gamma-1) c_v}{\beta} - p \right\} + c_v \frac{dT}{dt} \quad (\text{A.7})$$

and the modified energy equation (A.4) gives

$$\rho_0^f \operatorname{div} \underline{v} \frac{(\gamma-1) c_v}{\beta} + \rho^f c_v \frac{dT}{dt} - \kappa^f \nabla^2 T = 0 \quad (\text{A.8})$$

Similarly if $p = p(\rho^f, T)$ then $\frac{dp}{dt} = \left(\frac{\partial p}{\partial \rho^f} \right)_T \frac{d\rho^f}{dt} + \left(\frac{\partial p}{\partial T} \right)_{\rho^f} \frac{dT}{dt}$ (A.9)

and with (A.2) and (A.6); (A.9) becomes

$$\frac{dp}{dt} = \left(\frac{\partial p}{\partial \rho^f} \right)_T (-\rho_0^f \operatorname{div} \underline{v}) + B\beta \frac{dT}{dt} \quad (\text{A.10})$$

Now $\left(\frac{\partial p}{\partial \rho^f} \right)_T = \frac{B}{\rho^f} = \frac{c_0^f{}^2}{\gamma}$ and from (A.6) $B\beta = \frac{\rho^f \beta c_0^f{}^2}{\gamma}$

and noting that the small disturbance assumption makes the total and partial derivative with respect to time approximately equal e.g.

$$\frac{dv_i}{dt} = \frac{\partial v_i}{\partial t} + \frac{\partial v_i}{\partial x_j} \frac{\partial x_j}{\partial t} = \frac{\partial v_i}{\partial t} + \frac{\partial v_i}{\partial x_j} v_j \approx \frac{dv_i}{dt}$$

the time derivative of (A.3) becomes

$$\frac{d^2 \underline{v}}{dt^2} - \frac{c_0^f{}^2}{\gamma} \nabla \operatorname{div} \underline{v} + \frac{\beta c_0^f{}^2}{\gamma} \nabla \frac{dT}{dt} - N \nabla \operatorname{div} \frac{d\underline{v}}{dt} + \gamma \nabla \times (\nabla \times \frac{d\underline{v}}{dt}) = 0 \quad (\text{A.11})$$

where $N = \frac{1}{\rho_0^f} \left(\gamma + \frac{4}{3} \mu^f \right)$

Postulating a time dependence $\exp(-i\omega t)$, where all the variables take on the significance of amplitude variation from equilibrium values e.g.

$$T' = T_0 + T \exp(-i\omega t)$$

where T' represents the total value T previously used, then (A.11) may be written

$$\omega^2 \underline{v} + \frac{c_0^2}{\gamma} \nabla \operatorname{div} \underline{v} + \rho_0^f \frac{c_0^2}{\gamma} i\omega \nabla T - Ni\omega \nabla \operatorname{div} \underline{v} + i\omega \nu \nabla \times (\nabla \times \underline{v}) = 0 \quad (\text{A.12})$$

and (A.8) may be written

$$i\omega T + \sigma \gamma \nabla^2 T - \frac{(\gamma-1)}{\beta} \operatorname{div} \underline{v} = 0 \quad (\text{A.13})$$

Further, if the particle velocity is written in terms of potential functions viz.

$$\begin{aligned} \underline{v} &= -\nabla \phi + \operatorname{curl} \underline{A} \\ \operatorname{div} \underline{A} &= 0 \end{aligned} \quad (\text{A.14})$$

where ϕ and \underline{A} satisfy the scalar and vector Helmholtz equations respectively i.e.

$$\left. \begin{aligned} (\nabla^2 + \kappa_\phi^2) \phi &= 0 \\ (\nabla^2 + \kappa_A^2) \underline{A} &= 0 \end{aligned} \right\} \quad (\text{A.15})$$

then from (A.11)

$$\nabla \left[\omega^2 \phi + \left(\frac{c_0^2}{\gamma} - i\omega N \right) \nabla^2 \phi - \beta \frac{c_0^2}{\gamma} i\omega T \right] = \nabla \times \left[\omega^2 \underline{A} + i\omega \nu \nabla \times (\nabla \times \underline{A}) \right] \quad (\text{A.16})$$

The R.H.S. of this equation may be transformed to $\nabla \times \left[\omega^2 \underline{A} - i\omega\nu \nabla^2 \underline{A} \right]$
 by $\nabla \times (\nabla \times \underline{A}) = \nabla(\text{div} \underline{A}) - \nabla^2 \underline{A}$ and $\text{div} \underline{A} = 0$

This is zero by (A.15) if $\kappa_A^2 = \kappa_T^2 = \frac{i\omega}{\nu}$

$$\text{i.e.} \quad \kappa_T^f = (1+i) \left(\frac{\omega}{2\nu} \right)^{\frac{1}{2}} \quad (\text{A.17})$$

where κ_T^f represents the viscous wave propagation constant.

The L.H.S. of (A.16) may then be used with (A.13) to eliminate T and give the following biharmonic form for ϕ :-

$$\sigma^f \gamma^2 \left(\frac{c_0^f}{\gamma} - i\omega N \right) \nabla^4 \phi + \left[\begin{array}{l} \sigma^f \gamma^2 \omega^2 + c_0^f i\omega (\gamma-1) \\ + \gamma i\omega \left(\frac{c_0^f}{\gamma} - i\omega N \right) \end{array} \right] \nabla^2 \phi + \gamma i\omega^3 \phi = 0 \quad (\text{A.18})$$

which can be seen to correspond to two dilatational waves satisfying

$$(\nabla^2 + \kappa_1^{f2})\phi_1 = 0 \quad \text{and} \quad (\nabla^2 + \kappa_2^{f2})\phi_2 = 0 \quad \text{where} \quad \phi_1 + \phi_2 = \phi$$

and

$$\frac{1}{\kappa_1^{f2} \kappa_2^{f2}} = - \left(\frac{c_0^f}{\omega} \right)^4 [\epsilon f + i f] ; \quad \frac{1}{\kappa_1^{f2}} + \frac{1}{\kappa_2^{f2}} = \left(\frac{c_0^f}{\omega} \right)^2 [1 - i(\epsilon + \gamma f)]$$

ϵ and f representing the small quantities $\epsilon = \frac{N\omega}{c_0^{f2}}$ and $f = \frac{\sigma^f \omega}{c_0^{f2}}$
 which are both $< \frac{\omega}{c_0^{f2}} \sim 10^{-5}$ at 1000 Hz (as an upper limit)

$$\begin{aligned} \text{Hence} \quad \frac{1}{\kappa_1^{f2}} &= \left(\frac{c_0^f}{\omega} \right)^2 \left[1 - i(\epsilon + \gamma f) + i f \right] \\ \frac{1}{\kappa_2^{f2}} &= - \left(\frac{c_0^f}{\omega} \right)^2 i f \end{aligned}$$

where use has been made of the binomial expansion and the small quantities ϵ and f have been neglected above first order.

Inspection shows that κ_2^f may be identified completely with thermal wave

propagation, and κ_1^f with the usual compressional wave, i.e. one may write with further approx.

$$\kappa_D^f = \left(\frac{\omega}{c_D}\right) \left[1 + \frac{i\omega}{2c_D^2} (N + \sigma^f(\gamma - 1)) \right] \quad (\text{A.19})$$

and

$$\kappa_{TH}^f = (1 + i) \left(\frac{\omega}{2\sigma^f}\right)^{\frac{1}{2}} \quad (\text{A.20})$$

These two expressions correspond to those derived by Epstein and Carhart⁽⁴⁶⁾. The expression for κ_T^f is also derived by Mason⁽⁷⁵⁾.

APPENDIX B. SMALL AMPLITUDE WAVE PROPAGATION IN A LINEAR, ELASTIC, CONDUCTING SOLID

The equations of motion and energy balance for such a solid can be written as ⁽⁷⁶⁾:-

$$\rho^s \frac{d^2 \underline{u}}{dt^2} = \mu^s \nabla^2 \underline{u} + (\lambda + \mu^s) \nabla \operatorname{div} \underline{u} - \beta^s B^s \nabla T \quad (\text{B.1})$$

and

$$\rho^s c_v^s \frac{dT}{dt} + T_0 \beta^s B^s \operatorname{div} \frac{d\underline{u}}{dt} = \kappa^s \nabla^2 T \quad (\text{B.2})$$

respectively; where T_0 refers to the steady state temperature such that T represents the difference $(T' - T_0)$, T' being the actual temperature at time t . As with the fluid (Appendix A), postulating time dependence $\exp(-i\omega t)$ and considering $\underline{u} = -\nabla \phi + \operatorname{curl} \underline{A}$; $\operatorname{div} \underline{A} = 0$ and similar manipulations yield from (B.1):-

$$\nabla \left[\rho^s \omega^2 \phi + (\lambda + 2\mu^s) \nabla^2 \phi + \beta^s B^s T \right] = \nabla \times \left[\rho^s \omega^2 \underline{A} + \mu^s \nabla^2 \underline{A} \right] \quad (\text{B.3})$$

From the R.H.S. of this equation; the solution satisfying the vector Helmholtz equation for \underline{A} gives

$$\kappa_T^s = \omega \left(\frac{\rho^s}{\mu^s} \right)^{\frac{1}{2}} \quad (\text{B.4})$$

representing the standard shear wave propagation constant in the solid, which is real i.e. non-dissipative for a linear, elastic solid with no relaxation.

(B.2) may be transformed to

$$-i\omega\rho^s c_v^s T + T_0 \beta^s B^s i\omega \nabla^2 \phi = \kappa^s \nabla^2 T$$

which together with the L.H.S. of (B.3) and the third relation of (A.6) yields a biharmonic equation for ϕ

$$-\frac{i\omega\sigma^s \gamma^s}{c_0^{s2}} \left(\frac{c_0^s}{\omega}\right)^4 \nabla^4 \phi + \left(\frac{c_0^s}{\omega}\right)^2 \left[1 + \frac{\beta^s (\gamma^s - 1)}{\rho^s c_0^{s2}} - \frac{i\omega\sigma^s \gamma^s}{c_0^{s2}}\right] \nabla^2 \phi + \phi = 0 \quad (\text{B.5})$$

where $c_0^{s2} = \left(\frac{\lambda + 2\mu^s}{\rho^s}\right)$, the isothermal dilatational velocity of sound in the solid, may be obtained from setting $T = 0$ in the L.H.S. = 0 of (B.3) and use has been made of (A.6).

Analysing in a similar manner to that of Appendix A, the resultant propagation constant solutions may be written:-

$$\kappa_{1,2}^{s2} = -\left(\frac{\omega}{c_0^s}\right)^2 \frac{c_0^{s2}}{2i\omega\sigma^s \gamma^s} \left\{ A - \frac{i\omega\sigma^s \gamma^s}{c_0^{s2}} + A \left[1 - \frac{i\omega\sigma^s \gamma^s}{A c_0^{s2}} + \frac{2i\omega\sigma^s \gamma^s}{A^2 c_0^{s2}} \right] \right\}$$

where $A = 1 + \frac{B^s (\gamma^s - 1)}{\rho^s c_0^{s2}}$ and the small quantity $\frac{i\omega\sigma^s \gamma^s}{c_0^{s2}}$ has been neglected above first order in binomial expansions ($c_0^s \sim 5 \times 10^5$ cm/sec).

Under the further approximation that $(\gamma^s - 1)$ is small (this is necessary as $B^s \sim c_0^{s2}$), the propagation constants may be separated out as

$$\left. \begin{aligned} \kappa_1^s &= \left(\frac{\omega}{c_0^s}\right) \left\{ 1 - \frac{B^s (\gamma^s - 1)}{2\rho^s c_0^{s2}} \right\} \\ \kappa_2^s &= (1+i) \left(\frac{\omega}{2\sigma^s \gamma^s}\right)^{\frac{1}{2}} \left\{ 1 + \frac{B^s (\gamma^s - 1)}{\rho^s c_0^{s2}} \right\} \end{aligned} \right\} \quad (\text{B.6})$$

Using these in L.H.S. bracket of (B.3) = 0, with $\phi = \phi_1 + \phi_2$ where ϕ_1, ϕ_2 are associated with κ_1^s, κ_2^s respectively:-

$$\begin{aligned} T &= -\frac{1}{\beta^s B^s} \left\{ (\rho^s \omega^2 - \rho^s c_0^{s2} \kappa_1^{s2}) \phi_1 + (\rho^s \omega^2 - \rho^s c_0^{s2} \kappa_2^{s2}) \phi_2 \right\} \\ &= -\frac{\phi_1}{\beta^s B^s} \left[\rho^s \omega^2 \left(1 - \frac{1}{A}\right) \right] - \frac{\phi_2}{\beta^s B^s} \left[\frac{\omega^2 \rho^s}{A} - \frac{c_0^{s2} \rho^s i\omega}{\sigma^s \gamma^s} - \frac{i\omega B^s (\gamma^s - 1)}{\sigma^s \gamma^s} \right] \end{aligned}$$

$$= +g\phi_1 + G\phi_2, \text{ say} \quad (\text{B.7})$$

It can be seen from (B.6) and (B.7) that, it is convenient to make the approximation $\gamma^S = 1$ (a reasonable one for solids), for then the propagation constants may be identified with dilatational and thermal waves respectively, as in the fluid case (Appendix A) viz.

$$\left. \begin{aligned} \kappa_D^S &= \left(\frac{\omega}{c_0^S} \right) \\ \kappa_{TH}^S &= (1+i) \left(\frac{\omega}{2\sigma^S} \right)^{\frac{1}{2}} \end{aligned} \right\} \quad (\text{B.8})$$

and the temperature expression reduces to

$$\left. \begin{aligned} T &= G\phi_{TH}^S \\ \text{where } G &= -\frac{i\omega\rho^S}{\beta^S B^S} \left(i\omega + \frac{N^S}{\sigma^S} \right) \end{aligned} \right\} \quad (\text{B.9})$$

as for $\gamma^S \rightarrow 1$, $A \rightarrow 1$ and $g \rightarrow 0$

Here the results for κ_D^S and κ_T^S are standard and the form for κ_{TH}^S corresponds to that for κ_{TH}^f (Appendix A). $N^S = \frac{C_0^{S2}}{\gamma^S}$ above.

APPENDIX C

CALCULATION OF SINGLE FIBRE SCATTERING COEFFICIENTS

Elastic Fibre

C.1. The boundary conditions (3.1313), (3.1322), (3.1331) and (3.1332) for oblique incidence, may be collected together as below

$$\begin{aligned}
 & f \left[\epsilon_n J_n(a^f) + A_n^f H_n(a^f) \right] + F B_n^f H_n(b^f) = -G B_n^s J_n(b^s) \\
 & \kappa^f \left\{ f a^f \left[\epsilon_n J_n'(a^f) + A_n^f H_n'(a^f) \right] + F b^f B_n^f H_n'(b^f) \right\} = -\kappa^s G b^s B_n^s J_n'(b^s) \\
 & -a^f \left[\epsilon_n J_n'(a^f) + A_n^f H_n'(a^f) \right] - b^f B_n^f H_n'(b^f) + i \kappa c^f C_n^f H_n'(c^f) + n \kappa_T^f D_n^f H_n'(c^f) \\
 & \quad = -i \omega \left\{ -a^s A_n^s J_n'(a^s) - b^s B_n^s J_n'(b^s) + i \kappa c^s C_n^s J_n'(c^s) + n \kappa_T^s D_n^s J_n'(c^s) \right\} \\
 & n \left[\epsilon_n J_n(a^f) + A_n^f H_n(a^f) + B_n^f H_n(b^f) - i \kappa C_n^f H_n(c^f) \right] - \kappa_T^f c^f D_n^f H_n(c^f) \\
 & \quad = -i \omega \left\{ n \left[A_n^s J_n(a^s) + B_n^s J_n(b^s) - i \kappa C_n^s J_n(c^s) \right] - \kappa_T^s c^s D_n^s J_n(c^s) \right\} \\
 & -i \kappa \left[\epsilon_n J_n(a^f) + A_n^f H_n(a^f) + B_n^f H_n(b^f) \right] + (\kappa_T^{f2} - \kappa^2) C_n^f H_n(c^f) \\
 & \quad = -\kappa \omega \left\{ A_n^s J_n(a^s) + B_n^s J_n(b^s) \right\} - i \omega (\kappa_T^{s2} - \kappa^2) C_n^s J_n(c^s) \\
 & \mu^f \left[\epsilon_n \left\{ a^f J_n(a^f) + \left(\frac{c^{f2}}{2} - d^2 - n^2 \right) J_n(a^f) \right\} + A_n^f \left\{ a^f H_n(a^f) + \left(\frac{c^{f2}}{2} - d^2 - n^2 \right) H_n(a^f) \right\} \right. \\
 & \quad \left. + B_n^f \left\{ b^f H_n(b^f) + \left(\frac{c^{f2}}{2} - d^2 - n^2 \right) H_n(b^f) \right\} + i \kappa c^{f2} C_n^f H_n'(c^f) + n \kappa_T^f D_n^f \left\{ c^f H_n'(c^f) H_n(c^f) \right\} \right] \\
 & = \mu^s \left[A_n^s \left\{ a^s J_n(a^s) + \left(\frac{c^{s2}}{2} - d^2 - n^2 \right) J_n(a^s) \right\} + B_n^s \left\{ b^s J_n(b^s) + \left(\frac{c^{s2}}{2} - d^2 - n^2 \right) J_n(b^s) \right\} \right. \\
 & \quad \left. + i \kappa c^{s2} C_n^s J_n'(c^s) + n \kappa_T^s D_n^s \left\{ c^s J_n'(c^s) - J_n(c^s) \right\} \right] \\
 & \mu^f \left\{ n \left(\epsilon_n \left[a^f J_n'(a^f) - J_n'(a^f) \right] + A_n^f \left[a^f H_n'(a^f) - H_n'(a^f) \right] \right) + \frac{\kappa_T^f D_n^f}{2} \left(\frac{c^f H_n'(c^f)}{-n^2 H_n(c^f)} - c^{f2} H_n''(c^f) \right) \right\} \\
 & = \mu^s \left\{ n \left(A_n^s \left[a^s J_n'(a^s) - J_n'(a^s) \right] + B_n^s \left[b^s J_n'(b^s) - J_n'(b^s) \right] \right) + \frac{\kappa_T^s D_n^s}{2} \left(\frac{c^s J_n'(c^s)}{-n^2 J_n(c^s)} - c^{s2} J_n''(c^s) \right) \right\} \\
 & \mu^f \left\{ -i \kappa \left[\epsilon_n a^f J_n'(a^f) + A_n^f a^f H_n'(a^f) + B_n^f b^f H_n'(b^f) \right] + c^f C_n^f \left(\frac{\kappa_T^{f2} - \kappa^2}{2} \right) H_n'(c^f) + \frac{i n \kappa_T^f}{2} D_n^f H_n'(c^f) \right\} \\
 & = \mu^s \left\{ -i \kappa \left[A_n^s a^s J_n'(a^s) + B_n^s b^s J_n'(b^s) \right] + c^s C_n^s \left(\frac{\kappa_T^{s2} - \kappa^2}{2} \right) J_n'(c^s) + \frac{i n \kappa_T^s}{2} D_n^s J_n'(c^s) \right\}
 \end{aligned}$$

(C.1.1)

In particular the solutions for normal incidence for the elastic fibre case are required (Chapter 4).

At normal incidence the axial phase constant K is zero ($\mathcal{P} = 0$ in equation 3.125) and thus the Bessel function arguments a^{1f} , b^{1f} , c^{1f} etc. lose their dashes. Further it can be seen that with $k = 0$, the equations of (C.1.1) representing the continuity of V_θ and $P_{r\theta}$ can only be satisfied if C_n^f and C_n^s are arbitrary (or trivial viz. $C_n^f = C_n^s = 0$) i.e. the wave potentials ψ^f and ψ^s , representing the part of the vector field normal to the r coordinate surface⁽⁷⁷⁾ are redundant and therefore may be rejected.

Thus the equations of (C.1.1) have their z dependence removed and reduce to the six below:-

$$\begin{aligned}
 & f [\epsilon_n J_n(a^f) + A_n^f H_n(a^f)] + F B_n^f H_n(b^f) = - G B_n^s J_n(b^s) \\
 & \kappa^f \left\{ f a^f [\epsilon_n J_n'(a^f) + A_n^f H_n'(a^f)] + F b^f B_n^f H_n'(b^f) \right\} = - \kappa^s G b^s B_n^s J_n'(b^s) \\
 & - a^f [\epsilon_n J_n'(a^f) + A_n^f H_n'(a^f)] - b^f B_n^f H_n'(b^f) + n \kappa_r^f D_n^f H_n(c^f) \\
 & \quad = - i\omega \left\{ - a^s A_n^s J_n'(a^s) - b^s B_n^s J_n'(b^s) + n \kappa_r^s D_n^s J_n(c^s) \right\} \\
 & n [\epsilon_n J_n(a^f) + A_n^f H_n(a^f) + B_n^f H_n(b^f)] - \kappa_r^f c^f D_n^f H_n(c^f) \\
 & \quad = - i\omega \left\{ n [A_n^s J_n(a^s) + B_n^s J_n(b^s)] - \kappa_r^s c^s D_n^s J_n'(c^s) \right\} \\
 (C.1.2) & \left\{ \begin{aligned} & \epsilon_n [a^f J_n'(a^f) + (\frac{c^{f2}}{2} - n^2) J_n'(a^f)] + A_n^f [a^f H_n'(a^f) + (\frac{c^{f2}}{2} - n^2) H_n'(a^f)] \\ & + B_n^f [b^f H_n'(b^f) + (\frac{c^{s2}}{2} - n^2) H_n'(b^f)] + n \kappa_r^f D_n^f [c^f H_n'(c^f) - H_n(c^f)] \end{aligned} \right\} \\
 & \quad = \mu^s \left\{ A_n^s [a^s J_n'(a^s) + (\frac{c^{s2}}{2} - n^2) J_n'(a^s)] + B_n^s [b^s J_n'(b^s) + (\frac{c^{s2}}{2} - n^2) J_n'(b^s)] \right\} \\
 & \quad \quad + n \kappa_r^s D_n^s [c^s J_n'(c^s) - J_n(c^s)] \\
 & \mu^f \left[n \left\{ \begin{aligned} & \epsilon_n [a^f J_n'(a^f) - J_n(a^f)] + A_n^f [a^f H_n'(a^f) - H_n(a^f)] \\ & + B_n^f [b^f H_n'(b^f) - H_n(b^f)] \end{aligned} \right\} + \frac{\kappa_r^f D_n^f}{2} \left\{ \begin{aligned} & c^f H_n(c^f) - c^{f2} H_n''(c^f) \\ & - n^2 H_n(c^f) \end{aligned} \right\} \right] \\
 & \quad = \mu^s \left[n \left\{ A_n^s [a^s J_n'(a^s) - J_n(a^s)] + B_n^s [b^s J_n'(b^s) - J_n(b^s)] \right\} + \frac{\kappa_r^s D_n^s}{2} \left\{ \begin{aligned} & c^s J_n(c^s) - c^{s2} J_n''(c^s) \\ & - n^2 J_n(c^s) \end{aligned} \right\} \right]
 \end{aligned}$$

C.2. $n = 0$

For this situation, from the fourth and sixth equations of (C.1.2) the only possible solution for D_n^f and D_n^s is the trivial one $D_n^f = D_n^s = 0$. Otherwise D_n^f, D_n^s are arbitrary, their contribution for $n=0$ vanishing anyway from the remaining equations.

This means that as in the spherical case ⁽⁴⁶⁾, the zero order coefficients are independent of the shear wave potentials of both fluid and solid.

The boundary conditions may now be written:-

$$(C.2.1) \left\{ \begin{aligned} f [J_0(a^f) + A_0^f H_0(a^f)] + F B_0^f H_0(b^f) &= - G B_0^s J_0(b^s) \\ \kappa^f \left\{ f a^f [J_0'(a^f) + A_0^f H_0'(a^f)] + F b^f B_0^f H_0'(b^f) \right\} &= - \kappa^s G b^s B_0^s J_0'(b^s) \\ - a^f [J_0'(a^f) + A_0^f H_0'(a^f)] - b^f B_0^f H_0'(b^f) &= - i\omega \left\{ -a^s A_0^s J_0'(a^s) - b^s B_0^s J_0'(b^s) \right\} \\ \mu^f \left\{ [a^f J_0'(a^f) + \frac{c^{f2}}{2} J_0(a^f)] + A_0^f [a^f H_0'(a^f) + (\frac{c^{f2}}{2}) H_0(a^f)] + B_0^f [b^f H_0'(b^f) + (\frac{c^{f2}}{2}) H_0(b^f)] \right\} \\ &= \mu^s \left\{ A_0^s [a^s J_0'(a^s) + \frac{c^{s2}}{2} J_0(a^s)] + B_0^s [b^s J_0'(b^s) + (\frac{c^{s2}}{2}) J_0(b^s)] \right\} \end{aligned} \right.$$

Further, the following small argument Bessel Function expansions can be used for functions of a^f, a^s and c^s ; all of which are very small ($\sim 10^{-5}$);

$$\begin{aligned} J_0(x) &\sim 1 & J_0'(x) &= -J_1(x) \simeq -\frac{x}{2} \\ x J_0''(x) + J_0'(x) &= -x J_0(x) & \text{hence } J_0''(x) &\simeq -\frac{1}{2} \end{aligned}$$

also

$$H_0'(x) = -H_1(x)$$

where use has been made of the small argument relation ⁽⁸⁶⁾

$$J_n(x) \xrightarrow{x \rightarrow 0} \frac{1}{n!} \left(\frac{x}{2} \right)^n$$

(C.2.2) and the Recurrence relations, which apply where R_n is either J_n

or H_n ⁽⁸⁷⁾

$$\begin{aligned} x R_n'(x) &= n R_n(x) - x R_{n+1}(x) \\ x R_n''(x) + R_n'(x) &= \frac{n^2}{x} R_n(x) - x R_n(x) \end{aligned}$$

and thus the set (C.2.1) becomes:

$$(C.2.3.) \left\{ \begin{aligned} f [1 + A_0^f H_0(a^f)] + F B_0^f H_0(b^f) &= -G B_0^s J_0(b^s) \\ \kappa^f \left\{ f a^f \left[-\frac{a^f}{2} - A_0^f H_1(a^f) \right] - F b^f H_1(b^f) B_0^f \right\} &= -\kappa^s G b^s B_0^s J_1(b^s) \\ a^f \left[\frac{a^f}{2} + A_0^f H_1(a^f) \right] + b^f H_1(b^f) B_0^f &= -i\omega \left\{ \frac{c^{s2}}{2} A_0^s + b^s B_0^s J_1(b^s) \right\} \\ \mu^f \left\{ \frac{1}{2} (c^{f2} - a^{f2}) + A_0^f \left[\frac{c^{f2}}{2} H_0(a^f) - a^f H_1(a^f) \right] + B_0^f \left[\frac{c^{f2}}{2} H_0(b^f) - b^f H_1(b^f) \right] \right\} \\ &= \mu^s \left\{ \frac{1}{2} (c^{s2} - a^{s2}) A_0^s + B_0^s \left[\frac{c^{s2}}{2} J_0(b^s) - b^s J_1(b^s) \right] \right\} \end{aligned} \right.$$

from the first two equations of (C.2.3).

$$B_0^f = \frac{f \left\{ \frac{\kappa^f a^{f2}}{2 \kappa^s b^s J_1(b^s)} - \frac{1}{J_0(b^f)} \right\} + \left\{ \frac{\kappa^f a^f H_1(a^f)}{\kappa^s b^s J_1(b^s)} - \frac{H_0(a^f)}{J_0(b^f)} \right\} A_0^f}{\left\{ \frac{H_0(b^f)}{J_0(b^s)} - \frac{\kappa^f b^f H_1(b^f)}{\kappa^s b^s J_1(b^s)} \right\}}$$

$$= \frac{f}{F} [X + Y A_0^f] \frac{1}{P}, \quad \text{say}$$

and thus in the first equation

$$B_0^s = -\frac{f}{G J_0(b^s)} \left\{ 1 + \frac{X}{P} H_0(b^f) + A_0^f \left[H_0(a^f) + \frac{Y}{P} H_0(b^f) \right] \right\}$$

$$= -\frac{f}{G J_0(b^s)} [W + Z A_0^f], \quad \text{say}$$

where X, Y, W and Z have straightforward connotations.

In the third equation, substitution for B_0^f and B_0^s will not add appreciably to the coefficient of A_0^f ; $\frac{f}{F} Y$ and $-\frac{f}{G} \frac{Z}{J_0(b^s)}$ both being $\ll a^f H_1(a^f)$

since $\frac{f}{F}$ and $\frac{f}{G}$ are both very small, and $\alpha^f H_1(\alpha^f) \approx -\frac{2i}{\pi}$; further, of the constant terms $\frac{f}{F} \alpha^{f^2} \ll \alpha^{f^2}$ and $\frac{f}{G} < \frac{f}{F}$, it is possible to retain only the $-\frac{f}{FP} \left(\frac{1}{J_0(b^f)} \right)$ term from B_0^f , thus:-

$$\frac{\alpha^{f^2}}{2} + \alpha^f A_0^f H_1(\alpha^f) - \frac{f}{F} \mathcal{H} H_1(b^f) \left[\frac{1}{H_0(b^f) - \frac{\kappa^f b^f H_1(b^f)}{\kappa^f b^f J_1(b^f)}} \right] = -\frac{i\omega a^{s^2}}{2} A_0^s$$

Finally in the last equation:-

$$\begin{aligned} & \frac{\mu^f}{\mu^s} \left\{ \frac{1}{2} (c^{f^2} - a^{f^2}) + A_0^f \left[\frac{c^{f^2}}{2} H_0(\alpha^f) - \alpha^f H_1(\alpha^f) \right] + \frac{f}{FP} \left[\frac{c^{f^2}}{2} H_0(b^f) - b^f H_1(b^f) \right] (X + Y A_0^f) \right\} \\ & = -\frac{(c^{s^2} - a^{s^2})}{i\omega a^{s^2}} \left[\frac{\alpha^{f^2}}{2} + \alpha^f A_0^f H_1(\alpha^f) - \frac{f}{F} b^f H_1(b^f) \left\{ \frac{1}{H_0(b^f) - \frac{\kappa^f b^f H_1(b^f)}{\kappa^f b^f J_1(b^f)}} J_0(b^f) \right\} \right] \\ & \quad - \frac{f}{G J_0(b^f)} [W + Z A_0^f] \left[\frac{c^{s^2}}{2} J_0(b^s) - b^s J_1(b^s) \right] \end{aligned}$$

By inspection, as $\frac{\mu^f}{\mu^s} \sim 10^{-14}$, the L.H.S. is negligible compared in particular with terms in the first bracket on the R.H.S.; and neglecting again $\frac{f}{G}$ compared with $\frac{f}{F}$, and with α^{f^2} (this time)-

$$A_0^f = \frac{-\alpha^{f^2}}{2\alpha^f H_1(\alpha^f)} + \frac{f b^f H_1(b^f)}{S \alpha^f H_1(\alpha^f)} \quad \left. \vphantom{A_0^f} \right\} \quad (C.2.4)$$

$$\text{where } S = F \left[H_0(b^f) - \frac{\kappa^f b^f H_1(b^f)}{\kappa^f b^f J_1(b^f)} J_0(b^f) \right]$$

C.3. $n = 1$

For this case all six equations of the set (C.1.2) must be retained, however, the following small argument forms^(86,87) for the Bessel functions involving α^f , a^s and c^s may be used:-

$$(C.3.1) \quad \begin{aligned} J_1(x) &\approx \frac{x}{2} & J_2(x) &\approx \frac{x^2}{8} & J_0(x) &\approx 1 \\ J_1'(x) &= J_0(x) - \frac{1}{x} J_1(x) \approx 1 - \frac{1}{2} = \frac{1}{2} \quad \left(\begin{array}{l} \text{note} \\ \text{accurately } \frac{1}{2} - \frac{x^2}{8} \end{array} \right) \\ J_1''(x) &= -\frac{1}{x} J_1'(x) + \frac{1}{x^2} J_1(x) - J_1(x) \approx -\frac{x}{2} \end{aligned}$$

Further

$$\begin{aligned}
 x R_1'(x) - x^2 R_1''(x) - R_1(x) &= x R_1'(x) - [-x R_1'(x) + (1-x^2) R_1(x)] - R_1(x) \\
 &= x^2 R_1(x) - 2R_1(x) + 2x R_1'(x) \\
 &= x^2 R_1(x) - 2x R_2(x)
 \end{aligned}$$

In particular, when $R_1 = J_1$, this becomes $\lim_{x \rightarrow 0} \frac{x^3}{2} - \frac{x^3}{4} = \frac{x^3}{4}$

The set (C.1.2) may then be written (where $\epsilon_n = 2$ for $n = 1$):-

$$\begin{aligned}
 & f [a^f + A_1^f H_1(a^f)] + F B_1^f H_1(b^f) = -G B_1^s J_1(b^s) \\
 & \kappa^f \left\{ f a^f [1 + A_1^f H_1'(a^f)] + F b^f B_1^f H_1'(b^f) \right\} = -\kappa^s G b^s B_1^s J_1'(b^s) \\
 & -a^f [1 + A_1^f H_1'(a^f)] - b^f B_1^f H_1'(b^f) + \kappa_T^f D_1^f H_1(c^f) \\
 & \qquad \qquad \qquad = -i\omega \left\{ -a^s \frac{A_1^s}{2} - b^s B_1^s J_1'(b^s) + \kappa_T^s c^s \frac{D_1^s}{2} \right\} \\
 & a^f + A_1^f H_1(a^f) + B_1^f H_1(b^f) - \kappa_T^f c^f D_1^f H_1(c^f) \\
 & \qquad \qquad \qquad = -i\omega \left\{ A_1^s \frac{a^s}{2} + B_1^s J_1(b^s) - \frac{\kappa_T^s c^s D_1^s}{2} \right\} \\
 & \mu^f \left\{ \frac{a^f c^{f2}}{2} + A_1^f [a^f H_1'(a^f) + (\frac{c^{f2}}{2} - 1) H_1(a^f)] + B_1^f [b^f H_1'(b^f) + (\frac{c^{f2}}{2} - 1) H_1(b^f)] \right\} \\
 & \qquad \qquad \qquad + \kappa_T^f D_1^f [c^f H_1'(c^f) - H_1(c^f)] \\
 & \qquad \qquad \qquad = \mu^s \left\{ A_1^s \frac{a^s}{2} (\frac{c^{s2}}{2} - \frac{a^{s2}}{4}) + B_1^s [b^s J_1'(b^s) + (\frac{c^{s2}}{2} - 1) J_1(b^s)] - \frac{\kappa_T^s c^s D_1^s}{8} \right\} \\
 & \mu^f \left\{ -\frac{a^{f3}}{4} + A_1^f [a^f H_1'(a^f) - H_1(a^f)] + B_1^f [b^f H_1'(b^f) - H_1(b^f)] + \frac{\kappa_T^f D_1^f}{2} [c^{f2} H_1(c^f) - 2c^f H_1(c^f)] \right\} = \mu^s \left\{ \frac{A_1^s (-a^{s3})}{8} \right. \\
 & \qquad \qquad \qquad \left. + B_1^s [b^s J_1'(b^s) - J_1(b^s)] + \frac{\kappa_T^s c^{s3}}{8} D_1^s \right\}
 \end{aligned}$$

From the first two equations of (C.3.2), it is possible to write,

$$B_1^f = \frac{F}{F} \left\{ a^f \left(\frac{1}{J_1(b^f)} - \frac{\kappa^f}{\kappa^s b^s J_1'(b^s)} \right) + A_1^f \left(\frac{H_1(b^f)}{J_1(b^f)} - \frac{H_1(c^f) \kappa^f a^f}{\kappa^s b^s J_1'(b^s)} \right) \right\} \\
 \left[\left\{ \frac{\kappa^f b^f H_1'(b^f)}{\kappa^s b^s J_1'(b^s)} \right\} - \frac{H_1(b^f)}{J_1(b^f)} \right] \quad (C.3.3)$$

As with $n=0$, since $\left| \frac{F}{F} \right|$ is small (approx. 10^{-7} at 1000 c/s),

Substitution of (C.3.3) in either of the first two equations of (C.3.1) does not appreciably affect the coefficients of A_i^f (for instance $a^f H_i(a^f) \simeq -\frac{2i}{11}$) or the constant terms (a^f).

Further from the fifth equation of (C.3.2) if β_i^f may be written from (C.3.3).

$$\beta_i^f = \frac{f}{F} \frac{L}{M}, \quad \text{then}$$

$$\beta_i^s = \frac{f}{G J_i(b^s)} \left\{ \left[a^f + A_i^f H_i(a^f) \right] + H_i(b^f) \frac{L}{M} \right\} \quad (\text{C.3.4})$$

and the small size of $\left| \frac{f}{G} \right|$ ($\sim 10^{-14}$ at 1000 c/s) may again be called upon to indicate that β_i^s , also has a negligible effect on the last two equations of (C.3.2). Thus from these,

$$D_i^f = - \frac{a^f H_2(a^f)}{\kappa_T^f c^f H_2(c^f)} A_i^f \quad (\text{C.3.5})$$

It can further be seen, that in subtraction of the last two equations of (C.3.2) and neglecting $\frac{c^{s2}}{2}$ compared with 1 ($\frac{c^{s2}}{2} \sim 10^{-12}$ at 1000 c/s), β_i^s terms vanish anyway, and β_i^f terms do not contribute anything appreciable compared with other terms (by the previous arguments),

thus,

$$A_i^s \frac{a^s c^{s2}}{4} \mu^s - \frac{\kappa_T^s c^{s3}}{4} \mu^s D_i^s = \frac{\mu^f a^f c^{f2}}{2} + \frac{\mu^f c^{f2} H_1(a^f) A_i^f}{2} - \frac{\mu^f c^{f2} H_1(c^f) \kappa_T^f D_i^f}{2}$$

i.e. in the second equation of (C.3.1), D_i^s may be eliminated

$$a^f + A_i^f H_1(a^f) - \kappa_T^f c^f D_i^f H_1'(c^f) = \left(-\frac{j\omega}{\mu^s c^{s2}} \right) \left[\frac{\mu^f a^f c^{f2}}{2} + \frac{\mu^f c^{f2} H_1(a^f) A_i^f}{2} - \frac{\mu^f c^{f2} H_1(c^f) \kappa_T^f D_i^f}{2} \right]$$

giving, finally, with further use of relevant recurrence relations,

$$(C.3.6) \quad A_i^f = \frac{-a^f \left(1 + \frac{j\omega \mu^f c^{f2}}{\mu^s c^{s2}} \right)}{\left\{ H_1(a^f) \left(1 + \frac{j\omega \mu^f c^{f2}}{\mu^s c^{s2}} \right) + a^f H_2(a^f) \left[\left(1 + \frac{j\omega \mu^f c^{f2}}{\mu^s c^{s2}} \right) \frac{H_1(c^f)}{c^f H_2(c^f)} - 1 \right] \right\}}$$

It may be noted that the procedure used for A_0^f and A_1^f above involves a somewhat more refined argument, in each case, than that employed by Epstein and Carhart⁽⁴⁶⁾ for the spherical case (fluid/fluid). Where, for the corresponding A_0^f , the heat flow equation is divided through by $\kappa^f F$, and the term in $\frac{f}{F}$ then neglected; and for the corresponding A_1^f , the temperature and heat flow equations are made identically zero, neglecting β_1^f , and β_1^s , terms in the remaining equations.

C.4. Fibre rigidly fixed in space

For investigating the effect of variation in the angle of incidence of the incident plane wave on the scattering coefficients A_n^f , it is convenient to consider the simplified case of a fibre rigidly fixed in space.

This case is also, of interest, when considering the effect on the absorption characteristics of a fibre block of resin bonding (Chapter 5).

For a rigid fibre, the potentials ϕ_D^s , ϕ_{TM}^s , ψ^s , and χ^s vanish, i.e. the coefficients A_n^s , B_n^s , C_n^s and D_n^s are all zero. Thus if the fibre is also fixed in space, the boundary conditions which may be applied, are merely, continuity of temperature (i.e. zero variation) and the necessity for zero velocity (displacement) at the fibre boundary. The temperature gradient is not necessarily zero at this boundary, however, the conditions cited are sufficient to evaluate the A_n^f .

C.4.1 $n = 0$

From the set (C.1.1), the relations (C.2.2) and the argument of C.2 which concerns the D_n^f , the relevant conditions may be written:-

$$\left. \begin{aligned} f [1 + A_0^f H_0(a^f)] + F B_0^f H_0(b^f) &= 0 \\ a^f \left[\frac{a^f}{2} + A_0^f H_1(a^f) \right] + b^f B_0^f H_1(b^f) - i\kappa c^f C_0^f H_1(c^f) &= 0 \\ -i\kappa [1 + A_0^f H_0(a^f) + B_0^f H_0(b^f)] + (\kappa_T^{f2} - \kappa^2) C_0^f H_0(c^f) &= 0 \end{aligned} \right\} \quad (C.4.1.1)$$

From the first equation

$$B_0^f = -\frac{f}{F H_0(b^f)} \left\{ 1 + A_0^f H_0(a^f) \right\}$$

which can be substituted in the remaining two equations, neglecting terms in $\frac{f}{F}$ wherever possible i.e. in a similar manner to the procedure of C.2, giving:-

$$\begin{aligned} \left[\frac{a^{f2}}{2} - \frac{f b^f H_1(b^f)}{F H_0(b^f)} \right] + A_0^f a^f H_1(a^f) - i\kappa c^f C_0^f H_1(c^f) &= 0 \\ -i\kappa \left[-i\kappa H_0(a^f) \right] + (\kappa_T^{f2} - \kappa^2) C_0^f H_0(c^f) &= 0 \end{aligned}$$

Hence

$$A_0^f \approx \frac{\left[\frac{a^{f2}}{2} - \frac{f b^f H_1(b^f)}{F H_0(b^f)} \right] + \frac{\kappa^2 c^f H_1(c^f)}{(\kappa_T^{f2} - \kappa^2) H_0(c^f)}}{\left[\frac{-\kappa^2 c^f H_1(c^f) H_0(a^f)}{(\kappa_T^{f2} - \kappa^2) H_0(c^f)} - a^f H_1(a^f) \right]} \quad (C.4.1.2.)$$

C.4.2. $n = 1$

Similarly from the set (C.1.1) and the relations (C.3.1)

$$(C.4.2.1) \left\{ \begin{aligned} f [a^f + A_1^f H_1(a^f)] + F B_1^f H_1(b^f) &= 0 \\ -a^f [1 + A_1^f H_1(a^f)] - b^f B_1^f H_1(b^f) + i\kappa c^f H_1'(c^f) c^f \\ &\quad + \kappa_T^f D_1^f H_1(c^f) = 0 \\ a^f + A_1^f H_1(a^f) + B_1^f H_1(b^f) - i\kappa c^f H_1(c^f) - \kappa_T^f c^f H_1'(c^f) D_1^f &= 0 \\ -i\kappa [a^f + A_1^f H_1(a^f) + B_1^f H_1(b^f)] + (\kappa_T^{f2} - \kappa^2) C_1^f H_1(c^f) &= 0 \end{aligned} \right.$$

The first equation of this set, again shows that the effect of β_1^f in the other equations is entirely negligible.

Thus from the last equation of (C.4.2.1).

$$C_1^f = \frac{i\kappa}{(\kappa_T^2 - \kappa^2)} \frac{1}{H_1(c^f)} \left[a^f + A_1^f H_1(a^f) \right]$$

Substitution of this into the sum of the second and third equations of (C.4.2.1) then gives, after rearrangement

$$D_1^f = - \frac{1}{\kappa_T^2 c^f H_2(c^f)} \left\{ \left[a^f H_2(a^f) + \frac{\kappa^2}{(\kappa_T^2 - \kappa^2)} \frac{c^f H_2(c^f)}{H_1(c^f)} \frac{H_1(a^f)}{1} \right] A_1^f + \frac{\kappa^2 a^f c^f H_2(c^f)}{(\kappa_T^2 - \kappa^2) H_1(c^f)} \right\}$$

and finally, substitution for both C_1^f , and D_1^f into the third equation gives:-

$$A_1^f \approx \frac{- a^f \left\{ 1 + \frac{\kappa^2}{(\kappa_T^2 - \kappa^2)} \left[1 + \frac{c^f H_1'(c^f)}{H_1(c^f)} \right] \right\}}{\left[H_1(a^f) \left\{ 1 + \frac{\kappa^2}{(\kappa_T^2 - \kappa^2)} \left[1 + \frac{c^f H_1'(c^f)}{H_1(c^f)} \right] \right\} + a^f H_2(a^f) \frac{H_1'(c^f)}{H_2(c^f)} \right]}$$

(C.4.2.2)

C.5. Normal Incidence

For $\varphi = 0$ the boundary conditions existing and required reduce to three and four in number for $\lambda = 0$ and $\lambda = 1$, respectively, and the expressions for A_0^f and A_1^f for normal incidence are simply given by putting $k = 0$ in (C.4.1.2) and (C.4.2.2); and removing the dashes, viz:-

$$A_0^f \approx \frac{- a^f}{2 a^f H_1(a^f)} + \frac{f}{F} \frac{b^f H_1(b^f)}{H_2(b^f) a^f H_1(a^f)} \quad (C.5.1)$$

and

$$A_1^f \approx \frac{- a^f}{\left[H_1(a^f) + a^f H_2(a^f) \frac{H_1'(c^f)}{H_2(c^f)} \right]} \quad (C.5.2)$$

subject to the approximations involving $\frac{f}{F}$ made previously.

C.6. The effect of the scatterer properties on the A_n^f

C.6.1

It is easy to see that the expressions (C.5.1) and C.2.4) for A_0^f at normal incidence differ only as $FH_0(b^f)$ differs from S .

Thus allowing $\frac{\kappa^f}{\kappa^s} \rightarrow 0$ immediately makes the two expressions identical, i.e. allowing the fibre to become infinitely conducting, removes the dependence of A_0^f on the fibre properties.

It is also of interest to examine the effect of $\rho^s \rightarrow \infty$

$$\text{Now } b^s = (1+i) \left(\frac{\omega}{2\sigma^s} \right)^{\frac{1}{2}} R = (1+i) \left(\frac{\omega c \rho^s}{2\kappa^s} \right)^{\frac{1}{2}} R$$

Thus as $\rho^s \rightarrow \infty$, $b^s \rightarrow \infty$

and using the asymptotic forms of the Bessel functions introduced in

Appendix E,

$$J_0(b^s) \xrightarrow{b^s \rightarrow \infty} \left(\frac{2}{\pi b^s} \right)^{\frac{1}{2}} \cos \left[b^s - \frac{\pi}{4} \right]$$

$$\text{and } b^s J_1(b^s) \longrightarrow \left(\frac{2}{\pi b^s} \right)^{\frac{1}{2}} b^s \cos \left[b^s - \frac{3\pi}{4} \right]$$

$$\text{i.e. } \frac{J_0(b^s)}{b^s J_1(b^s)} \longrightarrow -\frac{1}{b^s} \left(\frac{\tan b^s + 1}{\tan b^s - 1} \right) \xrightarrow{b^s \rightarrow \infty} 0$$

Hence, the expected result that the value for A_0^f tends to that for a fibre rigidly fixed in space as the density of the scattering fibre increases.

C.6.2

Comparison of the expressions (C.5.2) and (C.3.6) for A_1^f at normal incidence, shows that they differ from each other only as the term $\frac{i\omega \mu^f c^2}{\mu^s c^2}$

differs from zero.

$$\text{Now } \frac{i\omega\mu^f c^f}{\mu^s c^s} = \frac{i\omega\mu^f \left(\frac{i\omega\rho^f}{\mu^f}\right) R^2}{\mu^s \left(\frac{i\omega\rho^s}{\mu^s}\right) R^2} = \frac{i\omega\rho^f}{\rho^s}$$

from the expressions (Appendix A and B) for κ_T^f, κ_T^s and the definitions of c^f, c^s (Chapter 3).

Hence, again the expected result that allowing $\frac{\rho^f}{\rho^s} \rightarrow 0$ implies the reduction of A_1^f to the value for a fibre rigidly fixed in space.

APPENDIX D CALCULATION OF ABSORPTION COEFFICIENTS AND SCATTERING
COEFFICIENTS; COMPUTER PROGRAMMES

D.1. Normal Incidence scattering coefficients

Using the expressions (C2.4), (C3.6), (C5.1) and (C5.2), from Appendix C, together with the approximate expansions of Bessel Functions given in Appendix F, the real and imaginary parts of the relevant scattering coefficients for an elastic fibre and a rigidly fixed fibre may be calculated as follows:-

Elastic fibre

$$\operatorname{Re} A_0^f = -\frac{\pi N (RA - WB)}{2(A^2 + B^2)}$$

$$\operatorname{Im} A_0^f = -\frac{\pi a^{f2}}{4} + \frac{\pi N (WA + RB)}{2(A^2 + B^2)}$$

where $\frac{f}{F} = iN$, $L = \operatorname{Re} H_0(b^f)$, $-M = \operatorname{Im} H_0(b^f)$

and $A = L - \frac{\kappa^f}{k^s} (WZ - RY)$

$$B = -M - \frac{\kappa^f}{k^s} (WY + RZ)$$

where

$$R = \operatorname{Re} [b^f H_1(b^f)] , \quad -W = \operatorname{Im} [b^f H_1(b^f)]$$

$$-Y = \operatorname{Re} \left[\frac{J_0(b^s)}{b^s J_1(b^s)} \right] , \quad +Z = \operatorname{Im} \left[\frac{J_0(b^s)}{b^s J_1(b^s)} \right]$$

$$\operatorname{Re} A_1^f = -\frac{\pi B' (1 - SL') a^{f2}}{2(A'^2 + B'^2)} , \quad \operatorname{Im} A_1^f = +\frac{A'}{B'} \operatorname{Re} A_1^f$$

where

$$L' = \frac{\omega \mu^f}{s^s c^s} , \quad c^{f2} = i\delta$$

$$A' = 2X(1 - SL') - 1 - SL' , \quad B' = 2Y(1 - SL')$$

and

$$X = \operatorname{Re} \left[\frac{A_1(c^f)}{c^f H_2(c^f)} \right] , \quad Y = \operatorname{Im} \left[\frac{H_1(c^f)}{c^f H_2(c^f)} \right]$$

Rigid fibre

$$\operatorname{Re} A_0^f = \frac{-\pi N(R_L + W_M)}{2(L^2 + M^2)}$$

$$\operatorname{Im} A_0^f = \frac{-\pi a^{f2}}{4} - \frac{\pi N(R_M - W_L)}{2(L^2 + M^2)}$$

$$\operatorname{Re} A_1^f = \frac{-\pi a^{f2} \gamma}{(2x-1)^2 + 4y^2}$$

$$\operatorname{Im} A_1^f = \frac{-\pi a^{f2}(2x-1)}{2[(2x-1)^2 + 4y^2]}$$

D.2 Oblique Incidence scattering coefficients

Similarly from the expressions (C4.1.2) and (C4.2.2) the oblique incidence scattering coefficients for a fibre rigidly fixed in space may be calculated as follows:-

$$\operatorname{Re} A_0^f = \frac{CA + BD}{A^2 + B^2}, \quad \operatorname{Im} A_0^f = \frac{AD - BC}{A^2 + B^2}$$

where

$$A = -G + HZ, \quad B = -H - GZ - \frac{2}{\pi}$$

$$C = -\frac{a^{f2}}{2} - E + G, \quad D = H - F$$

$$E = -\operatorname{Re} \left[\frac{F}{\bar{F}} \frac{b^{f*} H_1(b^f)}{H_0(b^f)} \right], \quad F = -\operatorname{Im} \left[\frac{F}{\bar{F}} \frac{b^{f*} H_1(b^f)}{H_0(b^f)} \right], \quad G = \operatorname{Re} \left[\frac{\kappa^2 c^{f*} H_1(c^f)}{(\kappa^2 - \kappa^{f2}) H_0(c^f)} \right]$$

$$H = \operatorname{Im} \left[\frac{\kappa^2 c^{f*} H_1(c^f)}{(\kappa^2 - \kappa^{f2}) H_0(c^f)} \right]$$

and the approximations

$$H_0(a^f) \approx 1 + iz$$

$$b^{f*} = b^f \left(1 + \frac{i\omega a^f}{c_0^{f2}} \sin \phi \right) \approx b^f, \quad c^{f*} = c^f \left(1 + \frac{i\omega a^f}{c_0^{f2}} \sin \phi \right) \approx c^f$$

have been made, which rely on the definitions of b^{lf} , c^{lf} given in Chapter 3 and the fact that $\frac{i\omega c^f}{c_0^{f2}}$ and $\frac{i\omega d^f}{c_0^{f2}}$ are small quantities. This is an equivalent approximation to the assumption that κ_D^f is real.

Similarly

$$\operatorname{Re} A_1^f = -\frac{\pi a^{f2}}{2z'} [a(b+2Y) - b(a+2X-2)]$$

$$\operatorname{Im} A_1^f = -\pi a^{f2} [a(a+2X-2) + b(b+2Y)]$$

where

$$a = 1 + l(1+A) - mB$$

$$b = m(1+A) + lB$$

$$\frac{\kappa^2}{(\kappa_T^2 - \kappa^2)} = l + im, \quad \frac{c^f H_1(c^f)}{H_1(c^f)} = A + iB$$

$$z' = (a + 2X - 2)^2 + (b + 2Y)^2.$$

and the approximation concerning b^{lf} , c^{lf} is again assumed

D.3 Absorption Coefficient

The Twersky theory in general (see Chapter 4) gives:

$$\kappa_b^2 = \kappa_D^{f2} - 4iNg + c^2(g^* + g)(g' - g)$$

where $c = \frac{2N}{\kappa_D^f \cos \alpha}$ and $g = \sum_n A_n^f$, $g' = \sum_n (-1)^n A_n^f$

The form of g is to the approximation suggested in Appendix E.

$$g = A_0^f + A_1^f$$

and

$$g' = A_0^f - A_1^f$$

A_0^f , A_1^f may be evaluated from D.1 and thus

$$\kappa_b^2 = \kappa_D^{f2} - 4iNg - 4c^2 A_0^f A_1^f$$

i.e. $\kappa_b = a + ib$

where generally
$$a = \frac{1}{\sqrt{2}} \left[A \pm (A^2 + B^2)^{\frac{1}{2}} \right]^{\frac{1}{2}}, \quad b = \frac{B}{2a}$$

$$A = \kappa_D^f + 4N \operatorname{Im} g - 4c^2 \left[\operatorname{Re} A_0^f \operatorname{Re} A_1^f - \operatorname{Im} A_0^f \operatorname{Im} A_1^f \right]$$

$$B = -4N \operatorname{Re} g - 4c^2 \left[\operatorname{Re} A_0^f \operatorname{Im} A_1^f + \operatorname{Im} A_0^f \operatorname{Re} A_1^f \right]$$

To be consistent with the previously used convention for a forward travelling wave (Chapter 3), (a) must be real and positive.

i.e.
$$a = + \left[\frac{1}{2} \left\{ A + (A^2 + B^2)^{\frac{1}{2}} \right\} \right]^{\frac{1}{2}}$$

Further from Chapter 4, the relative characteristic impedance is given by

$$\left(\frac{1-Q}{1+Q} \right) = v + iw$$

$$v = \frac{eg + df}{g^2 + f^2}, \quad w = \frac{dg - ef}{g^2 + f^2}$$

$$e = 2c \operatorname{Re} A_1^f - b, \quad d = \kappa_D^f + 2c \operatorname{Im} A_1^f + a$$

$$g = 2c \operatorname{Re} A_0^f - b, \quad f = \kappa_D^f + 2c \operatorname{Im} A_0^f + a$$

and the surface normal impedance

$$z_n = \rho_0^f c_0^f (v + iw)(R + iS)$$

where

$$R + iS = \frac{\left\{ 1 + e^{-2bd} (\cos 2ad + i \sin 2ad) \right\}}{\left\{ 1 - e^{-2bd} (\cos 2ad + i \sin 2ad) \right\}}$$

Thus finally

$$a_0 = \frac{4(VR - SW)}{(VR - SW + 1)^2 + (RW + VS)^2}$$

The following computer program, written in Algol 60 for use with the English Electric - Leo-Marconi KDF-9 machine at Leeds University, was

used for calculation of normal incidence absorption coefficients according to expression (D.3).

The various materials for which experimental values existed, were typed in terms of mean fibre radius, slab density and slab thickness and this data together with the constants tabled in Appendix F were input.

It should be noted that the program, as written, outputs values of a_0 , for a given slab density and thickness, for each of the values of mean fibre radius fed in.

This program was modified to calculate absorption coefficients for oblique incidence in the XY plane, by including an extra loop for values of incident angle from 0° to 90° , and by replacing the expressions for K_b , α_o , V and W , as in D.3 by deviations of them based on expressions 4.2.17 to 4.2.19. Similarly a program was written to compute oblique incidence scattering coefficients according to the expressions (4.2.17 to 4.2.19).

```

begin           comment  Calculation of normal incidence absorption coefficient
                    against frequency for fibre glass by a scattering theory
                    developed by Attenborough. Variation with fibre radius
                    slab density and slab thickness is also considered.;

                    library A0,A6;

                    integer i,j,k,n,m,s,kt,l,f0,f1,f2,f3;

                    real   w,gamma,rof,ros,kf,ks,cpf,cps,muf,mus,pi,rog,b,af,Cof,
                    Cos,N,nuf,kdf,C,cs,c,Z,Y,W,R2,L,M,A,B,ReAOf,ImAOf,P,Q,
                    S,T,LL,YY,X,x,ReA1f,ImA1f,ReRigAOf,ImRigAOf,ReRigA1f,
                    ImRigA1f,yxz,V,gg,WW,RR,SS,kfg,a0,NN,Reg,Img,d,e,ff,g,mm,
                    pp,AA,BB,AAA,BBB,sigmaf,sigmas,delta,a,bb,ll,yy,xx;

                    open(20);           open(70);

                    f0:= format([2s+d.ddd10+nd]);
                    f1:= format([2s+nddd.ddddd]);
                    f2:=format([2s+d.ddd10+ndc]);
                    f3:= format([2s+nddd]);

```

```
Cof:=read(20); gamma:=read(20); rof:=read(20);  
rog:= ros:=read(20); kf:=read(20); ks:=read(20);  
cpf:=read(20); cps:=read(20); Cos:=read(20);  
muf:=read(20); mus:=read(20); n:=read(20);  
m:=read(20); s:=read(20); kt:=read(20);
```

```
begin integer array f[1:n];  
  array R[1:m], t[1:s], ro[1:kt];  
  for i:=1 step 1 until n do f[i]:=read(20);  
  for i:=1 step 1 until m do R[i]:=read(20);  
  
  for i:=1 step 1 until s do t[i]:=read(20);  
  for i:=1 step 1 until kt do ro[i]:=read(20);  
  close(20);  
  pi:=3.142; nuf:=muf/rof; sigmaf:=kf/(rof*cpf);  
  sigmas:=ks/(ros*cps);  
  write text(70,[[2c]i[2s]j[2s]l[2s]k[2s]V[6s]WW[6s]a[6s]  
bb[6s]a0[4s]ImRigA1f[2c]]);
```

```

for i:= 1 step 1 until n do
begin w:=2* $\pi$ *f[i]; N:=( $\gamma$ -1)*w*x* $\sigma$ /Cof $\uparrow$ 2;
      kdf:=w/Cof;
      for j:=1 step 1 until m do
      begin b:=sqrt(w/(2*x* $\sigma$ ))*R[j]; af:=w*R[j]/Cof;
            cs:=sqrt( $\rho$ / $\mu$ )*R[j]*w;
            c:=(w/nuf)*R[j] $\uparrow$ 2;
            Z:=(-12-b $\uparrow$ 4/36)/(48+b $\uparrow$ 4);
            Y:=(48+2*b $\uparrow$ 4)/(48*b $\uparrow$ 2+b $\uparrow$ 6)*(-1);
            x:=w*R[j] $\uparrow$ 2/(4*x* $\sigma$ ); W:=2/ $\pi$ +x;
            xx:=(ln(sqrt(w/ $\sigma$ )/2*R[j]));
            R2:=2*x/ $\pi$ -4*x/ $\pi$ *(xx+0.5772); L:=0.5+(xx+0.5772)*2*x
                                                    x/ $\pi$ -2*x/ $\pi$ ;
            M:=0.5*x-(xx+0.5772)*2/ $\pi$ ;
            A:=L-kf/ks*(R2*Z+W*Y); B:=-M-kf/ks*(R2*Y-W*Z);
            delta:=w/nuf*R[j] $\uparrow$ 2;

```

$$\text{ReAof} := -\pi \times N \times (R2 \times A - W \times B) / (2 \times (A \uparrow 2 + B \uparrow 2));$$

$$\text{ImAof} := -\pi \times a \uparrow 2 / 4 + \pi \times N \times (W \times A + R2 \times B) / (2 \times (A \uparrow 2 + B \uparrow 2));$$

$$yy := (0.5772 + 0.5 \times \ln(c) - \ln(2));$$

$$P := c / (2 \times \pi) - c / \pi \times yy + c \uparrow 2 / 32; Q := 2 / \pi - c \uparrow 2 / 8 \times 1$$

$$/ \pi \times (-5/4 + yy) + c$$

$$/ 4;$$

$$S := c / \pi - c \uparrow 3 / 48 \times 1 / \pi \times yy - c \uparrow 2 / 16;$$

$$T := 4 / \pi + c \uparrow 2 / (16 \times \pi) \times (4 \times yy - 3);$$

$$X := (P \times S + Q \times T) / (S \uparrow 2 + T \uparrow 2);$$

$$LL := m \uparrow f \times w / m \uparrow s \times c \uparrow 2;$$

$$AA := 2 \times X \times (1 - \text{delta} \times LL) - 1 - \text{delta} \times LL;$$

$$YY := (T \times P - Q \times S) / (S \uparrow 2 + T \uparrow 2);$$

$$BB := 2 \times YY \times (1 - \text{delta} \times LL);$$

$$\text{ReA1f} := -\pi \times BB \times (1 - \text{delta} \times LL) \times a \uparrow 2 / (2 \times (AA \uparrow 2 + BB \uparrow 2));$$

$$\text{ImA1f} := \text{ReA1f} \times AA / BB;$$

$$\text{ReRigAof} := -0.5 \times \pi \times N \times (R2 \times L + W \times M) / (L \uparrow 2 + M \uparrow 2);$$

$$\text{ImRigAof} := -\pi \times a \uparrow 2 / 4 - \pi \times N / 2 \times (R2 \times M - W \times L) / (L \uparrow 2 + M \uparrow 2);$$

$$\text{ReRigA1f} := -\pi \times a \uparrow 2 \times YY / ((2 \times X - 1) \uparrow 2 + 4 \times YY \uparrow 2);$$

$$\text{ImRigA1f} := 0.5 \times \text{ReRigA1f} \times (2 \times X - 1) / YY;$$

```

for l:=1 step 1 until kt do
  begin NN:=ro[1]/(pi×R[j]↑2×rog);
        C:= 2×NN/kdf;Reg:=ReAOf+ReA1f;
        Img:= ImAOf+ImA1f;
        AAA:=kdf↑2+4×NN×Img-4×C↑2×
              (ReA1f×ReAOf-ImA1f×ImAOf);
        BBB:=-4×NN×Reg-4×C↑2×
              (ReAOf×ImA1f+ImAOf×ReA1f);
        a:=sqrt(0.5×(AAA+sqrt(AAA↑2+BBB↑2)));
        bb:=BBB/(2×a);
        d:=kdf+2×C×ImA1f+a;e:=2×C×ReA1f-bb;
        ff:=kdf+2×C×ImAOf+a;g:=2×C×ReAOf-bb;
        for k:=1 step 1 until s do
          begin yxz:=exp(-2×bb×t[k]);
                ll:=1+yzx×sin(2×a×t[k]);
                mm:=yzx×cos(2×a×t[k]);
                pp:=1-yzx×sin(2×a×t[k]);
                gg:=g↑2+ff↑2;kfg:=pp↑2+mm↑2;
                V:=(exg+d×ff)/gg;WW:=(d×g-exff)/gg;
                RR:=(ll×pp-mm↑2)/kfg;SS:=mm×(pp+ll)/kfg;

```

```

a0:=-4x(VXRR-SSxWW)/((VXRR-SSxWW+1)↑2
+(RRxWW+VXSS)↑2);
write(70,f3,i);write(70,f3,j);write(70,f3,l);write
(70,f3,k);write(70,f1,V);write(70,f1,WW);write(70,f1,a
); write(70,f1,bb);write(70,f1,a0);write(70,f2,ImRigA1f);
end;
Reg:=ReRigA0f+ReRigA1f;
Img:=ImRigA0f+ImRigA1f;
AAA:=kdf↑2+4xNNxImg-4xC↑2x
(ReRigA1fxReRigA0f-ImRigA1fxImRigA0f);
BBB:=-4xNNxReg-4xC↑2x(ReRigA0fxImRigA1f
+ImRigA0fxReRigA1f);
a:=sqrt(0.5x(AAA+sqrt(AAA↑2+BBB↑2)));
bb:=BBB/(2xa);
d:=kdf+2xCxImRigA1f+a;e:=2xCxReRigA1f-bb;
ff:=kdf+2xCxImRigA0f+a;g:=2xCxReRigA0f-bb;

```

```

for k:=1 step 1 until s do
begin yxz:=exp(-2×bb×t[k]);
      ll:=1+yzx×sin(2×axt[k]);
      mm:=yzx×cos(2×axt[k]);
      pp:=1-yxz×sin(2×axt[k]);
      gg:=g↑2+ff↑2;kfg:=pp↑2+mm↑2;
      V:=(exg+dxff)/gg;WW:=(dxg-exff)/gg;
      RR:=(11×pp-mm↑2)/kfg;
      SS:=mm×(pp+11)/kfg;
      a0:=4×(V×RR-SS×WW)/((V×RR-SS×WW+1)↑2
                        +(RR×WW+V×SS)↑2);

```

```

write(70,f3,i);write(70,f3,j);write(70,f3,l);write(
70,f3,k);write(70,f1,V);write(70,f1,WW);write(70,f1,a);
write(70,f1,bb);write(70,f2,a0);

```

end

end end end end;close(70)

end→

APPENDIX E. ATTENUATION DUE TO A SINGLE CYLINDRICAL SCATTERER

E.1. The Dissipation Integral

Briefly outlining Epstein and Carhart's approach⁴⁶⁾ for fluid spheres, the time average of the overall energy loss consists of viscous and thermal parts** viz:-

$$W = W_{\mu} + W_{\sigma}$$

where

$$W_{\mu} = \int_F \left\langle v_j P_{Nj} \right\rangle_{Av} dF + \int_V \left\langle P \nabla \cdot \tilde{v} \right\rangle_{Av} dV$$

and

$$W_{\sigma} = \int_V \left\langle \frac{\kappa^f}{T_0} (\nabla^2 T) \right\rangle_{Av} dV$$

in which N signifies the component of P_{ij} in the direction of the outward normal drawn from the surface F of a large volume V surrounding the scatterer concerned.

Remembering that v_j and P_{Nj} contained in the time average are complex and have time dependence $e^{(-i\omega t)}$; and introducing the complex number notation

**

The energy losses are given by the integration and time average of the viscous and thermal dissipation functions

$$\phi_{\mu} = \frac{1}{2} P'_{ij} d_{ij}$$

and

$$\phi_{\sigma} = \frac{\kappa^f}{T_0} (\nabla T)^2$$

(P'_{ij} is the dissipative part of the total stress tensor)

respectively.

The viscous dissipation function ϕ_{μ} has the standard form introduced by Rayleigh ("Theory of Sound" vol. I. Ch. 4), the tensor expression above being used by Mason⁽⁷¹⁾. The thermal dissipation function ϕ_{σ} is derived by Tolman and Fine (Rev. Mod. Phys. 20, 51, 1948).

$$\text{Re} \langle x \rangle = \frac{1}{2} [x + x^*]$$

the time mean can be considered from

$$\begin{aligned} \langle \text{Re} [x e^{-i\omega t} y e^{-i\omega t}] \rangle_{Av} &= \frac{1}{4} \langle (x e^{i\omega t} + x^* e^{-i\omega t})(y e^{i\omega t} + y^* e^{-i\omega t}) \rangle \\ &= \frac{1}{2} \text{Re}(x^* y) = \frac{1}{2} \text{Re}(x y^*) \end{aligned}$$

as the terms in $e^{-2i\omega t}$ and $e^{2i\omega t}$ vanish in the time averaging.

Thus the dissipation expressions above can be written in the forms

$$\begin{aligned} W_\mu &= \frac{1}{2} \text{Re} \left\{ \int_F v_j^* P_{Nj} dF + \int_V p^* \nabla \cdot \underline{v} dV \right\} \\ W_\sigma &= \frac{1}{2T_0} \text{Re} \left\{ K^f \int_F T^* \left(\frac{\partial T}{\partial N} \right) dF - K^f \int_V T^* \nabla^2 T dV \right\} \end{aligned}$$

The analysis⁽⁴⁶⁾ shows that the sum of the second terms (i.e. the volume integrals) of each expression is zero whilst the first term of W_σ is negligible leaving the total

$$W = \frac{1}{2} \text{Re} \int_F v_j^* P_{Nj} dF \quad (\text{E.1})$$

in which the time dependence is now suppressed.

This argument is unaffected by change from a spherical to a cylindrical coordinate system, thus for a single cylindrical fibre choosing V to be a large concentric cylindrical volume, radius B and surface F_1 , the integral (E.1) can be evaluated again following Epstein and Carhart⁽⁴⁶⁾ where the contributions of the surface integrals over the interior and exterior surfaces F_2 and F_3 of the scatterer cancel, due to the continuity of both the v_j and P_{Nj} across the scatterer boundary (the P_{Nj} being equal and opposite for F_2 and F_3).

If the radius B is chosen sufficiently large the highly damped thermal and viscous potentials will not contribute at F_1 and in the expressions for v_j and P_{Nj} viz. (3.1312) and (3.1321) terms in r^{-1} may

be neglected compared with terms in r^0 , and r^{-2} terms neglected against r^{-1} terms.

Thus it is possible to write

$$v_r = -\frac{\partial \bar{\phi}}{\partial r} \quad v_\theta = -\frac{1}{r} \frac{\partial \bar{\phi}}{\partial \theta} \quad v_z = -\frac{\partial \bar{\phi}}{\partial z}$$

and

$$P_{rr} = i\omega \rho_0^f \bar{\phi} + 2\mu^f \frac{\partial^2 \bar{\phi}}{\partial r^2}$$

$$P_{\theta\theta} = \mu^f \left[-\frac{2}{r} \frac{\partial^2 \bar{\phi}}{\partial r \partial \theta} + \frac{2}{r^2} \times \frac{\partial^2 \bar{\phi}}{\partial \theta^2} \right]$$

$$P_{rz} = \mu^f \left(-2 \frac{\partial^2 \bar{\phi}}{\partial r \partial z} \right)$$

where $\bar{\phi} = \phi_i + \phi_b^f$

For large r , obviously the product $v_\theta^* P_{r\theta}$ may be neglected (e.g. compared with $v_r^* P_{rr}$) as it decreases with $\frac{1}{r^2}$; thus it is required to obtain only

$$W = \frac{1}{2} \operatorname{Re} \int_{F_1} (v_r^* P_{rr} + v_z^* P_{rz}) dF_1 \quad (\text{E.2})$$

E.2. Oblique incidence

In general (89) the element of area on the surface $\xi_1 = \text{const.}$ in curvilinear coordinates ξ_1, ξ_2, ξ_3 with parameters h_1, h_2, h_3 is

$$dF_1 = h_2 h_3 d\xi_2 d\xi_3$$

i.e. for cylindrical polars $dF_1 = B d\theta dz$ and $\int_{F_1} dF_1 = \int_0^\pi 2B d\theta \int_0^L dz$

where L is the length of the cylindrical fibre.

Further, defining

$$\lambda_n = e_n J_n(k_0^f r) + A_n^f H_n(k_0^f r)$$

then

$$\bar{\phi} = \exp(ikz) \sum_{n=0}^{\infty} i^n \lambda_n(k_0^f r) \cos(n\theta)$$

and

$$\frac{1}{2} \operatorname{Re} \int_{F_1} v_r^* P_{rr} dF_1 = \int \frac{1}{2} \operatorname{Re} (v_r P_{rr}^*) dF_1$$

$$= \frac{1}{2} \operatorname{Re} \int_{F_1} \left\{ \left[-\exp(ikz) \sum_{n=0}^{\infty} i^n k_0^f \lambda_n'(k_0^f B) \cos(n\theta) \right] \times \right.$$

$$\left. \left[(-i\omega \rho_0^f - 2\mu^f k^2) \exp(-ikz) \sum_{n=0}^{\infty} (-i)^n \lambda_n^*(k_0^f B) \cos(n\theta) \right] \right\} dF_1$$

the orthogonality of $\cos(\lambda B)$ then picks out the $m = n$ terms, leaving

$$\frac{1}{2} \operatorname{Re} \int_{F_1} v_r^* P_r dF_1 = \frac{1}{2} \operatorname{Re} \left\{ 2(i\omega\rho_0^f + 2\mu^f \kappa^2) L \kappa_0^f B \sum_{n=0}^{\infty} \frac{\pi}{\epsilon_n} \lambda_n' \lambda_n^* \right\} \quad (\text{E.3})$$

Similarly

$$\frac{1}{2} \operatorname{Re} \int_{F_1} v_z^* P_z dF_1 = \frac{1}{2} \operatorname{Re} \left\{ 4\mu^f \kappa^2 L \kappa_0^f B \sum_{n=0}^{\infty} \frac{\pi}{\epsilon_n} \lambda_n' \lambda_n^* \right\} \quad (\text{E.4})$$

where

$$\epsilon_n = \begin{cases} 1 & n=0 \\ 2 & n>0 \end{cases}$$

Now assuming κ_0^f is real i.e. neglecting the damping of the fluid dilatational wave (the order of small quantities, see Appendix A),

$$\begin{aligned} \sum_{n=0}^{\infty} \lambda_n' \lambda_n^* &= \sum_{n=0}^{\infty} \left[\epsilon_n J_n'(\kappa_0^f B) + A_n^f H_n'(\kappa_0^f B) \right] \left[\epsilon_n J_n(\kappa_0^f B) + A_n^{f*} H_n^*(\kappa_0^f B) \right] \\ &= \sum_{n=0}^{\infty} \left[\epsilon_n^2 J_n J_n' + \epsilon_n A_n^f H_n' J_n + \epsilon_n A_n^{f*} J_n' H_n^* + A_n^f A_n^{f*} H_n' H_n^* \right] \end{aligned}$$

and as $\frac{1}{2} \operatorname{Re}(ix) = \frac{1}{4} i(x - x^*)$

$$\frac{1}{2} \operatorname{Re} \left(i \sum_{n=0}^{\infty} \lambda_n' \lambda_n^* \right) = \frac{1}{2} \operatorname{Re} \left\{ i \sum_{n=0}^{\infty} \left[\epsilon_n A_n^f (J_n H_n' - J_n' H_n) + A_n^f A_n^{f*} H_n' H_n^* \right] \right\}$$

Then using the recurrence relation ⁽⁸⁷⁾ (E.5)

$$x R_n'(x) + n R_n(x) = x R_{n-1}(x) \quad \text{where } R_n = J_n \text{ or } H_n$$

and the large argument approximations ⁽⁹⁰⁾,

$$J_n^{(1)}(x) \xrightarrow{x \rightarrow \infty} \left(\frac{2}{\pi x} \right)^{\frac{1}{2}} \cos \left[x - \frac{1}{2} \pi \left(n + \frac{1}{2} \right) \right]$$

$$H_n^{(1)}(x) \xrightarrow{x \rightarrow \infty} \left(\frac{2}{\pi x} \right)^{\frac{1}{2}} \exp \left[ix - \frac{1}{2} i \pi \left(n + \frac{1}{2} \right) \right]$$

$$\begin{aligned} J_n H_n' - J_n' H_n &= \left(H_{n-1} - \frac{n}{x} H_n \right) J_n - \left(J_{n-1} - \frac{n}{x} J_n \right) H_n \\ &= H_{n-1} J_n - J_{n-1} H_n \\ &\approx \left(\frac{2}{\pi x} \right) \left\{ \exp \left[ix - \frac{1}{2} i \pi \left(n - \frac{1}{2} \right) \right] \cos \left[x - \frac{1}{2} \pi \left(n + \frac{1}{2} \right) \right] \right. \\ &\quad \left. - \cos \left[x - \frac{1}{2} \pi \left(n - \frac{1}{2} \right) \right] \exp \left[ix - \frac{1}{2} i \pi \left(n + \frac{1}{2} \right) \right] \right\} \\ &= \left(\frac{2}{\pi x} \right) \left\{ \exp \left[ix - \frac{1}{2} i \pi \left(n + \frac{1}{2} \right) \right] \left\{ i \cos \left[x - \frac{1}{2} \pi \left(n + \frac{1}{2} \right) \right] \right\} \right. \\ &\quad \left. + \sin \left[x - \frac{1}{2} \pi \left(n + \frac{1}{2} \right) \right] \right\} \\ &= \left(\frac{2i}{\pi x} \right) \quad (\text{E.6}) \end{aligned}$$

Similarly

$$H_n' H_n^* \approx \left(\frac{2i}{\pi x} \right) - \left(\frac{2n}{\pi x^2} \right)$$

The second term vanishes anyway for $\lambda = 0$, and may be neglected otherwise if the condition $x \rightarrow \infty$, which allowed the approximate forms of J_n and H_n to be used, obtains

$$\text{i.e. write } H_n' H_n^* \simeq \left(\frac{2i}{\pi x} \right) \quad (\text{E.7})$$

It should be noted that this argument requires B to be very large (as κ_D^f is small) viz. $B \sim 10 \text{ cm}$ at 10 kc/s and $B \sim 10^3 \text{ cm}$. at 50 kc/s .

Further from the "generalised Snell's law" of (3.125) and also from Appendix A.

$$\kappa^2 = \kappa_r^f \sin^2 \Theta^f = \frac{i\omega\beta_0^f}{\mu^f} \sin^2 \Theta^f \quad (\text{E.8})$$

$$\left(\sin \Theta^f = \frac{\kappa_0^f}{\kappa_r^f} \sin \varphi \right)$$

thus using (E.3) - (E.8) in (E.2)

$$W = -2\omega\beta_0^f (1 + 4\sin^2 \Theta^f) L \text{Re} \left[\sum_{\lambda=0}^{\infty} \left(A_\lambda^f + \frac{1}{\epsilon_\lambda} A_\lambda^f A_\lambda^{f*} \right) \right] \quad (\text{E.9})$$

where the A_λ^f have their oblique incidence values (Appendix C4).

E.3. Normal Incidence

For the particular case of normal incidence required in Chapter 4, $K = 0$ (the z components of the V_j and P_{Nj} vanish) the A_n^f take on their normal incidence values (Appendix C) and the time averaged energy loss per scatterer of length L is given by

$$W = -2\omega\beta_0^f L \text{Re} \left[\sum_{\lambda=0}^{\infty} \left(A_\lambda^f + \frac{1}{\epsilon_\lambda} A_\lambda^f A_\lambda^{f*} \right) \right] \quad (\text{E.10})$$

As can be seen from Appendix C, the values of the A_n^f will involve orders of higher powers of α^f as n increases e.g. A_2^f will be at least $\alpha^f \times A_1^f$ as $J_2(\alpha^f) \sim \frac{\alpha^{f2}}{8}$ and $J_1(\alpha^f) \sim \frac{\alpha^f}{2}$. Thus as $\alpha^f \sim 10^{-5}$ over the audio frequency range of interest, it seems a satisfactory approximation (following Epstein and Carhart⁽⁴⁶⁾) to consider only the values of A_0^f and A_1^f i.e. it is possible to write

$$W \simeq -2\omega\beta_0^f L \text{Re} (A_0^f + A_1^f) \quad (\text{E.11})$$

where further $A_n^f A_n^{f*}$ has been neglected compared with A_n^f (calculation showing that $A_0^f \sim 10^{-6}$, $A_1^f \sim 10^{-5}$ even at higher frequencies).

APPENDIX FA. Material Constants used in calculations (46, 91, 111, 112)

AIR	GLASS
$\mu = 0.1825 \times 10^{-3} \text{ g cm}^{-1} \text{ sec}^{-1}$	$41 \times 10^{10} \text{ dynes/cm}^2 \text{ (fibre)}$
$\rho = 1.17 \times 10^{-3} \text{ g cm}^{-3}$	2.3 g cm^{-3}
$C_0 = 3.44 \times 10^4 \text{ cm sec}^{-1}$	$5.749 \times 10^5 \text{ cm sec}^{-1}$
$C_p = 0.240 \text{ cal gm}^{-1} \text{ }^\circ\text{C}^{-1}$	$0.198 \text{ cal gm}^{-1} \text{ }^\circ\text{C}^{-1}$
$\delta = 1.4$	1.0
$K = 0.000058 \text{ cal sec}^{-1} \text{ }^\circ\text{C}^{-1} \text{ cm}^{-1}$	$0.00155 \text{ cal sec}^{-1} \text{ }^\circ\text{C}^{-1} \text{ cm}^{-1}$
	$-6.021 \times 10^{10} \text{ dynes cm}^{-2}$
$B = P_{AT}$	$4.0 \times 10^{11} \text{ dynes cm}^{-2} \text{ (fibre)}$
$\beta = 1/T \text{ (absolute)}$	$2.5 \times 10^{-5} \text{ }^\circ\text{K}^{-1}$

B. Approximate expansions of Bessel Functions

Using the well-known expansions⁽⁸⁷⁾ for the cylindrical Bessel function of the first kind and the Weber Bessel function of the second kind respectively, i.e.

$$J_n(z) = \sum_{k=0}^{\infty} (-1)^k \frac{\left(\frac{1}{2}z\right)^{n+2k}}{k!(n+k)!}$$

$$Y_n(z) = \frac{2}{\pi} \left\{ \gamma + \ln\left(\frac{1}{2}z\right) \right\} J_n(z) - \frac{1}{\pi} \sum_{k=0}^{n-1} \frac{(n-k-1)!}{k!} \left(\frac{z}{2}\right)^{n-2k} \\ - \frac{1}{\pi} \sum_{k=0}^{\infty} (-1)^k \frac{\left(\frac{1}{2}z\right)^{n+2k}}{k!(n+k)!} \left\{ \left(1 + \frac{1}{2} \dots \frac{1}{k}\right) + \left(1 + \frac{1}{2} \dots \frac{1}{n+k}\right) \right\}$$

where γ (Euler's constant) = 0.5772 ...

the following approximate expressions can be derived:-

$$c^f H_1(c^f) = \frac{1}{2} \frac{\delta}{\pi} - \frac{\delta}{\pi} \left\{ \gamma + \frac{1}{2} \ln \delta - \ln 2 \right\} + \frac{\delta^2}{32} - i \left[\frac{\delta}{\pi} + \frac{\delta}{4} - \frac{\delta^2}{8\pi} \left\{ \frac{-5}{4} + \gamma + \frac{1}{2} \ln \delta - \ln 2 \right\} \right] \quad (F.1)$$

where $c^{f2} = i\delta$ and c^f is small such that for higher powers than 4 it may be neglected compared with 1.

Similarly

$$c^{f+} H_2(c^f) = \frac{\delta}{\pi} - \frac{\delta^2}{16} - \frac{\delta^3}{48\pi} \left(\gamma + \frac{1}{2} \ln \delta - \ln 2 \right) + \frac{\delta^2}{\pi} \cdot \frac{17}{256} - i \left[\frac{4}{\pi} + \frac{\delta^2}{16\pi} \left\{ 4 \left(\gamma + \frac{1}{2} \ln \delta - \ln 2 \right) - 3 \right\} \right] \quad (F.2)$$

Further

$$\operatorname{Re} J_0(b^3) = 1 - \frac{1}{16} b^4 + \frac{1}{6(24)^2} b^8 \quad (F.3)$$

$$\operatorname{Im} J_0(b^3) = -\frac{b^2}{2} + \frac{b^6}{8 \cdot 36} \quad (F.4)$$

$$\operatorname{Re} b^3 J_1(b^3) = \frac{b^4}{4} - \frac{b^8}{(64)(48)} \quad (F.5)$$

$$\operatorname{Im} b^3 J_1(b^3) = b^2 - \frac{b^6}{48} \quad (F.6)$$

where $b^3 = (1+i) \left(\frac{\omega}{2\sigma^3} \right)^{\frac{1}{2}} R = (1+i)b$, say, and b is small such that powers of b higher than the fourth may be neglected compared with 1.

The expression (F.1) for c^f , also applies for b^f which is of the same order $\left[b^f = (1+i) \left(\frac{\omega}{2\sigma^f} \right)^{\frac{1}{2}} R \right]$

Further

$$H_0(b^f) = 0.5 + \frac{2x}{\pi} (\gamma + \gamma) - \frac{2x}{\pi} + \frac{2i}{\pi} (\gamma + \gamma) - \frac{1}{2} ix \quad (F.7)$$

where $x = \frac{\omega R^2}{4\sigma^f}$, $y = \ln \left[\frac{1}{2} \left(\frac{\omega}{\sigma^f} \right)^{\frac{1}{2}} R \right]$

the zero order Weber Bessel function being given by

$$Y_0(b^f) = \frac{2}{\pi} \left[\ln \left(\frac{1}{2} b^f \right) + \gamma \right] J_0(b^f) - \frac{2}{\pi} \sum_{k=1}^{\infty} \frac{\left(-\frac{1}{4} x^2 \right)^k}{(k!)^2} \left(1 + \frac{1}{2} \dots \frac{1}{k} \right)$$

similar expressions to (F.7) also being valid for c^f .

C. Fibrous materials examined

Rocksil and Rocksil -K resin bonded materials were used, supplied by Cape Insulation Limited in 1" and 2" thick circular disc samples, as specified below:-

Name and specified Density (lb/ 3)	Measured Density g. cm ⁻³	Average fibre radius R
Rocksil-K 1	0.0184	3
" 1.5	0.02462	3
" 2	0.0288	3
" (M.D.S.) 5	0.0825	3
" (H.D.S.) 6	0.0863	3
Rocksil Building Slab	0.0874	5
Rocksil Acoustic Blanket	0.0636	5

Appendix HViscoelastic Absorber

Following Nowacki (Dynamics of Elastic Systems 1963 Chapman and Hall Ltd.) neglecting thermoelasticity, the constitutive relation for the standard viscoelastic model, may be written.

$$(1 + t_1 \frac{d}{dt}) (\sigma_{ij} - B e_{kk} \delta_{ij}) = 2\mu^s (1 + t_2 \frac{d}{dt}) (e_{ij} - \frac{1}{3} e_{kk} \delta_{ij})$$

$$\text{i.e. } \sigma_{ij} = 2\mu^s \frac{(1 + t_2 \frac{d}{dt})}{(1 + t_1 \frac{d}{dt})} e_{ij} + \left[B - \frac{2}{3} \mu^s \frac{(1 + t_2 \frac{d}{dt})}{(1 + t_1 \frac{d}{dt})} \right] e_{kk} \delta_{ij}$$

(6.1)

for a periodic situation, $\frac{d}{dt} = -i\omega$ and on comparison with the tensor constitutive relation for a normally elastic solid viz.

$$\sigma_{ij} = 2\mu^s e_{ij} + \lambda e_{kk} \delta_{ij}$$

it can be seen that the effect of viscoelasticity is to replace the elastic real constants by frequency dependent complex variables i.e. if

$$\begin{aligned} \mu^s &\rightarrow \mu^s (1 + \mu') \\ \lambda &\rightarrow \lambda (1 + \lambda') \end{aligned}$$

where μ' and λ' are given by (6.1) the form of the constitutive relation, propagation constants and stress expressions for the normally elastic problem may be retained.

This corresponds to the Voigt case as given by Kolsky (Stress Waves in Solids 1953).

In detail

$$1 + \mu' = \frac{(1 - i\omega t_2)}{(1 - i\omega t_1)}$$

and

$$1 + \lambda' = \frac{1}{\lambda} \left[\lambda + \frac{2}{3} \mu^s - \frac{2}{3} \mu^s \frac{(1 - i\omega t_2)}{(1 - i\omega t_1)} \right]$$

$$\begin{aligned}
 &= \frac{1}{\lambda} \left[\lambda + \frac{2}{3} \mu^s - \frac{2}{3} \mu^s (1 + \mu') \right] \\
 &= \frac{1}{\lambda} \left[\lambda - \frac{2}{3} \mu^s \mu' \right] \\
 &= 1 - \frac{2}{3} \frac{\mu^s \mu'}{\lambda}
 \end{aligned}$$

i.e. $\lambda' = -\frac{2}{3} \mu^s \mu' / \lambda$ in this case therefore it is only

necessary to retain one frequency dependent elastic coefficient.

N.B. this relationship is equivalent to putting $B^1 = 0$, $[B \rightarrow B(1 + B^1)]$ found to be roughly true for rubber-like materials as the effect of B^1 is very much smaller than for μ^1 .

The wave propagation constants may then be written

$$\begin{aligned}
 \kappa_D^{VES} &= \omega \left[\frac{\rho}{2\lambda(1+\lambda') + \mu^s(1+\mu')} \right]^{\frac{1}{2}} \\
 &= \omega \left[\frac{\rho}{(2\lambda + \mu) + 2\lambda\lambda' + \mu^s\mu'} \right]^{\frac{1}{2}} \\
 &= \omega \left[\frac{\rho}{(2\lambda + \mu) - \frac{4}{3}\mu^s\mu' + \mu^s\mu'} \right]^{\frac{1}{2}} \\
 &= \frac{\omega}{c_0^{VES}} \left[\frac{1}{1 - \frac{\mu\mu'}{3(2\lambda + \mu)}} \right]^{\frac{1}{2}} \approx \frac{\omega}{c_0^{VES}}
 \end{aligned}$$

when

$$\lambda \gg \mu^s$$

and

$$\begin{aligned}
 \kappa_T^{VES} &= \omega \left(\frac{\rho}{\mu(1+\mu')} \right)^{\frac{1}{2}} \\
 &= \kappa_T^{VES} \left(\frac{1}{1+\mu'} \right)^{\frac{1}{2}}
 \end{aligned}$$

Consider now the model of the hypothetical absorber to be a continuous viscoelastic solid matrix, containing a random distribution of spherical or cylindrical cavities sealed off from each other and from the surface by intervening layers of viscoelastic material. This model is obviously susceptible to the same kind of scattering approach as that employed for the fibrous material.

Firstly, it is necessary to consider the problem of scattering by a spherical or cylindrical cavity imbedded in a semi-infinite viscoelastic solid.

(a) Spherical

For simplicity the amplitude of the incident wave may be taken as unity (it is immaterial to the expression for the attenuation due to a single scatterer).

Then the coefficients representing the scattering inside a viscoelastic solid are given simply by the boundary conditions for a cavity inside a normally elastic solid with the real elastic coefficients and constants replaced by the relevant complex ones viz.

$$\begin{aligned} & \left[a^{VES} \lambda^{VES} N^{VES} j_n'(a^{VES}) + 2a^{VES} \lambda^{VES} j_n'(a^{VES}) + n(n+1) \lambda^{VES} j_n(a^{VES}) \right] \\ & + A_n^{VES} \left[a^{VES} \lambda^{VES} N^{VES} h_n''(a^{VES}) + 2a^{VES} \lambda^{VES} h_n'(a^{VES}) + n(n+1) \lambda^{VES} h_n(a^{VES}) \right] \\ & + 2\mu^{VES} n(n+1) C_n^{VES} \left(h_n(c^{VES}) - c^{VES} h_n'(c^{VES}) \right) = 0 \end{aligned}$$

$$\mu^{VES} \left\{ \left[j_n(a^{VES}) - a^{VES} j_n'(a^{VES}) \right] + A_n^S \left[h_n(a^{VES}) - a^{VES} h_n'(a^{VES}) \right] \right. \\ \left. + C_n^S \left[\left(\frac{1}{2} n(n+1) + 1 \right) h_n(c^{VES}) - \frac{1}{2} c^{VES 2} h_n''(c^{VES}) \right] \right\} \\ = 0.$$

which express the fact that the radial and θ comp. of stress at the boundary of the cavity must be zero.

$$\left[N^{VES} = 2\mu^{VES} + \lambda^{VES}, \quad a^{VES} = \kappa_D^{VES} R, \quad c^{VES} = \kappa_T^{VES} R \right]$$

From these equations, where use has been made of the relation

$$\frac{1}{\sin \theta} \frac{d}{d\theta} (\sin \theta \cdot P_n') = n(n+1) P_n(\cos \theta) \\ \left[P_n' = - \frac{dP_n(\cos \theta)}{d\theta} \right]$$

for $n = 0$ the θ dependence vanishes

$$a^{VES 2} N^{VES} j_0''(a^{VES}) + 2a^{VES} \lambda^{VES} j_0'(a^{VES}) + A_0^{VES} \left[a^{VES 2} N^{VES} h_0''(a^{VES}) \right. \\ \left. + 2a^{VES} \lambda^{VES} h_0'(a^{VES}) \right] = 0$$

thus

$$A_0^{VES} = - \frac{\left[a^{VES 2} N^{VES} j_0''(a^{VES}) + 2a^{VES} \lambda^{VES} j_0'(a^{VES}) \right]}{\left[a^{VES 2} N^{VES} h_0''(a^{VES}) + 2a^{VES} \lambda^{VES} h_0'(a^{VES}) \right]}$$

Now the functions j_n and h_n satisfy Bessel's differential equation

$$R_n'' + \frac{2}{x} R_n' + \left(1 - \frac{n(n+1)}{x^2}\right) R_n = 0$$

$$\text{i.e. } R_0'' + \frac{2}{x} R_0' + R_0 = 0$$

$$\therefore R_0'' = -\frac{2}{x} R_0' - R_0$$

$$\text{and as } R_0' = -R_1$$

$$R_0'' = +\frac{2}{x} R_1 - R_0$$

Further the small argument forms for $j_n(a^{VES})$ from Epstein and Carhart may be used. viz.

$$j_0(a^{VES}) \approx 1 \quad j_1(a^{VES}) \approx \frac{1}{3}x \quad j_2(a^{VES}) \approx \frac{x^2}{15}$$

$$\left(\text{i.e. } j_0'' \approx -\frac{1}{3}\right)$$

$$\begin{aligned} \therefore A_0^{VES} &\approx - \frac{\left[-\frac{1}{3} a^{VES 2} N^{VES} - \frac{2}{3} a^{VES 2} \lambda^{VES} \right]}{\left[a^{VES 2} N^{VES} h_0''(a^{VES}) + 2a^{VES} \lambda^{VES} h_0'(a^{VES}) \right]} \\ &= \frac{a^{VES 2} \beta^{VES}}{\left[a^{VES 2} N^{VES} h_0''(a^{VES}) + 2a^{VES} \lambda^{VES} h_0'(a^{VES}) \right]} \end{aligned}$$

similarly

$$\begin{aligned} &a^{VES 2} N^{VES} j_1''(a^{VES}) + 2a^{VES} \lambda^{VES} j_1'(a^{VES}) + 2\lambda^{VES} j_1(a^{VES}) \\ &+ A_1^{VES} \left[a^{VES 2} N^{VES} h_1''(a^{VES}) + 2a^{VES} \lambda^{VES} h_1'(a^{VES}) + 2\lambda^{VES} h_1(a^{VES}) \right] \\ &+ 4\mu^{VES} c_1^{VES} \left[h_1(c^{VES}) - c^{VES} h_1'(c^{VES}) \right] = 0 \end{aligned}$$

$$\mu^{VES} \left\{ \left[j_1(a^{VES}) - a^{VES} j_1'(a^{VES}) \right] + A_1^S \left[h_1(a^{VES}) - a^{VES} h_1'(a^{VES}) \right] \right. \\ \left. + C_n^S \left[2h_1(c^{VES}) - \frac{1}{2} c^{VES 2} h_1''(c^{VES}) \right] \right\} = 0$$

$$\therefore A_1^{VES} \approx \frac{\begin{array}{cc} \frac{A}{3} a^{VES} \lambda^{VES} & - a^{VES 3} / 15 \\ 32i \mu^{VES} / c^{VES} & - \frac{2i}{c^{VES 3}} + \frac{3i}{c^{VES 2}} \end{array}}{\begin{array}{cc} -i \left(8\lambda^{VES} + 4\mu^{VES} \right) / a^{VES 2} & - \mu^S a^{VES 3} / 15 \\ 3i / a^{VES} & - \frac{2i}{c^{VES 3}} + \frac{3i}{c^{VES 2}} \end{array}}$$

cylindrical For generality oblique incidence is considered. However, this means that even when the surface of the material is closed with an impervious layer, the existence of end effects at the cylindrical channel intersections with the material boundaries is a complication which requires consideration over and above the following, where they are neglected.

From Appendix (C); again neglecting thermoelasticity, where the symbols have obvious meanings, dropping superscripts, where redundant:-

$$\text{for } \underline{n=0} \quad \mu \left\{ a' J_0'(a') + \left(\frac{c^2}{2} - \kappa^2 \right) J_0(a') + A_0 \left[a' H_0'(a') + \left(\frac{c^2}{2} - \kappa^2 \right) H_0(a') \right] + i\kappa c^2 (C_0 H_0''(c')) \right\} = 0$$

$$\mu \left\{ -i\kappa \left[a' J_0'(a') + A_0 a' H_0'(a') \right] + c' C_0 \left(\kappa \frac{c^2}{2} - \kappa^2 \right) H_0'(c') \right\} = 0$$

and for n = 1

$$2 [a' J_1'(a') + (c_2^2 - \kappa^2 - 1) J_1(a')] + A_1 [a' H_1'(a') + (c_2^2 - \kappa^2 - 1) H_1(a')] + i\kappa c_1^2 C_1 H_1''(c') + \kappa D_1 [c' H_1'(c') - H_1(c')] = 0$$

$$2 [a' J_1'(a') - J_1(a')] + A_1 [a' H_1'(a') - H_1(a')] + i\kappa C_1 [c' H_1'(c') - H_1(c')] + D_1 [c' H_1'(c') - c'^2 H_1''(c') - H_1(c')] = 0$$

$$-i\kappa [2a' J_1'(a') + A_1 a' H_1'(a')] + c' C_1^2 (\kappa_{1/2}^2 - \kappa^2) H_1'(c') + i\kappa \kappa_{1/2} D_1 H_1(c') = 0$$

Appendix G.

Solid stress in spherical polar coordinates for a normally elastic solid.

$$\sigma_{ij} = 2\mu e_{ij} + \lambda e_{kk} \delta_{ij}$$

$$e_{rr} = \frac{du_r}{dr} \quad e_{r\theta} = \frac{1}{2} \left[\frac{1}{r} \frac{du_r}{d\theta} + r \frac{d}{dr} \left(\frac{u_\theta}{r} \right) \right]$$

$$e_{\theta\theta} = \frac{d}{d\theta} \left(\frac{u_\theta}{r} \right) + \frac{u_r}{r} \quad e_{\phi\phi} = \frac{u_r}{r} + u_\theta \frac{\cot\theta}{r}$$

and for the axially symmetric problem (ind. of ϕ) $e_{r\phi} = e_{\theta\phi} = 0$

thus

$$\sigma_{rr} = 2\mu e_{rr} + \lambda e_{kk} = 2\mu \frac{du_r}{dr} + \lambda \text{div } u$$

$$\sigma_{r\theta} = 2\mu e_{r\theta} = \left[\frac{1}{r} \frac{du_r}{d\theta} + r \frac{d}{dr} \left(\frac{u_\theta}{r} \right) \right]$$

also

$$u_r = -\frac{\partial\phi}{\partial r} + \frac{1}{r \sin\theta} \frac{d}{d\theta} (\sin\theta \cdot A^s)$$

and

$$u_\theta = -\frac{1}{r} \frac{\partial\phi}{\partial\theta} - \frac{1}{r} \frac{d}{dr} (r A^s)$$

thus

$$\sigma_{rr} = 2\mu \left\{ -\frac{\partial^2\phi}{\partial r^2} - \frac{1}{r \sin\theta} \frac{d}{d\theta} (\sin\theta \cdot A^s) + \frac{1}{r \sin\theta} \frac{d^2}{dr d\theta} (\sin\theta \cdot A^s) \right\} + \lambda \text{div } u$$

and thus after some manipulation

$$\sigma_{r\theta} = -\frac{2}{r} \frac{\partial^2\phi}{\partial r \partial\theta} - \frac{2}{r^2} \frac{\partial\phi}{\partial\theta} + \frac{1}{r^2} \frac{d}{d\theta} \left(\frac{1}{\sin\theta} \frac{d}{d\theta} (\sin\theta \cdot A^s) \right) + \frac{2}{r^2} A^s - \frac{\partial^2 A^s}{\partial r^2}$$

Plate 1 Plan view of sample of Rocksil Acoustic Blanket

Plate 2 Side elevation of Acoustic Blanket showing the tendency of the fibres to lie in layers parallel to the surface (netting) of the sample.

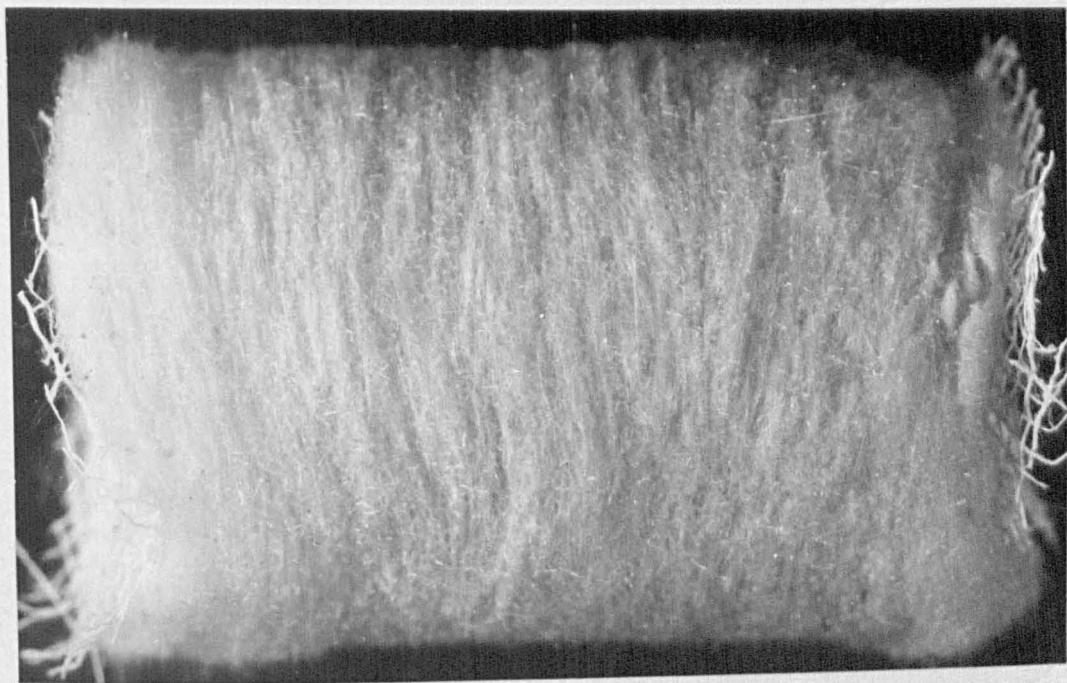
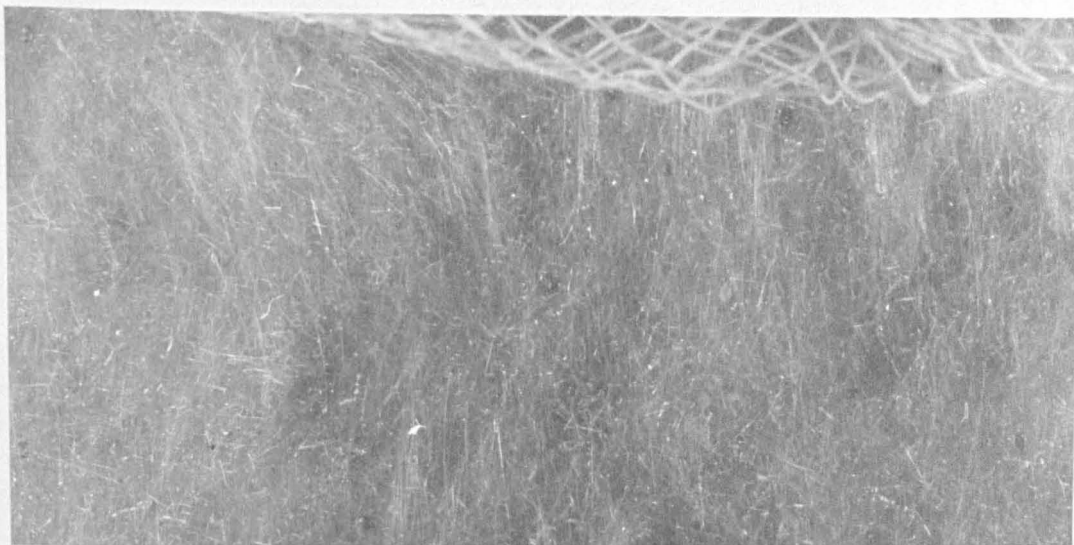


Plate 3 Surface of rigid polyurethane foam sample (approx 5 x magnification)

Plate 4 Sample of coarse, flexible polyurethane foam in which all "skins" have been dissolved. The basic "fibrous" lattice framework is clearly shown.

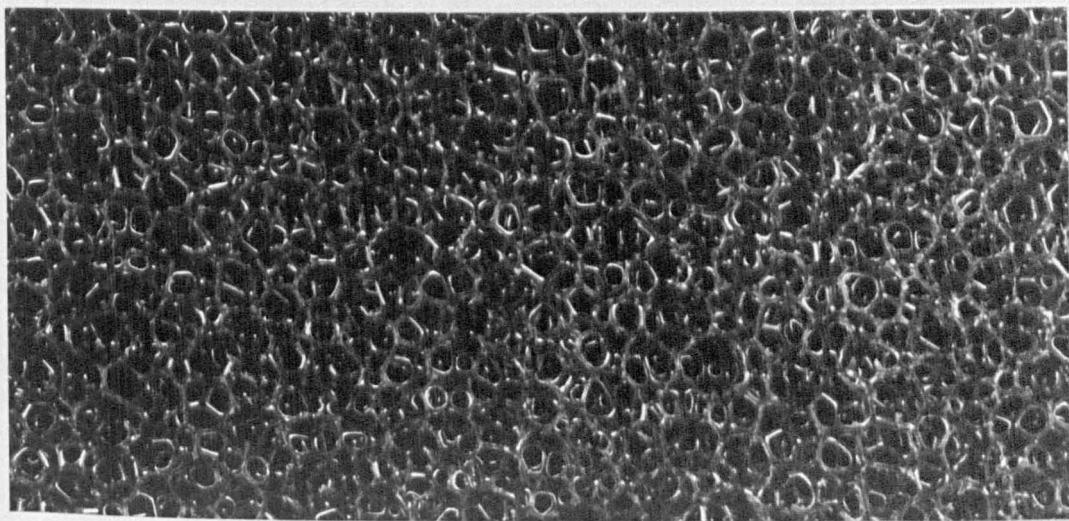
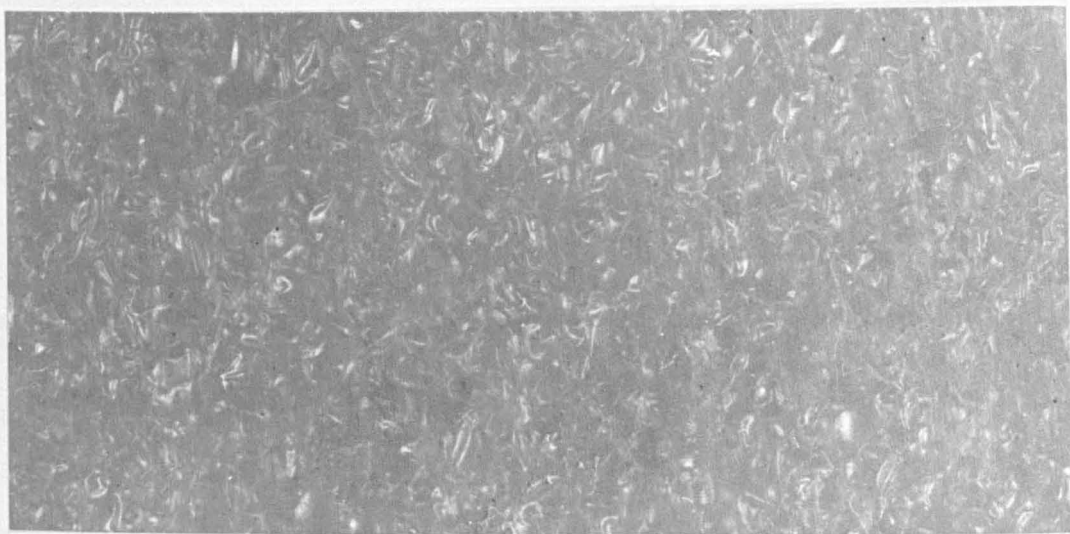
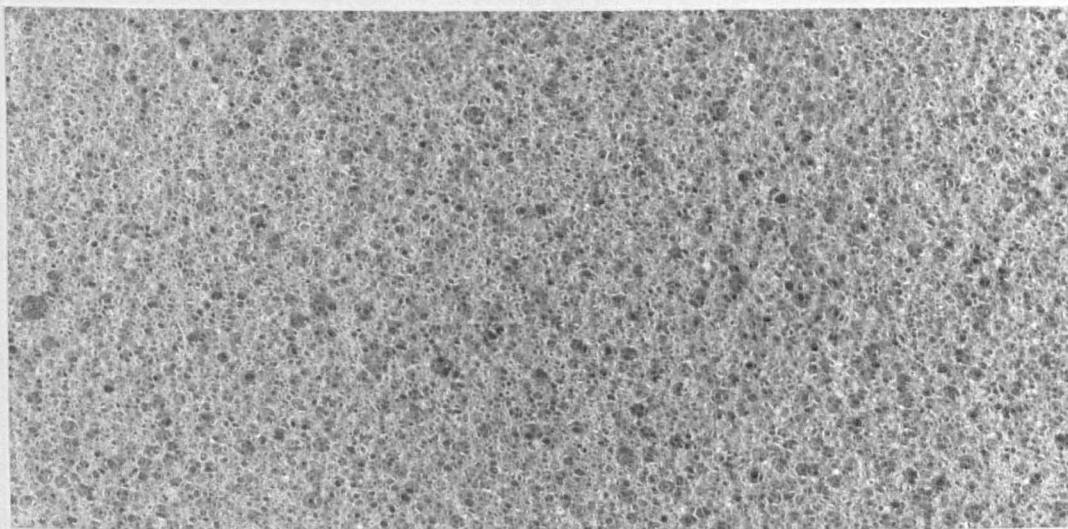


Plate 5 Finer sample of flexible polyurethane foam in which the "skins" are retained.

Plate 6 Surface of Rocksil-K Resin Bonded sample, showing the tendency towards "clumping".

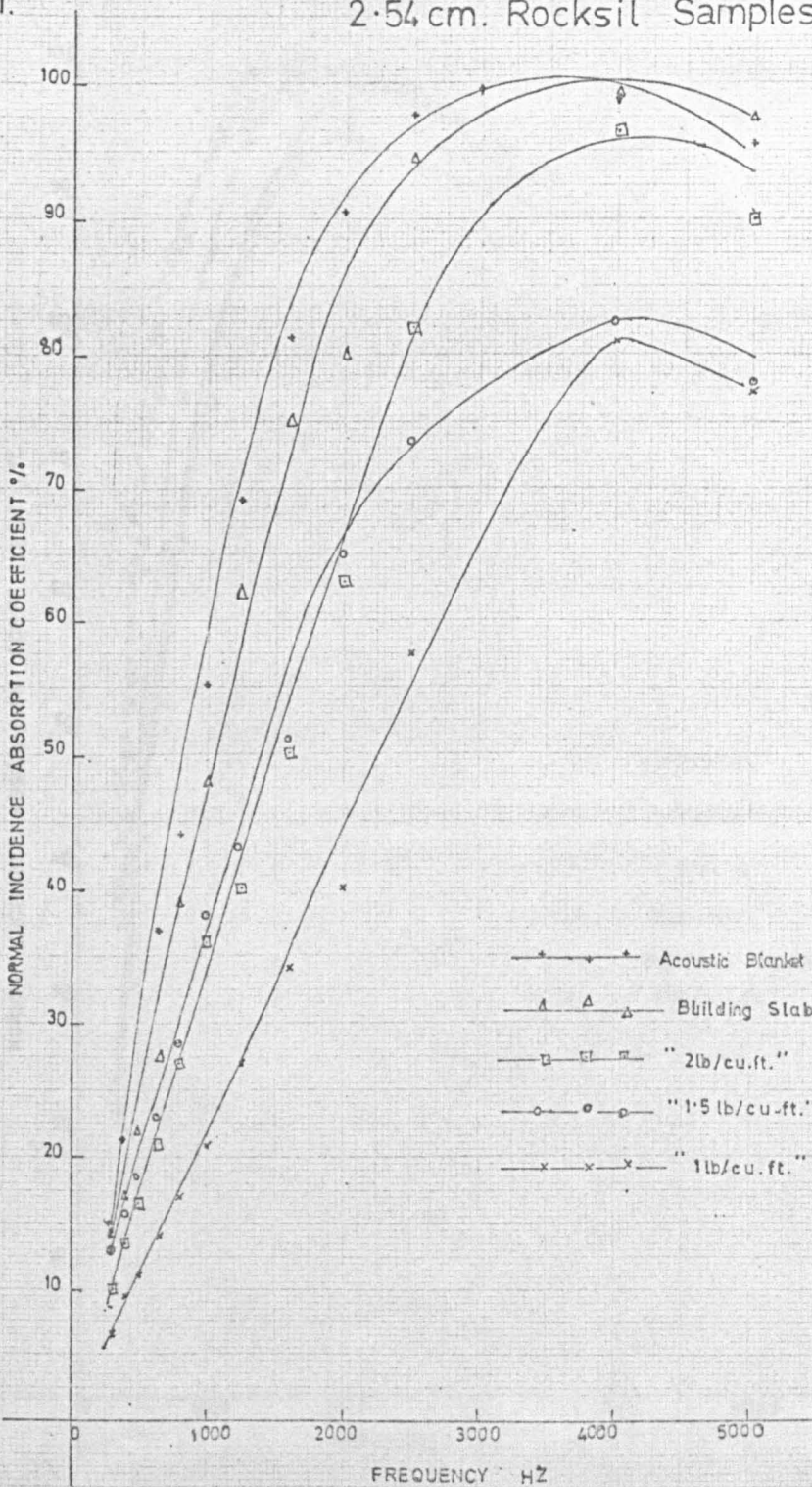


RESUMÉ OF DATA RELATING TO FIBROUS MATERIALS

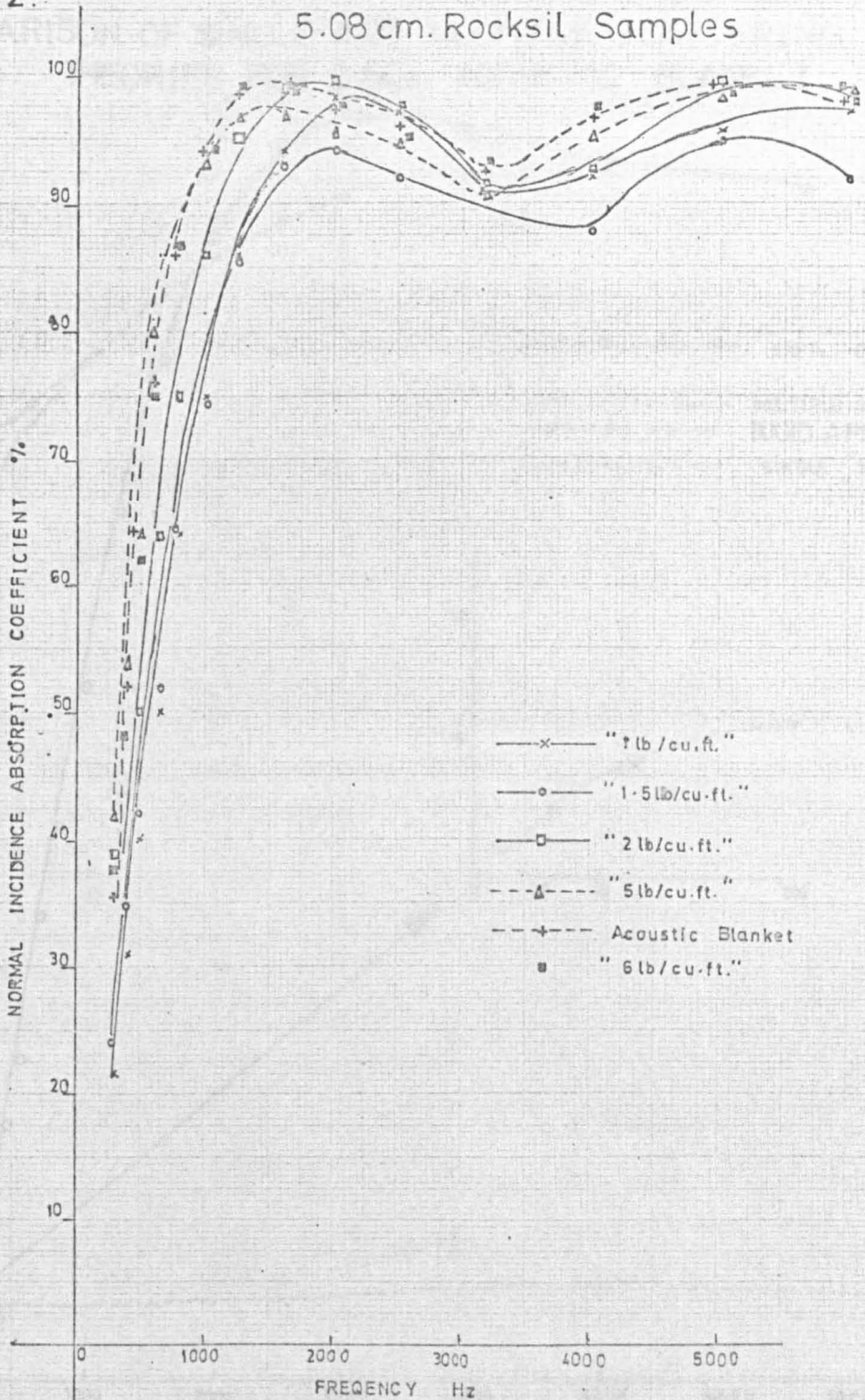
Name and specified Density (lb/ft ³)		Measured Density g. cm ⁻³	Average fibre radius R (microns)
Rocksil-K	1	0.0184	3
"	1.5	0.02462	3
"	2	0.0288	3
" (M.D.S.)	5	0.0825	3
" (H.D.S.)	6	0.0863	3
Rocksil Building Slab		0.0874	5
Rocksil Acoustic Blanket		0.0636	5

1.

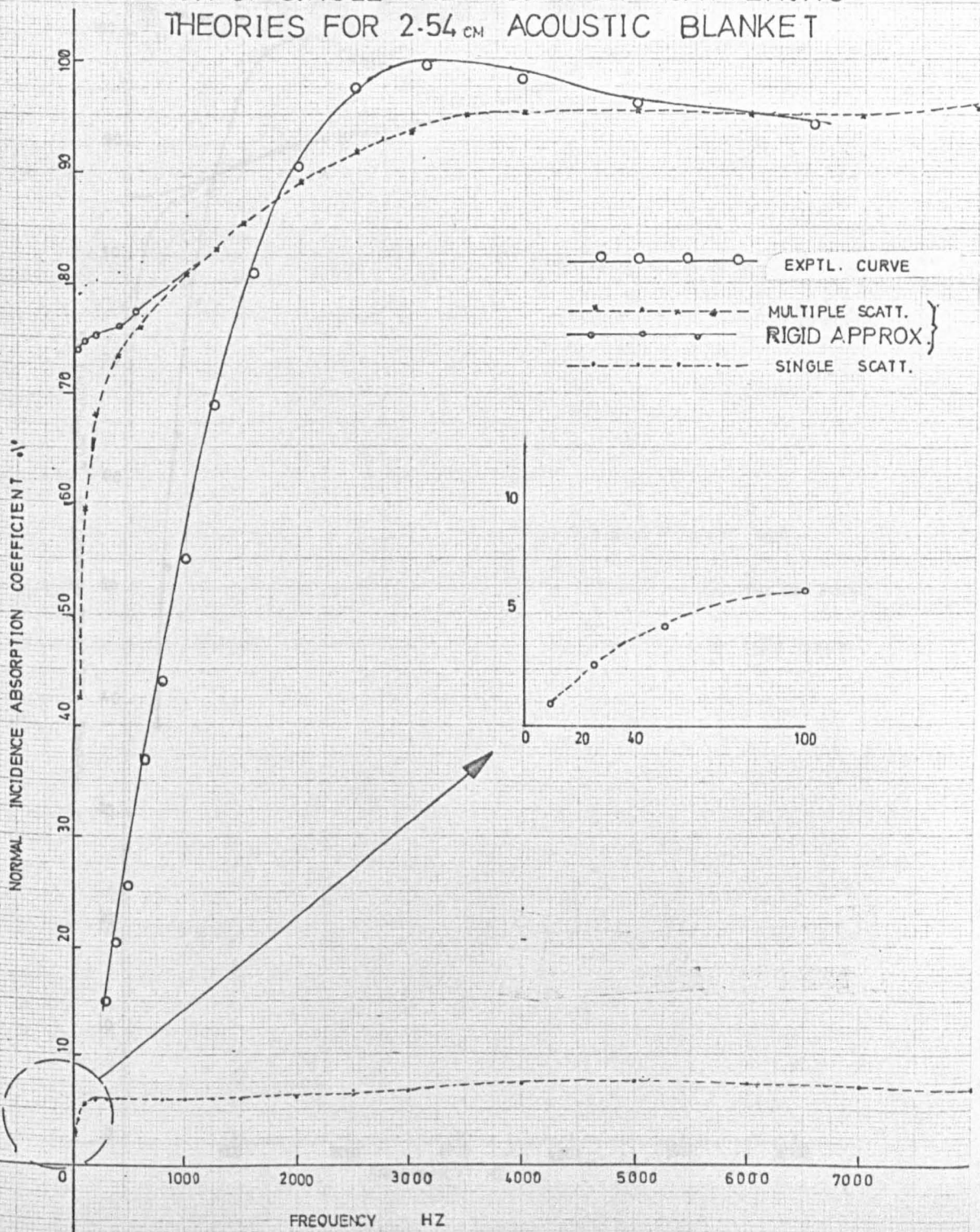
2.54 cm. Rocksil Samples



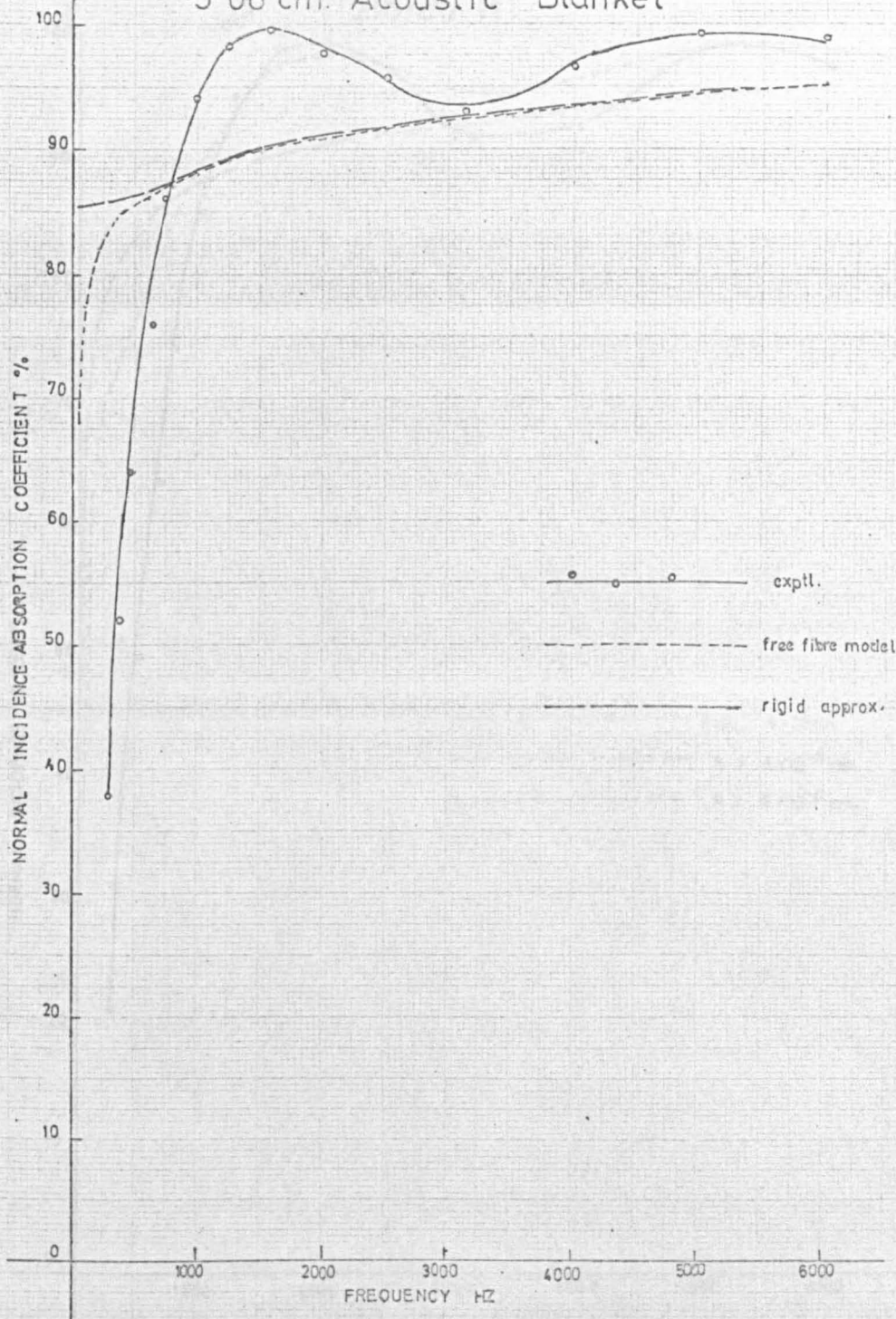
5.08 cm. Rocksil Samples



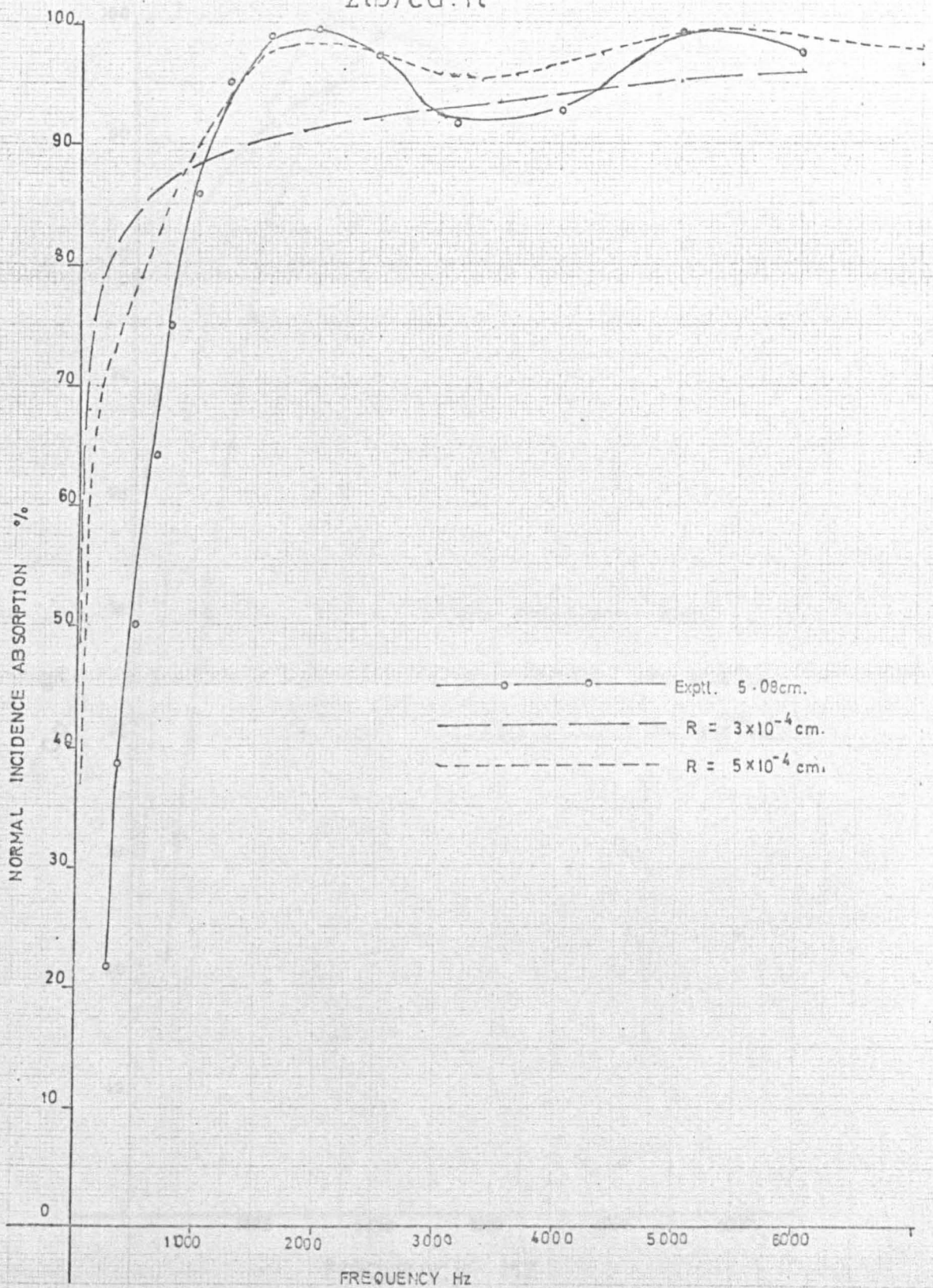
3. COMPARISON OF SINGLE AND MULTIPLE SCATTERING THEORIES FOR 2.54_{CM} ACOUSTIC BLANKET



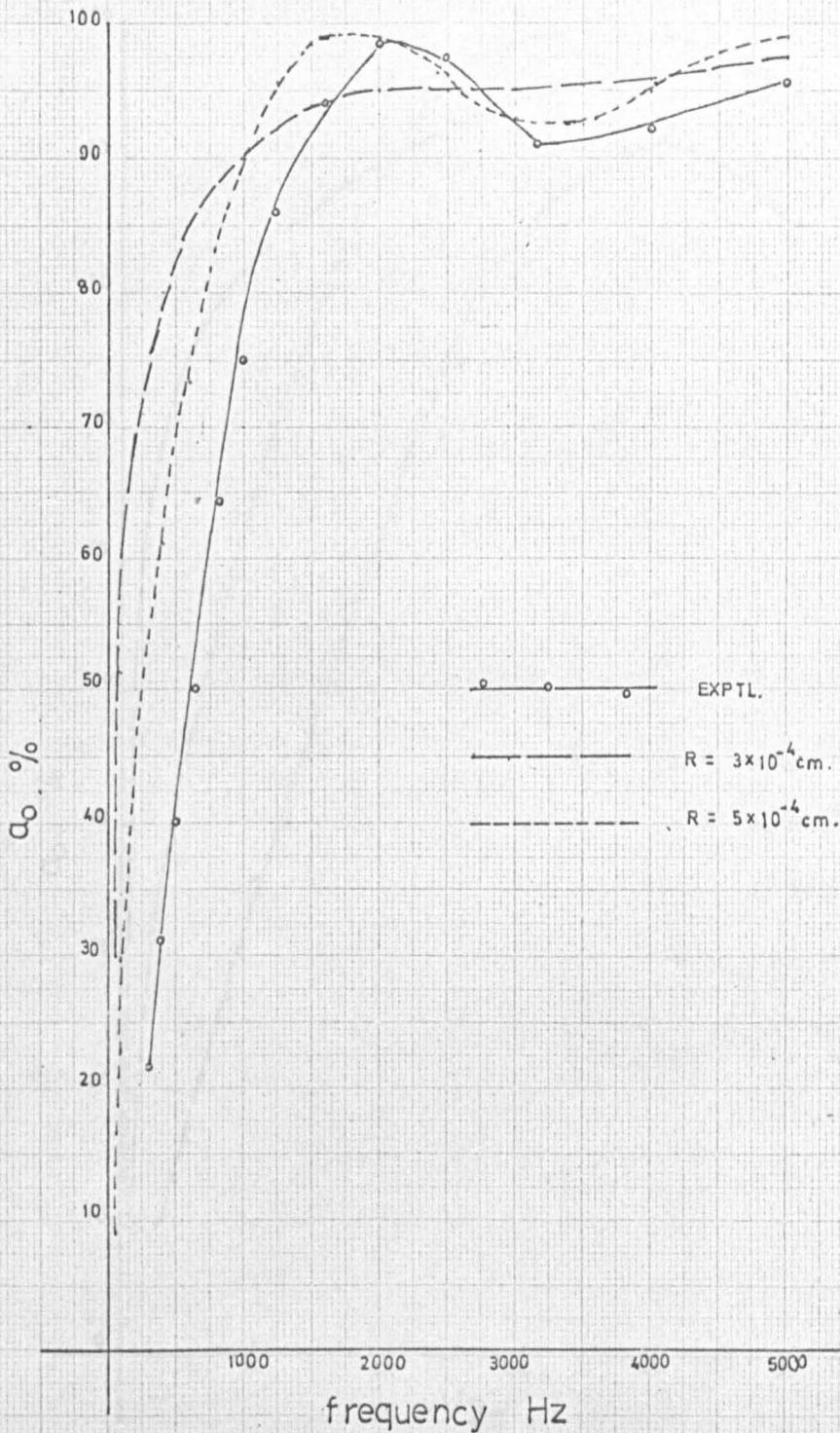
4. Comparison of theory and expt.
5.08 cm. Acoustic Blanket



5a.

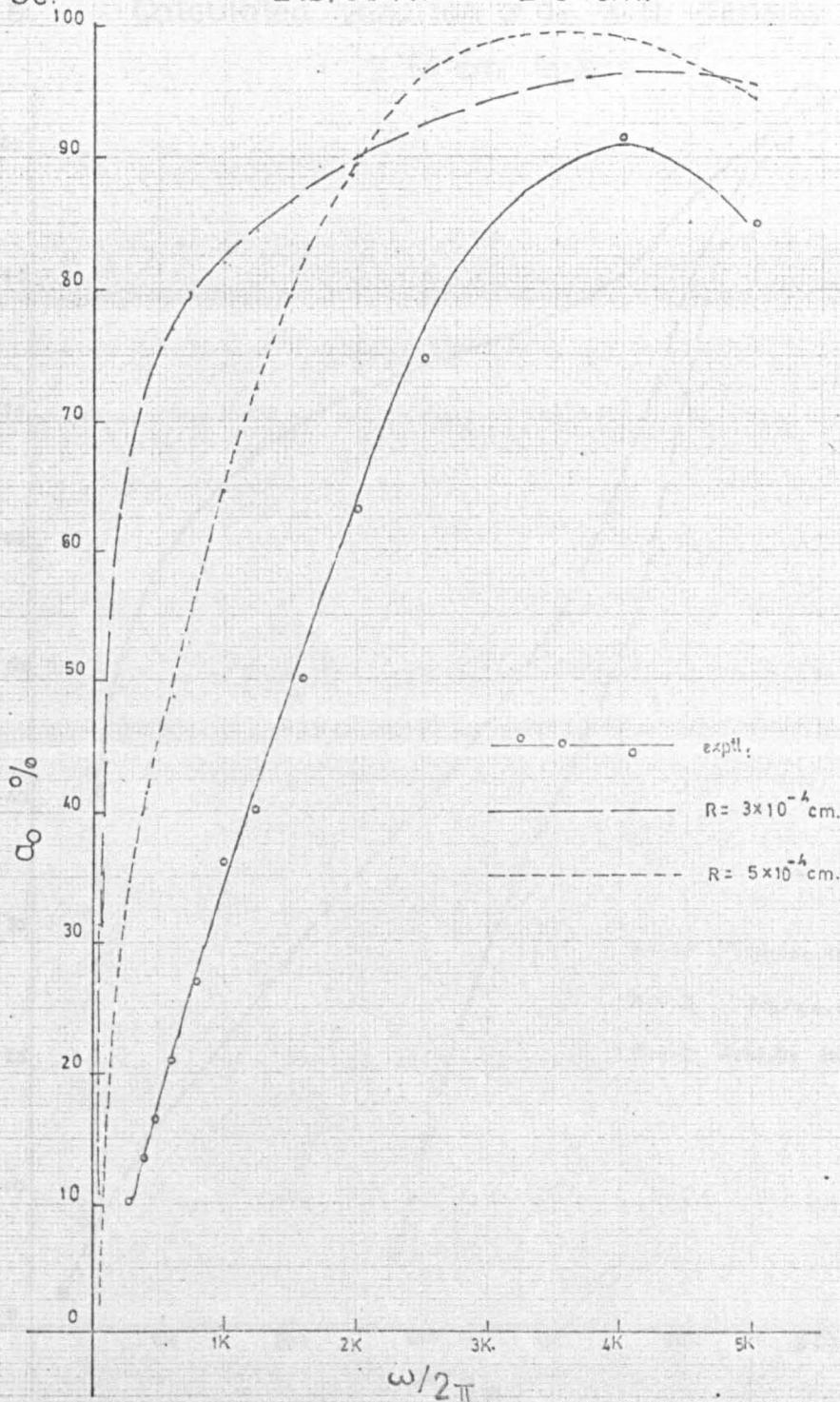
Comparison of theory and expt.
"2lb/cu.ft"

5b. "1lb/cu.ft" 5.08 cm.

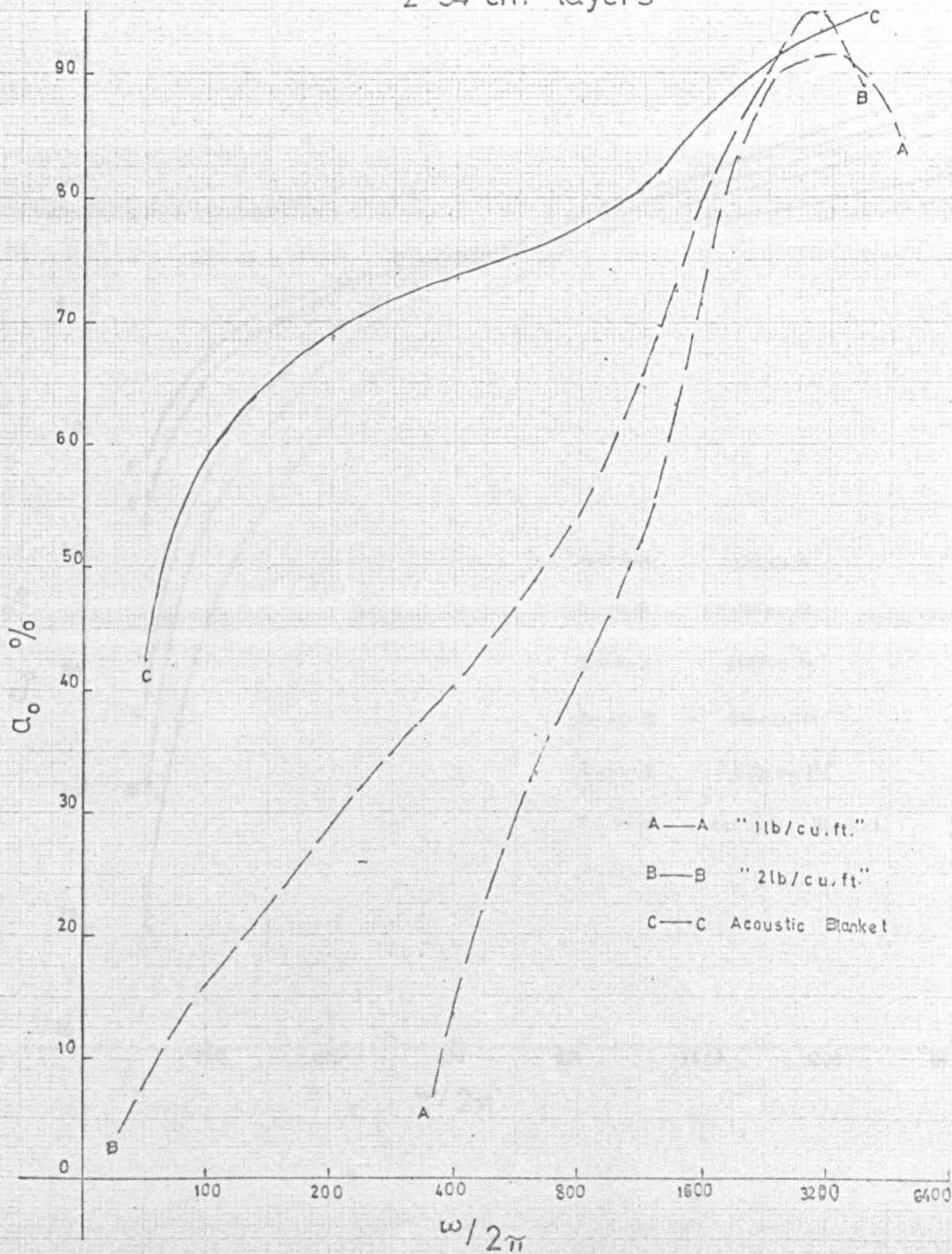


5c.

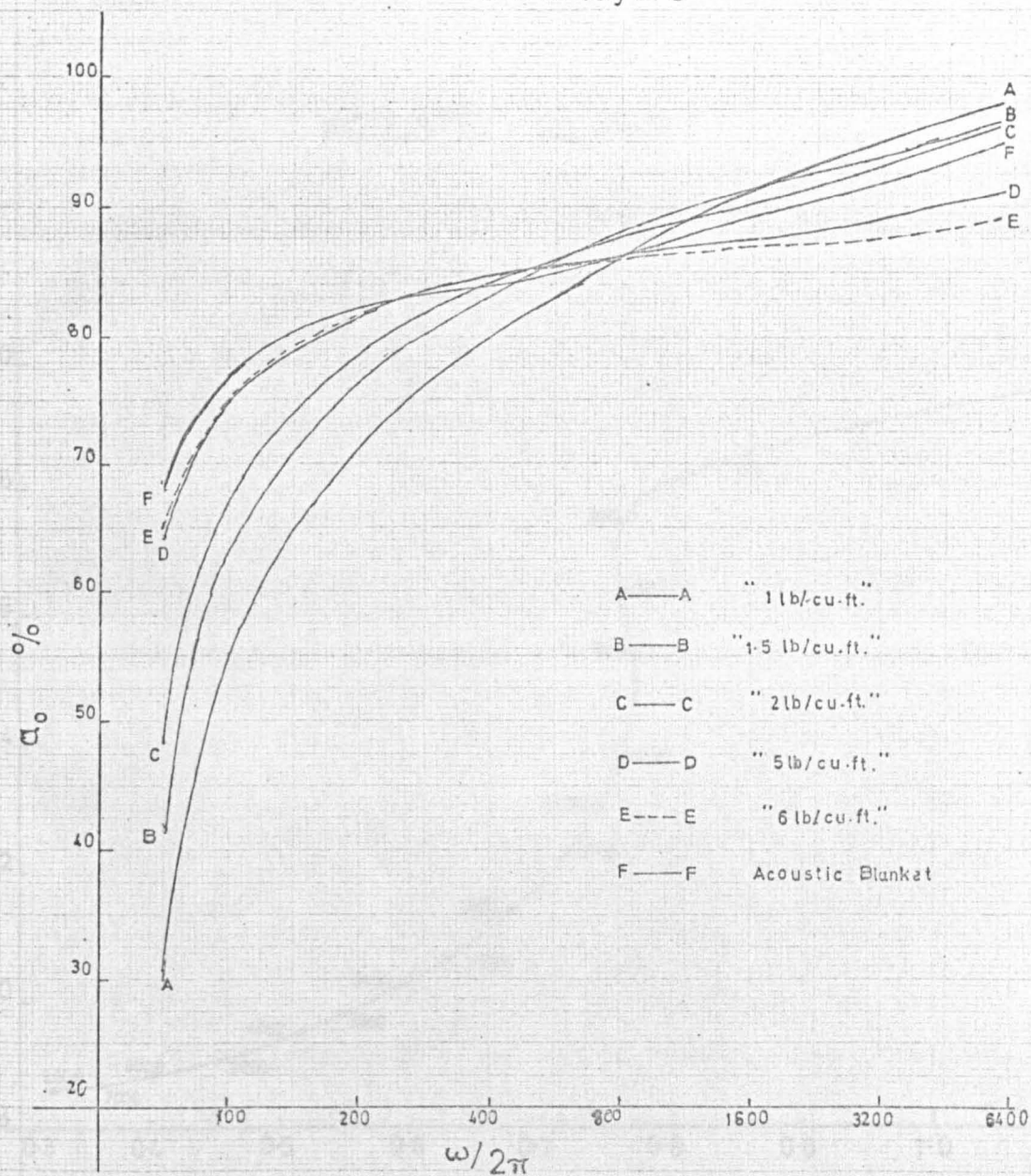
" 2lb/cu.ft." 2.54cm.



6. Calculated variation of α_0 with density
2.54 cm layers

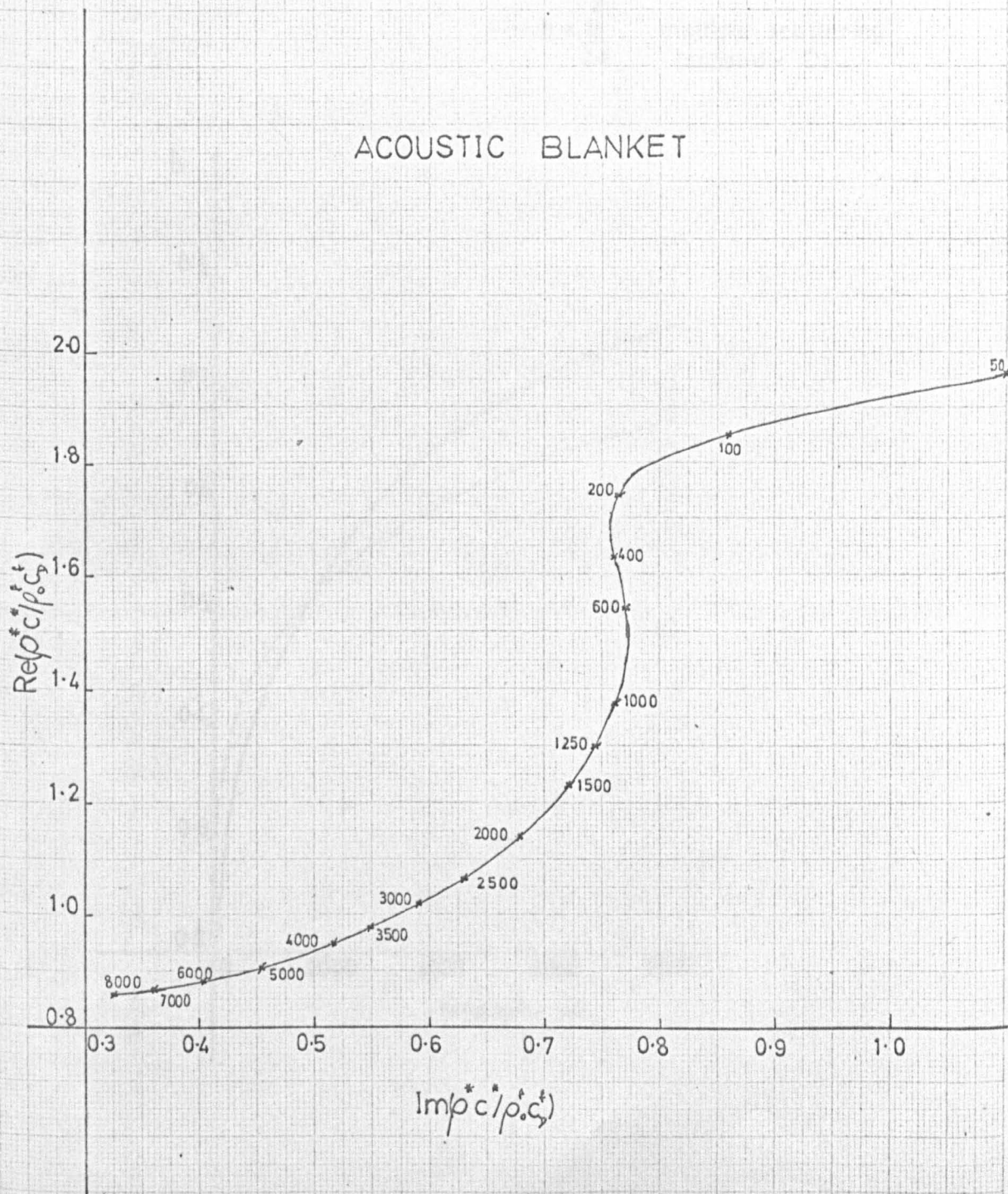


7. Calculated variation of α_0 with density
5.08 cm. layers



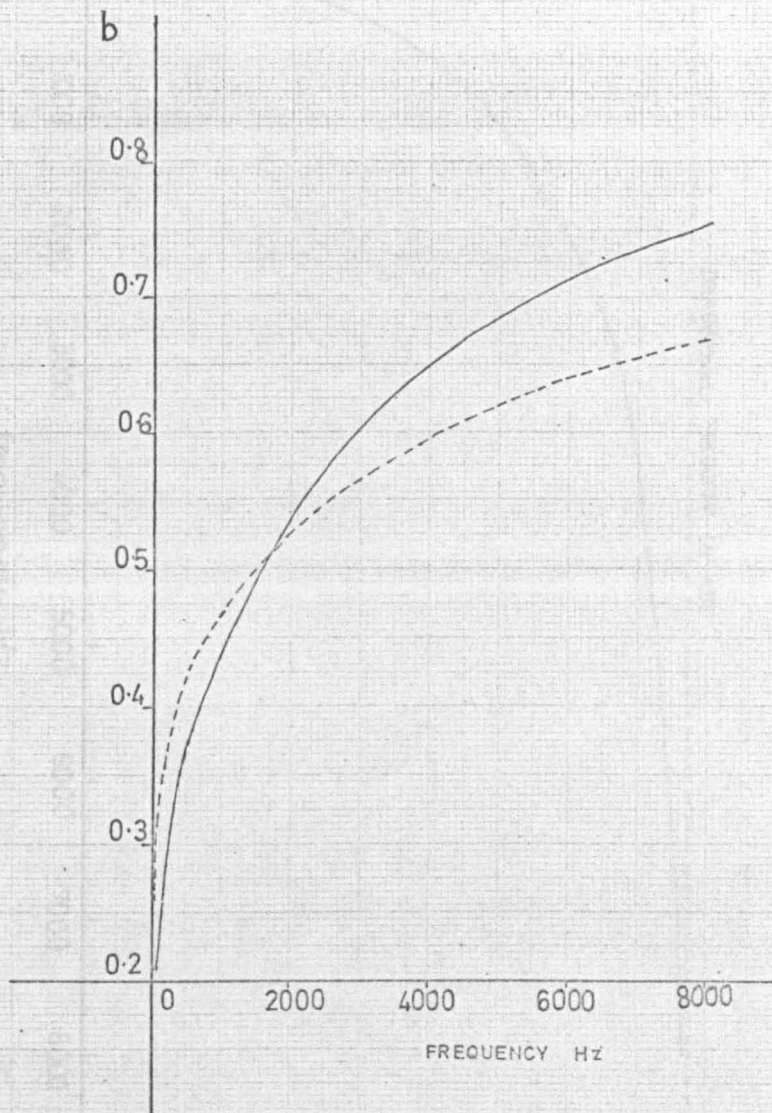
8. RELATIVE CHARACTERISTIC IMPEDANCE

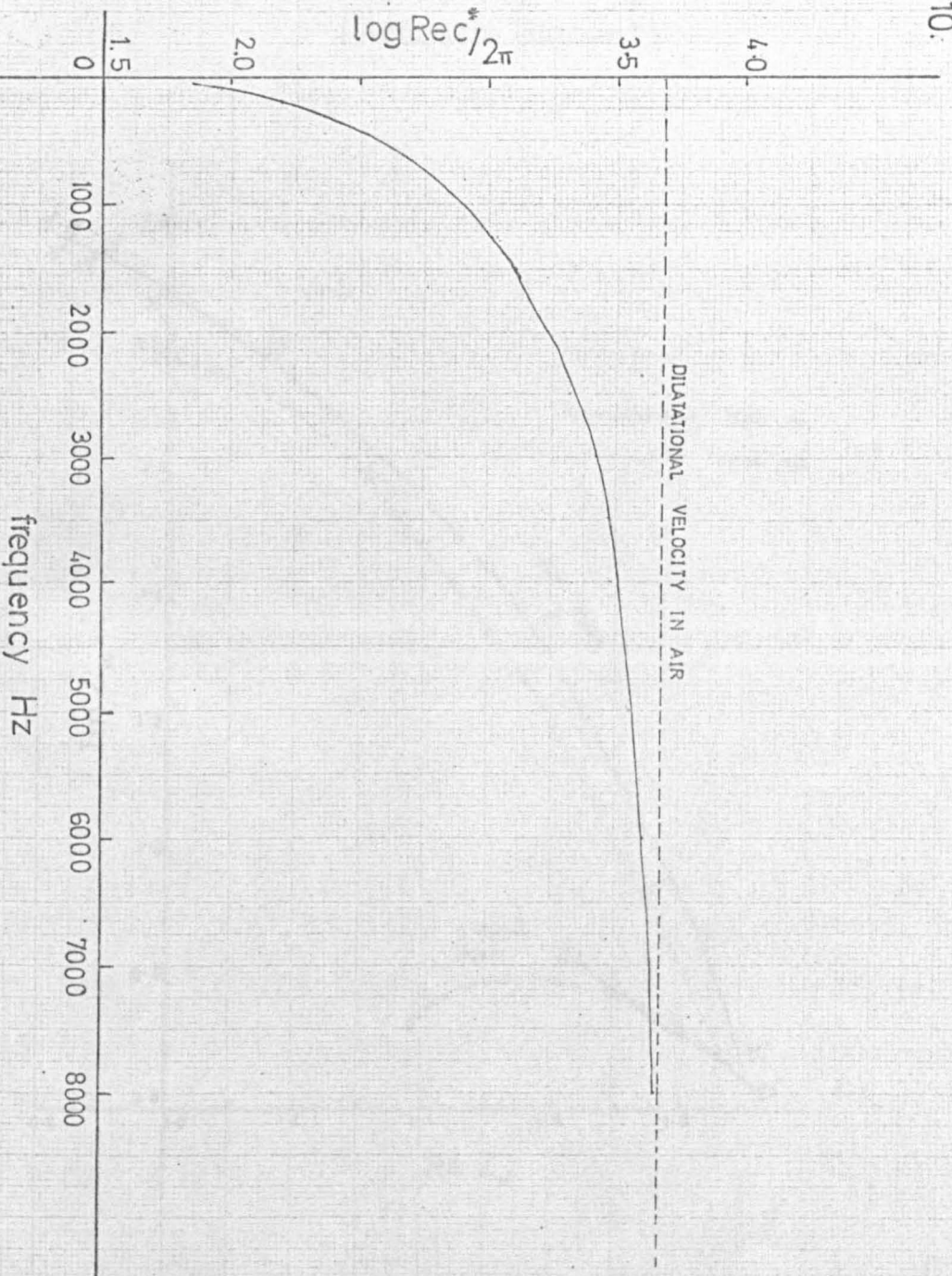
ACOUSTIC BLANKET



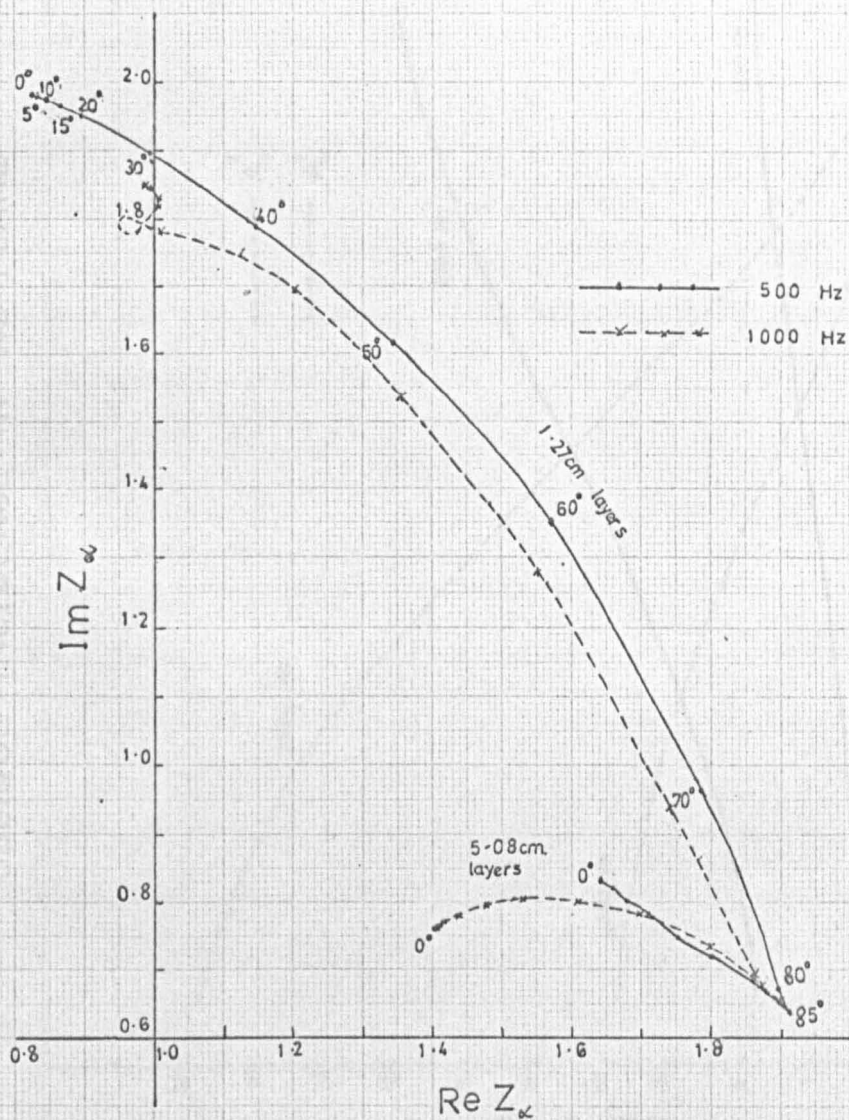
9.

ATTENUATION --- $b = \frac{N\sigma}{2}$ single scattering
— $b = \frac{B}{2a}$ multiple scattering
(appendix D)



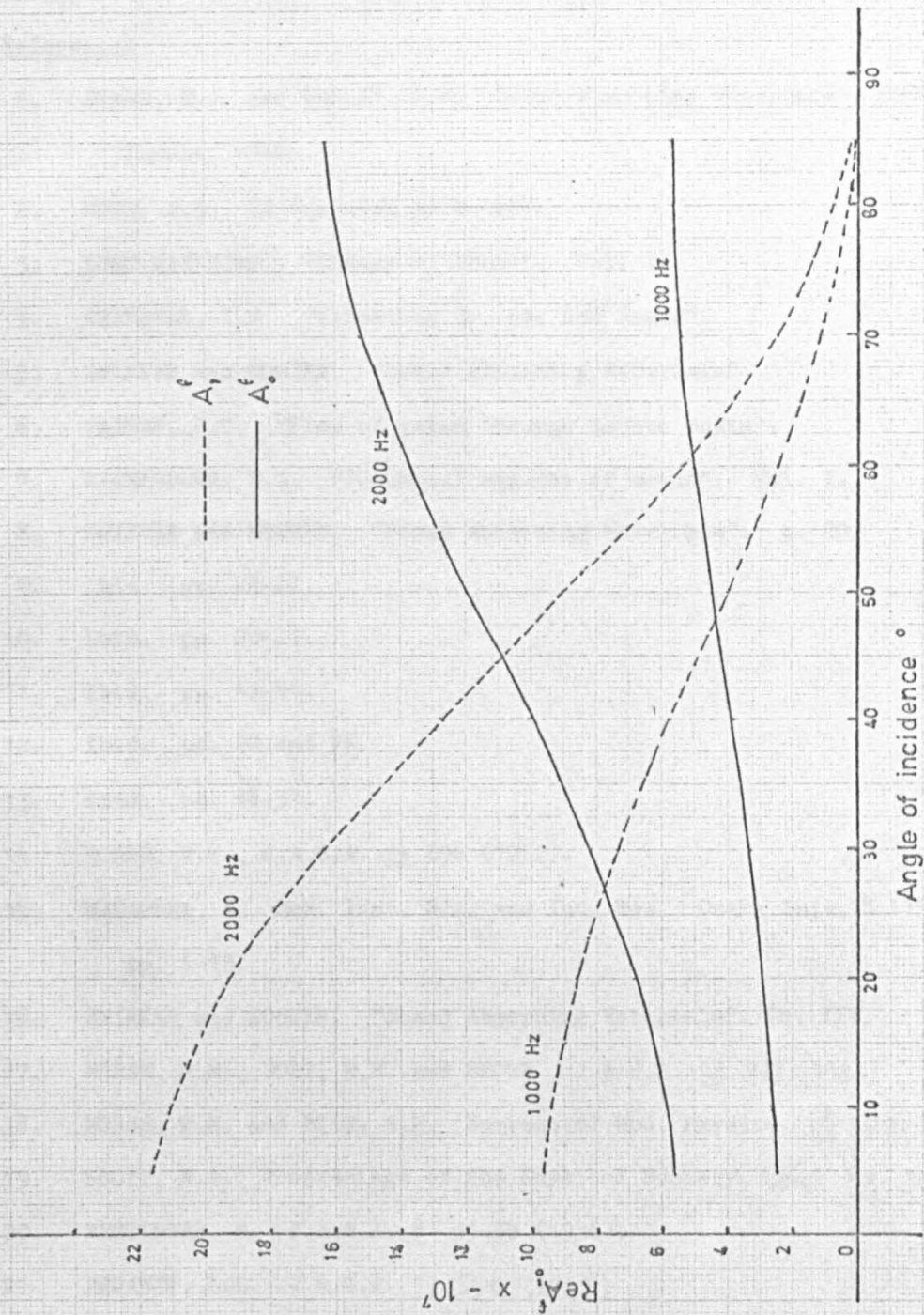


11. VARIATION OF SURFACE IMPEDANCE WITH ANGLE OF INCIDENCE IN "XY" PLANE (Acoustic Blanket)



SCATTERING COEFFICIENTS OBLIQUE INCIDENCE IN "XZ" PLANE

12.



References

1. EVANS, E.J. and BAZLEY, E.N. "Sound Absorbing Materials". HMSO
London, 1960.
2. WOOD, A.B. "A Textbook of Sound".
3. LORD RAYLEIGH. "Theory of Sound". Vol. II.
4. CRANDALL, I.B. "Vibrating Systems and Sound".
5. ZWIKKER and KOSTEN. "Sound Absorbing Materials".
6. CARMAN, P.C. "Flow of gases through porous media".
7. RICHARDSON, E.G. "Technical aspects of sound". Vol. I.
8. ZWIKKER and KOSTEN. "Sound Absorbing Materials". p. 20.
9. *ibid.* pp. 26-28.
10. *ibid.* pp. 20-21.
11. *ibid.* pp. 42-44.
12. *ibid.* pp. 22 and 76.
13. *ibid.* pp. 48-51.
14. MORSE, R.W. J.A.S.A. 24 696 (1952).
15. NAKAMURA, A. Mem. Inst. Sci. and Ind. Res. Osaka Univ. 18 (1961)
pp. 1-13.
16. ZWIKKER and KOSTEN. "Sound Absorbing Materials". Ch. III.
17. MORSE, P.M., BOLT, R.H. and BROWN. J.A.S.A. 12 217 (1940)
18. MORSE, P.M. and BOLT, R.H. Reviews of Mod. Physics. 16 69-150 (1944)
19. SCOTT, R.A. Proceedings of the Physical Society, Lond. 58 358 (1946)
20. RETTINGER, M. J.A.S.A. 8 53-59 (1936).
21. BERANEK, L.L. J.A.S.A. 19 556 (1947)
22. KOSTEN, C.W. and JANSSEN, J.H. Acustica 372-378 2 (1957).
23. ZWIKKER and KOSTEN. "Sound Absorbing Materials". Ch. VI.

24. PATERSON, N.R. *Geophysics* 21 69-714 (1956).
25. BRANDT, A. *Journal of Applied Mechanics* 22, 479 seq. (1955).
26. DUFFY, J. and MINDLIN, R.D. *J. Appl. Mech. Am. Soc. Mech. Eng.*
24 585 (1957).
27. KAWASIMA, V. *Acustica* 10 208 (1960).
28. BIOT, M.A. *J. Appl. Phys.* 26 182 (1955).
29. BIOT, M.A. (i) and (ii). *J.A.S.A.* 28 179 (1956).
30. *ibid.* pp. 185.
31. BIOT, M.A. *J. Appl. Phys.* 33 1482 (1962).
32. GASSMAN, F. *Geophysics* 16 4 673-685 (1951).
33. BIOT, M.A. *J. Appl. Phys.* 25 1385 (1954) and 27 462 (1956).
34. BIOT, M.A. *J.A.S.A.* 34 1254 (1962).
35. HARDIN, B.O. and RICHART, F.E. *Proceedings of the Am. Soc. Civ. Eng.;* *Soil Mechanics Division*, 89(i) 33 (1965).
36. BRUTSAERT, W. *J. Geophys. Research* 69 2 243 (1964).
37. BERANEK, L.L. *J.A.S.A.* 14 (1942).
38. McGRATH, J.W. *J.A.S.A.* 24 305 (1952).
39. TYUTEKIN, V.V. *Soviet Physics - Acoustics* 2 3 309 (1956).
40. (a) NESTEROV, V.S. *Soviet Physics - Acoustics* 5 344 (1959).
(b) BYSOVA, N.L., and NESTEROV, V.S. *ibid.* 419 (1959)
41. URICK, R.J. and AMENT, W.S. *J.A.S.A.* 21 115 (1949).
42. LORD RAYLEIGH. "Theory of Sound" Vol. II Art 395.
43. LAMB, H. "Hydrodynamics" pp. 647.
44. SEWELL, C.J.T. *Phil. Trans. (A)* 210, 239 (1910).
45. EPSTEIN, P.S. *Applied Mechanics Theo. Von. Karman Anniv. Vol.* p. 558
(1941).

46. EPSTEIN, P.S. and CARHART, R.R. J.A.S.A. 25 553 (1953).
47. CHOW, J.F.C. J.A.S.A. 36(iii) 2395 (1964).
48. DEVLIN, C. J.A.S.A. 31 2 1654 (1959).
49. (a) ZINK, J.W. and DELSASSO, L.P. J.A.S.A. 30 765 (1958).
(b) ZINK, J.W. Ph.D. Dissertation, October, 1957. Univ. Calif.
50. YING, C.F. and TRUPELL, R. J.Appl.Phys. 27 1086 (1955).
51. BHATIA, A.B. J.A.S.A. 31(i) 16 (1959).
52. MORSE, P.M. and FESHBACH, H. "Methods of theoretical Physics" Vol. II
p. 1495.
53. WATERMAN, and TRUPELL, R. J. Math. Phys. 2 512 (1961).
54. TWERSKY, V.F. J. Math. Phys. 3 700-715 (1962).
55. TWERSKY, V.F. J. Math. Phys. 3 724-734 (1962).
56. TWERSKY, V.F. J.A.S.A. 36(ii) 1314 (1964).
57. EMBLETON, J.A.S.A. 40(i) 667 (1966).
58. DOMBROVSKII, R.V. Sov. Physics - Acoustics 12 419 (1967).
59. ZWIKKER and KOSTEN "Sound Absorbing Materials" p. 109.
60. BRISTOL SYMPOSIUM ON POROUS MATERIALS (Colston Papers) p. 151.
61. WOMERSLEY, J. W.A.D.C. Technical Report TR 56-614.
62. ZWIKKER and KOSTEN "Sound Absorbing Materials" p. 79.
63. JONES, R., LISTER, N., THROWER, E.N. "The Dynamic behaviour of Soils
and Foundations". Symposium on Vibration in Civil Engineering
held in the I.C. of Sc. & Tech. April, 1965,
64. KAWASIMA, V. Acustica 10 p. 209. (1960).
65. HARRIS, C.M. and MULLOY, C.T. J.A.S.A. 24 1-7 (1952).
66. KAWASIMA, V. Acustica 10 212. (1960).
67. *ibid.* p. 215.
68. URICK, R.J. J.A.S.A. 20 (3) 283 (1948).

69. CARSTENSEN, E.L. and SCHWAN, H.P. J.A.S.A. 31 185 (1959).
70. B.R.S. Report No. 36 "Sound Absorbant Treatments". (As given in "Building Materials" Feb. 1965).
71. MASON, W.P. "Physical Acoustics" Volume I Part A. p. 9. (1964).
72. *ibid.* p. 50.
73. *ibid.* p. 17.
74. *ibid.* p. 45.
75. *ibid.* p. 64.
76. *ibid.* p. 75.
77. WHITE, R.M. J.A.S.A. 30 771-785 (1958).
78. TYUTEKIN, V.V. Soviet Physics - Acoustics 5 105 (1959).
79. TYUTEKIN, V.V. Soviet Physics - Acoustics 6 97 (1960).
80. LAMB, H. "Hydrodynamics" pp 645 (1916).
81. MORSE, P.M. "Vibration and Sound".
82. MORSE, P.M. and FESHBACH, H. "Methods of Theoretical Physics" pp.1376.
83. *ibid.* Vol. II p. 1766.
84. see for example RUTHERFORD, D.E. "Vector Methods" p. 69.
85. REDWOOD, M. "Mechanical Waveguides".
86. MORSE, P.M. and FESHBACH, H. "Methods of Theoretical Physics" Vol. II p. 1563.
87. See for example SNEDDON, I.N. "Special Functions of Mathematical Phys. and Chem". pp. 107-108.
88. *ibid.* p. 139-140.
89. See for example RUTHERFORD, D.E. "Vector Methods" p. 70.
90. for example SNEDDON, J.N. as above p. 139-140.
91. KINSLER, and FREY. "Fundamentals of Acoustics". p. 133.
92. DUYKERS, L.R., J.A.S.A. 41 1330 (1967)

93. See for ex. Beranek 'Acoustic Measurements' p.p. 317 et seq.
94. Zwicker and Kosten "Sound Absorbing Materials". 1949. Ch. 5.
95. Morse, P.M. and Bolt, R.H. Rev. Mod. Phys. 16 96 (1944)
96. Taylor, H.D. J.A.S.A. 24, 701, (1952).
97. "Sound Absorbing Materials". pp. 166 et seq.
98. Pyett, E.T. Acustica 3, 375-382 (1953).
99. Ford, P., Landau, B.V. and West, H., J.A.S.A. 44, 2, 531-536 (1968).
100. Goodier, J.N. and Bishop, R.E.D. J. Appl. Phys. 23, 124-126, (1952).
101. Junger, M.C., J. Appl. Mech. 22, 227-231 (1955).
102. Chester, W., Proc. Roy. Soc. A 203, 33-42, (1950).
103. "Sound Absorbing Materials". p. 70.
104. Lang, W., Proc. of Int. Symp. on Acoustics. Ed. L. Cremer (1959).
105. "Sound Absorbing Materials". pp. 13-18.
106. Furrer, N. "Room and Building Acoustics and Noise Abatement" p. 64.
107. Kolsky, H. "Stress Waves in Solids". p. 100.
108. Vovk, Pasternak, and Tyutekin. Sov. Phys. Ac. 4 22 (1958).
109. Biot, M.A., J. Appl. Phys., 23, 997 (1952).
110. Lyamshev, L.N., Sov. Phys. Ac. 5, 56, (1959).
111. MEREDITH, J. Text. Inst. 45 T 489 (1954)
112. KAYE, G.W.C. and LABY, T.H. "Physical and Chemical Constants"
p.63.